UCRL-17790
C.2

# University of California

# Ernest O. Lawrence Radiation Laboratory

A COMPARATIVE STUDY OF (p, t) AND (p, $^3$He) REACTIONS ON LIGHT NUCLEI

Donald George Fleming
(Ph.D. Thesis)

August 1967

TWO-WEEK LOAN COPY

*This is a Library Circulating Copy which may be borrowed for two weeks. For a personal retention copy, call Tech. Info. Division, Ext. 5545*

Berkeley, California

UCRL-17790 C.2

## DISCLAIMER

This document was prepared as an account of work sponsored by the United States Government. While this document is believed to contain correct information, neither the United States Government nor any agency thereof, nor the Regents of the University of California, nor any of their employees, makes any warranty, express or implied, or assumes any legal responsibility for the accuracy, completeness, or usefulness of any information, apparatus, product, or process disclosed, or represents that its use would not infringe privately owned rights. Reference herein to any specific commercial product, process, or service by its trade name, trademark, manufacturer, or otherwise, does not necessarily constitute or imply its endorsement, recommendation, or favoring by the United States Government or any agency thereof, or the Regents of the University of California. The views and opinions of authors expressed herein do not necessarily state or reflect those of the United States Government or any agency thereof or the Regents of the University of California.

UCRL-17790

UNIVERSITY OF CALIFORNIA
Lawrence Radiation Laboratory
Berkeley, California

AEC Contract No. W-7405-eng-48

# A COMPARATIVE STUDY OF (p,t) AND (p,$^3$He) REACTIONS ON LIGHT NUCLEI

Donald George Fleming

(Ph.D. Thesis)

August 1967

# A COMPARATIVE STUDY OF (p,t) AND (p,$^3$He) REACTIONS ON LIGHT NUCLEI

Contents


Abstract . . . . . v

I. Introduction . . . . . 1

II. Experimental Procedures . . . . . 3

A. Machine and External Beam-Facilities . . . . . 3

B. Detectors and Electronics . . . . . 5

C. Gas Targets . . . . . 8

D. Data Analysis . . . . . 8

III. Theory . . . . . 10

A. Direct Transitions . . . . . 10

1. General Discussion . . . . . 10

2. Selection Rules . . . . . 15

3. The Effect of a Spin-Dependent Force on the Cross Section . . . . . 16

4. Cross Section Ratios for Mirror (p,t) and (p,$^3$He) Transitions . . . . . 18

5. Two-Nucleon Parentage Factors . . . . . 19

B. Core Excitation . . . . . 22

IV. Experimental Results and Nuclear Spectroscopy . . . . . 25

A. $^{15}$N(p,t)$^{13}$N and $^{15}$N(p,$^3$He)$^{13}$C . . . . . 25

1. Experimental Results . . . . . 25

2. Optical Model Parameters . . . . . 31

3. Intermediate Coupling Theory and Nuclear Structure Calculations . . . . . 44

4. Spectroscopy of Individual Transitions . . . . . 47

B. $^{13}$C(p,t)$^{11}$C and $^{13}$C(p,$^3$He)$^{11}$B . . . . . 71

1. Experimental Results . . . . . 71

2. Optical Model Parameters . . . . . 75

3. Spectroscopy of Individual Transitions . . . . . 75

V. Theoretical Cross Sections . . . . . 105

A. Mirror State Cross Section Ratios . . . . . 106

1. Discussion of Results . . . . . 106

2. Possible Explanations . . . . . 120

B. Comparison of Relative Cross Sections . . . . . 122
1. $^{15}N(p,t)^{13}N$ and $^{15}N(p,^{3}He)^{13}C$ Transitions . . . . . 122
2. $^{13}C(p,t)^{11}C$ and $^{13}C(p,^{3}He)^{11}B$ Transitions . . . . . 129
VI. Conclusions . . . . . 132
Acknowledgements . . . . . 133
Appendix . . . . . 134
References . . . . . 144

# A COMPARATIVE STUDY OF (p,t) AND (p,$^3$He) REACTIONS ON LIGHT NUCLEI

Donald George Fleming

Lawrence Radiation Laboratory
University of California
Berkeley, California

September 1967

## ABSTRACT

The (p,t) and (p,$^3$He) reactions on $^{15}$N and $^{13}$C targets have been investigated. Transitions to mirror final states in the mass 13 and mass 11 final nuclei were studied over 15 and 12.5 MeV of excitation, respectively. Several new spin and parity assignments are made. In particular, the lowest 1p shell T=3/2 states in these nuclei have been identified.

The DWBA predictions of the angular distributions arising from these (p,t) and (p$^3$He) transitions were generally found to well reproduce experiment. For the $^{15}$N(p,t)$^{13}$N and $^{15}$N(p,$^3$He)$^{13}$C reactions, these calculations were carried out using intermediate coupling wave functions to describe the final state; for the $^{13}$C(p,t)$^{11}$C and $^{13}$C(p,$^3$He)$^{11}$B reactions, pure jj configurations were assumed. In addition to giving a good account of the observed angular distributions, the DWBA calculations of relative cross sections for the (p,t) transitions were also found to be in good agreement with experiment.

Comparative measurements of these (p,t) and (p,$^3$He) reactions populating mirror final states has been used to test some of the assumptions made in current theories of direct two-nucleon transfer reactions. The agreement in cross section ratios of mirror (p,t) to (p,$^3$He) transitions is found to improve in every case with the inclusion of a strongly spin-dependent force in the nucleon-nucleon interaction, but overall satisfactory agreement is not obtained. The (p,t) transitions are found to be generally stronger than expected relative to their mirror (p,$^3$He) transitions and three cases are discussed where the experimental ratios of these cross sections exceed the theoretical upper limit. Interference terms arising either through the spin-orbit interaction in the optical potential or through a core-excitation mechanism are suggested as accounting for this result.

# I. INTRODUCTION

The successful interpretation of the single-nucleon transfer reaction as a simple direct reaction has led to its use as a spectroscopic tool for many years.[1,2] Although less thoroughly investigated, direct two-nucleon transfer reactions are equally important as spectroscopic probes (for example, the (p,t) reaction can be used to study nuclei two neutrons removed from stability) and their recent treatment by DWBA theories[3-6] permits an interpretation of the two-nucleon cross section in terms of the details of nuclear structure. In particular, the two-nucleon transfer reaction can be a sensitive test of the shell model configurations present in initial and final states.

If one assumes that the nucleon pair is transferred in a relative $\ell=0$ state of motion, then the Pauli Principle restricts the (p,t) reaction to a pure $^{13}S$ spin-isospin transfer. The (p,$^3$He) reaction, however, is not similarily restricted and, in particular, for reactions on targets with $T_z \neq 0$ leading to final states with $T = |T_z(\text{target})|$, it may proceed by both $^{31}S$ <u>and</u> $^{13}S$ spin-isospin transfers of the neutron-proton pair. In a comparison of (p,t) and (p,$^3$He) reactions populating mirror final states, the S=0 restriction on the spin transfer of the (p,t) reaction may manifest itself in two ways:

(1) Some (p,t) transitions may not be observed because they are "J-forbidden". For transitions <u>within</u> the 1p shell, this results when a J=3 transfer is required by angular momentum selection rules, whereas J=2 is the maximum transfer possible. An example of this occurs in the search for the intermediate coupling predicted[7-9] $7/2^-$ level in $^{13}N$ and $^{13}C$ via the $^{15}N$(p,t) and $^{15}N$(p,$^3$He) reactions, as is later discussed.

(2) Particularly in the lower part of the 1p shell, where LS coupling is more appropriate, some (p,t) transitions may not be observed because they are "S-forbidden". This occurs whenever the spin multiplicity of the initial and final states is not the same. Several striking examples of this were found in a recent comparative study of (p,t) and (p,$^3$He) reactions populating mirror final states in mass 7 and 5 nuclei.[10]

Other than what is discussed in Ref. 10, the spectroscopic utility of comparative (p,t) and (p,$^3$He) reactions to mirror final states has not been explored. Individually, the (p,t) reaction has received some study, particularly in medium and heavy nuclei[11] with Hintz and his co-workers making some detailed studies in this region.[12] By contrast, there has been relatively little (p,t) work reported in light nuclei,[13,14] and the (p,$^3$He) reaction, in general, has received only scant attention.[15,16] Moreover, with the exception of Ref. 10, the (p,t) and (p,$^3$He) reactions studied to date have covered only a limited range of excitation.

In addition to their spectroscopic utility, comparative measurements of (p,t) and (p,$^3$He) reactions on odd mass (T=1/2) targets populating mirror final states also provides one with a sensitive test of some of the assumptions made in current theories of direct two-nucleon transfer reactions.[3-6] Of particular interest is an increased understanding of the theoretical treatment necessary to interpret the greater flexibility in spin-isospin transfer allowed in the (p,$^3$He) reaction. The population of mirror final states permits such comparisons with minimal uncertainty in the final state wave functions. In general, it is found that (p,t) cross sections to mirror final states - when not inhibited by nuclear structure considerations - are strongly enhanced over the corresponding (p,$^3$He) transitions, sometimes by factors as large as 6 or 7. The implications of this enhancement will be considered in a detailed study of two (T=1/2) target nuclei, $^{15}$N and $^{13}$C, leading to mirror final states in the mass 13 and mass 11 final nuclei, respectively.

Further, since a T=1 transfer is allowed in both (p,t) and (p,$^3$He) reactions, their simultaneous observation can be a particularly valuable tool for locating states of high isospin. Measurement of the absolute cross sections of such transitions can be used to test the hypothesis that the specifically nuclear part of the nucleon-nucleon interaction is charge independent. The comparison of (p,t) and (p,$^3$He) reactions populating analogue final states ($T \geq 3/2$) has been employed previously to investigate the lowest T=2 levels in mass 16 and mass 20[17] and to investigate the lowest T=3/2 levels in mass 7.[18] Herein, are reported observations of the lowest (1p shell) T=3/2 states in the mass 13 and mass 11 isospin quartets.

## II. EXPERIMENTAL PROCEDURES

### A. Machine and External-Beam Facilities

The external beam facilities of the Berkeley 88" Cyclotron were used in these experiments. This is a variable energy sector-focused machine and its operation has recently been described by Conzett and Harvey.[19] The physical layout of the cyclotron and target area, together with the overall beam optics, is illustrated in Fig. 1. In the radial plane, the first set of quadrupole magnets (Quad. 1) creates an image of the virtual source just prior to the entrance of the switching magnet. The beam is then deflected 38° by the switching magnet through a second set of quadrupole magnets (Quad. 3) which produces a radial focus at the analyzing slit. For these experiments, this slit consisted of two vertical tantalum plates, 125 mils thick, and normally set 60 mils apart. In the vertical plane, only one focus is required prior to the scattering chamber. This occurs at the exit of the switching magnet. Beyond the analyzing slit, two quadrupole lens doublets (Quad. 21, Quad. 22) were required to bring the beam to a radial and vertical focus at the center of a 20" diameter scatter chamber. Typical beam spot sizes at this point were 80 mils wide × 100 mils high, with variable beam intensities between 0.05 and 1.5 μa.

Proton induced reactions were studied at 43.7 MeV on a $^{15}N$ target, at 43.7 and 49.6 MeV on a $^{13}C$ target and at 43.7 and 54.1 MeV on an $^{16}O$ target.

The beam intensity was measured in a Faraday cup (which employed a carbon block 3/4 of an inch thick) using an integrating electrometer. The incident beam energy was determined by a range-energy measurement using aluminum absorbers of known thickness and the tables of Williamson and Boujot.[20] Two separate counter assemblies were operated, both of which were positioned 10° out of the horizontal plane. The smallest possible scattering angle that could be attained was then 10°. The two counter packs were external to the scatter chamber (20 in. from the center), which made for easy access; in addition, they could be independently rotated to any desired scattering angle. The scatter chamber and supporting beam pipe was kept under vacuum ($10^{-4}$ mm of mercury) by an oil diffusion pump, backed by a Kinney mechanical pump.

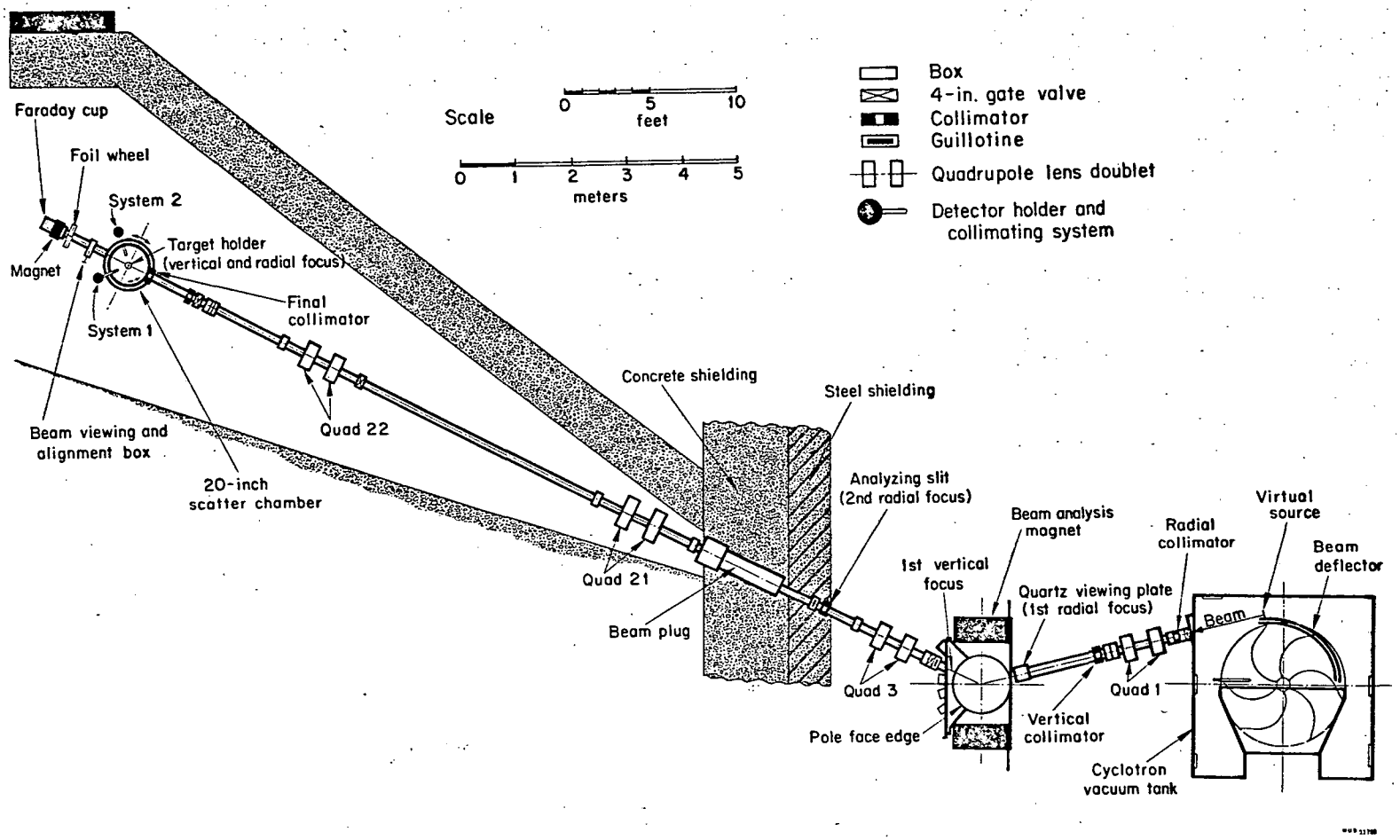


Fig. 1. Cyclotron area and beam optics.

## B. Detectors and Electronics

Reaction events were measured in two separate counter telescopes, each consisting of a 5.5 mil phosphorous diffused silicon $\Delta E$ detector and a 120 mil Li-drift silicon E detector. The development and application of solid state counters has been well described[21] and will not be discussed here. Each $\Delta E$-E counter pair was backed by a 20 mil Li-drift silicon detector, which served only to eliminate energy signals from long-range events that passed through the first two detectors. Electrical contact was made by a stainless steel spring and the detector voltages were typically 150 V and 500 V for the $\Delta E$ and E counters, respectively.

A block diagram of the electronics is shown in Fig. 2. Signals from the three detectors ($\Delta E$, E, E rej.) were first sent to charge sensitive preamplifiers which then fed the main amplifiers in the circuit. In the main amplifier, these pulses were integrated with a 0.2 μsec time constant, amplified and shaped and then stretched to a 3 μsec width. A slow coincidence ($2\tau$ = 1 μsec) was demanded between the $\Delta E$ and E signals and pulses which satisfied this requirement were sent to a Goulding-Landis particle identifier.[22] This identifier depends on the empirical relation $R = aE^{1.73}$, were R is the range of the particle, E its total energy and a is a characteristic constant dependent on particle type. Thus, for a particle passing through the $\Delta E$ and E detectors,

$$\frac{T}{a} = (E + \Delta E)^{1.73} - E^{1.73}$$

so that the identification signal is proportional to T/a, where T is effectively the thickness of the $\Delta E$ counter. For protons a = 32.2 and for $\alpha$ particles a = 2.95, so that for a given $\Delta E$ detector, one expects a larger identification signal for $\alpha$ particles than for protons. A typical particle identifier spectrum is shown in Fig. 3.

Particle identifier signals were gated in a four-channel router, in coincidence with their total ($E + \Delta E$) energy signal. Since relatively thin $\Delta E$ detectors were used, relatively small particle identification signals resulted for Z=1 particles and consequently it was not always possible to completely separate deuterons and tritons. Thus a safety

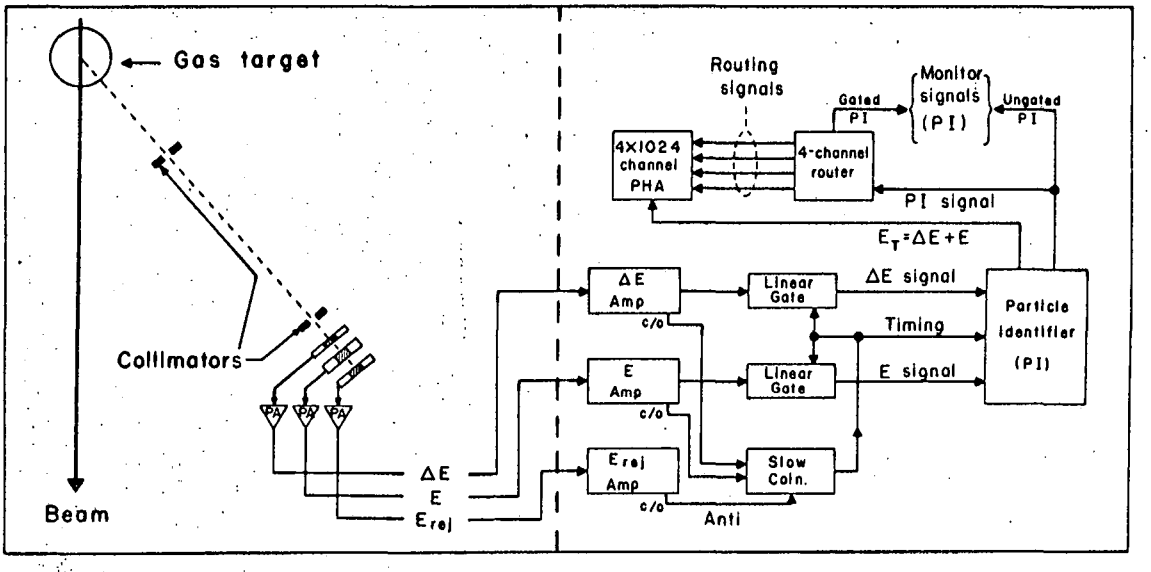


Fig. 2. Counter assembly and block diagram of the electronics used in these experiments.

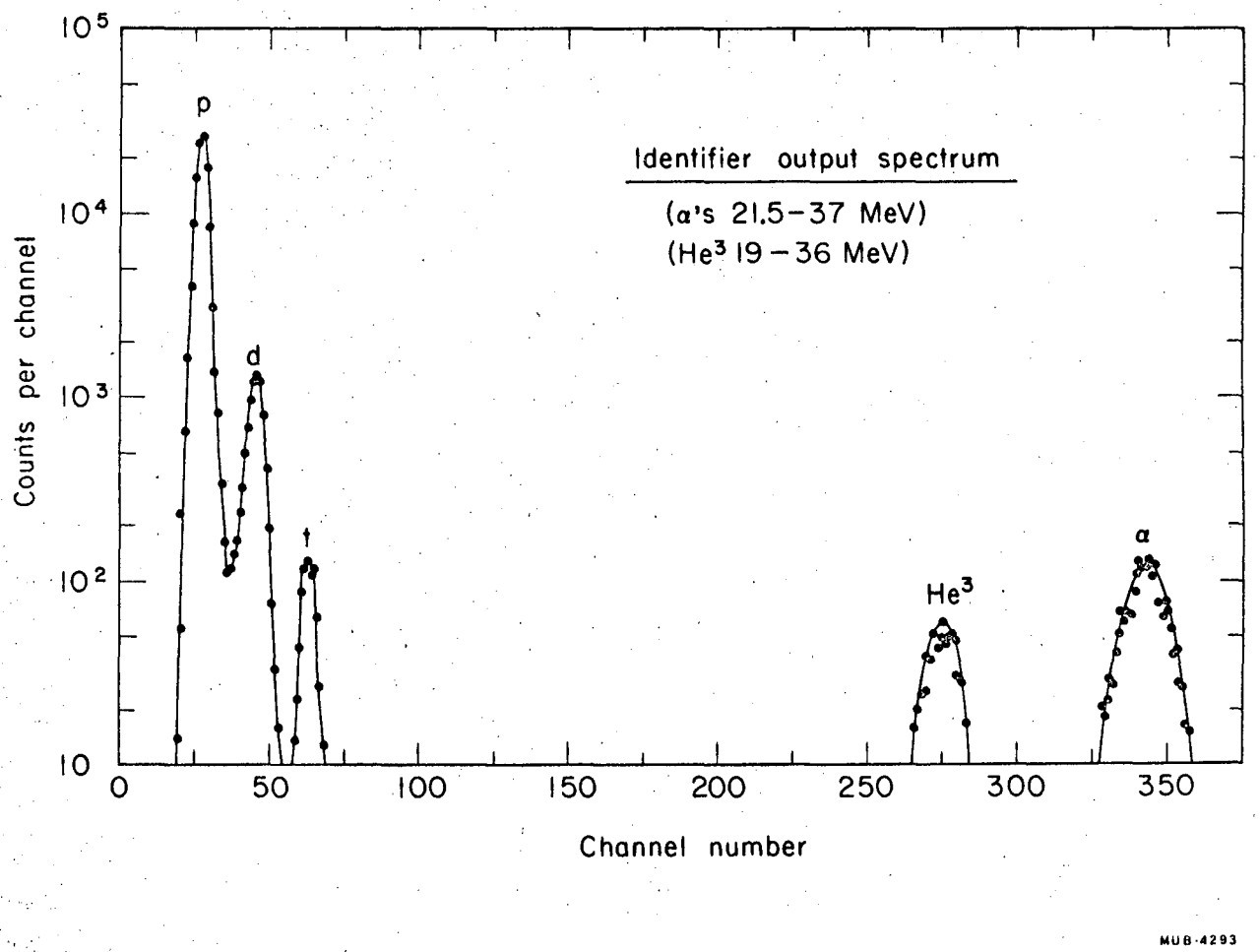


Fig. 3. A typical particle identifier spectrum.

group was always observed in which any leak-through tritons were collected. Valid triton, helium-3 (and alpha) particle events were recorded in the appropriate channel of a Nuclear Data pulse height analyzer or in an on-line PDP-5 computer, both normally operating in the 4 × 1024 channel mode. Typical energy resolutions (FWHM) of 150 and 180 keV were obtained for tritons and helium-3, respectively.

## C. Gas Targets

The targets used were pure ($^{16}O$) or nearly pure (99% $^{15}N$, 93% $^{13}C$) gases. They were contained in a three-inch diameter gas target cylinder which was filled externally. The 315° gas target window was covered with 0.1 mil Havar foil[23] which easily withstood pressures of 30 cm of mercury. The target thickness and beam energy were constantly monitored by a 120 mil Li-drift silicon detector fixed at 27.5° to the beam. This was particularly important for the $^{13}C$ reaction, since methane is known to decompose under radiation.

## D. Data Analysis

Total energy signals (E + ΔE) stored in the pulse height analyzer or computer were written on magnetic tape for later analysis. The first information to be extracted from the energy spectrum was the determination of the energies of the various final states populated in the reaction. The energies of the "known" final states ($^{13}N$ g.s., $^{13}N^*$ 3.51, $^{13}N^*$ 7.38 MeV levels in the $^{15}N(p,t)^{13}N$ reaction, for example) were then used to determine the energy scale, from which the excitations of all other levels in the spectrum could be determined. Enough angles were studied to insure that the transition of interest had the correct kinematic behavior and was therefore not due to some unknown impurity. The average excitation was then determined and a standard deviation calculated.

The total number of counts in each peak (after background correction) was determined for all the levels of interest and the differential

cross section calculated at each angle. For a gas target, the target thickness is determined by the solid angle ($\Omega$) subtended by the defining collimators (two are needed, as shown in Fig. 2) and thus varies with the angle of observation. The (center-of-mass) differential cross section was calculated from the formula

$$\left(\frac{d\sigma}{d\Omega}\right)_{cm} = \frac{JC(T + 273)\ \mathrm{Sin}\ \theta_L \times (\ell_1 + \ell_2)^2 \times Z \times 6.53 \times 10^{-7}}{B\ N\ P\ W_1\ W_2\ H_2\ (1 + \ell_1/\ell_2)} \ (\mathrm{mb/sr})$$

where $T$ and $P$ are the gas temperature (°C) and pressure (cm of Hg), respectively, $\theta_L$ is the laboratory scattering angle, C/B is the total number of counts per $\mu$c of incident beam of charge Z, and $\ell_1$, $\ell_2$, $W_1$, $W_2$, $H_2$ are geometrical parameters defining, respectively, the distance from the center of the target to the front face of the first collimator, the distance from the front of the first collimator to the rear of the back collimator, the width of these two collimators and the height of the rear collimator. All dimensions are measured in inches. $N$ is the number of nuclei/mole ($N = 2$ for $^{15}N$) and $J$ is the Jacobian for transformation from lab to center-of-mass coordinates.

The total cross section is obtained by integration of the above expression:

$$\sigma_T = 2\pi \int_0^{\pi} \frac{d\sigma}{d\Omega} \sin\theta\ d\theta = 2\pi \int_{-1}^{1} \frac{d\sigma}{d\Omega}\ d(\cos\theta)$$

In practice, this integral was evaluated graphically and the range of integration was typically 10 - 80° in the center-of-mass. Absolute cross sections are expected to be good to within ± 10%.

# III. THEORY

## A. Direct Transitions

### 1. General Discussion

Two-nucleon transfer reactions have received considerable theoretical attention over the past ten years. The bulk of these theories,[24] however, have been extensions of single nucleon plane wave theories, and have had only marginal success in fitting the data.[25] Distorted wave theories of direct two-nucleon transfer reactions[3-6] have been developed and although several DWBA analyses have appeared in the literature,[26] until recently, relatively little detailed experimental verification of the theory has been published.

The formulation of the theory of direct two-nucleon transfer reactions by most authors[3,4,6] is essentially equivalent. (An exception is the work of Rook et al.[5] who, in addition to the zero range interaction employed by others, also use a point triton approximation). However, since the formulation of Ref. 3 was made with particular emphasis on the role played by the structure of nuclear states in the reaction, it was more suitable for this analysis and will consequently be used throughout. This theory fully takes into account the configurations of both the target nucleus and the residual state, spatial correlations between the nucleons and coherent effects in the picked up pair. The salient features of the theory are discussed below.

Assuming that the spin-orbit interaction can be neglected in the optical model, then the differential cross section of a two-nucleon transfer reaction can be written as an incoherent sum over all the angular momentum quantum numbers (L,S,J,T) of the transferred pair:

$$\frac{d\sigma}{d\Omega} \alpha \frac{k_f}{k_i} C_{ST}^{\ 2} \sum_{LSJT} \sum_{M} \left| \sum_{N} G_{NLSJT} \, B^{M}_{NL}(k_i,k_f) \right|^2 \qquad (1)$$

This is quite different from a similar expression obtained for a single-nucleon transfer reaction where it is well known[2] that the cross section can be factored into two terms, one containing the nuclear structure information and the other depending on the kinematics:

$$\frac{d\sigma}{d\Omega} \propto \frac{k_f}{k_i} \sum_{\ell jm} \beta_{j\ell}^2 |B_{n\ell}^m|^2 \tag{2}$$

One is unable to achieve a similar factorization in the two-nucleon transfer reaction because of coherent effects, which are absent in the single-nucleon cross section of Eq. (2) and which will be discussed more fully below. Nevertheless, the transition matrix element (Eq. (1)) can be separated into a factor depending only upon the details of nuclear structure ($G_{NLSJT}$), and a transfer amplitude ($B_{NL}^M$) which represents the probability of transferring a structureless pair to or from the target nucleus. This allows a separate treatment of the dependence of the cross section on the details of nuclear structure, independently of the spectroscopically uninteresting transfer amplitude with its attendant distorted wave calculation.

The $C_{ST}^2$ term in Eq. (1), for a pickup reaction, has the form

$$C_{ST}^2 = b_{ST}^2 |\langle t_f\ m_f TM_T | t_i\ m_i \rangle|^2 \tag{3}$$

where $b_{ST}^2$ is an overlap integral involving the spin-isospin wave functions of the transferred pair and the light particle (A=3 ground state in this discussion) and the Clebsch-Gordon coefficient couples the isospin of initial and final nuclear states by the isospin $(T,M_T)$ transferred in the reaction. This equation is discussed in more detail in a later section.

The transfer amplitude $B_{NL}^M$ is completely analogous to a similarly denoted term in the theory of single-nucleon transfer reactions (Eq. (2)) and for the (p,t) reaction it can be represented by the integral

$$B_{NL}^M(k_p,k_t) \propto \int \chi_t^{*(-)}(k_t,R_t)\ U_{NL}^{M*}(2\nu R^2)\ Y_{LM}^*(R)\ V(\rho)\ \Phi_t(\rho)\ \chi_p^{(+)}(k_p,R_p) dR\ dR_p dR_t \tag{4}$$

where $\chi_p^{(+)}$ and $\chi_t^{(-)}$ are the familiar optical model solutions of the elastic scattering problem for the entrance and exit channels, respectively. The center-of-mass coordinate of the transferred pair is given by $R$; $\rho = |R-R_p|$ and $R_p$ and $R_t$ are the center-of-mass coordinates of the

incident proton and exit triton, respectively. The internal wave function of the triton is given by $\Phi_t(\rho)$ and $V(\rho)$ is the two-body interaction potential between the incident proton and the center-of-mass of the picked-up neutrons. The optical model potential has the form

$$-U(r) = V\, f(r) + 4ai\, W_D\, f'(r) + iW\, f(r) - V_c(r) \qquad (5)$$

where V, W, and $W_D$ are the real, volume absorption and surface absorption potentials, respectively. Saxon-Wood or derivative Saxon-Wood form factors are used throughout[27] and no spin-orbit coupling is included. The Coulomb potential is given by $V_c(r)$ and is evaluated with a spherical charge distribution.

The wave function $U^M_{NL}(2\nu R^2)$ represents the center of mass motion of the transferred pair. It depends, as it does in a single-nucleon transfer reaction, on the principal quantum number (N) and the transferred orbital angular momentum (L). However, unlike single-nucleon transfer reactions, several radial states (those with different N) may be required to completely describe the center of mass motion of two nucleons and these enter coherently into the two-nucleon cross section (Eq. (1)). Such a coherence has no analog in a single nucleon transfer reaction. The bound state wave function is represented by a harmonic oscillator in the interior of the nucleus. In order to give this wave function a more proper asymptotic behavior than that afforded by a pure harmonic oscillator, it is matched to a Hankel function tail at the nuclear surface, the argument of which is proportional to the separation energy of the pair. In a pickup reaction, this has the effect of compressing the bound state wave function for excited states.

An alternate procedure is to evaluate the bound state wave function using the single particle eigenfunctions of a Woods-Saxon potential. This will yield a wave function for the center-of-mass of the pair which is improved over a pure harmonic oscillator wave function in the sense that it does not decay so rapidly; hence it should yield improved results for the calculated angular distribution, as was recently emphasized by Drisko and Rybicki.[28] However, especially if many single particle states

are required to describe the center-of-mass motion of the transferred pair, it is not clear[6] that the wave function calculated from a Woods-Saxon well will have the proper asymptotic behavior associated with the separation energy of the pair. Moreover, the use of harmonic oscillator single particle wave functions allows one to immediately exploit their convenient analytical properties, as is later discussed.

The coherent nuclear structure factors, as manifest in the $G_{NLSJT}$ of Eq. (1), can have a drastic effect on the two-nucleon cross section, resulting in strong transitions to those levels for which they are constructive. These structure factors are discussed in some detail, since the cross section is essentially proportional to a sum of their squares. Following Ref. 3, the nuclear structure factor can be written as a product of three factors:

$$G_{NLSJT} = \sum_{\gamma} g^{\gamma} \beta^{\gamma}_{LSJT}\, \Omega_n \langle n0, NL;\ L | n_1 \ell_1,\ n_2 \ell_2;\ L \rangle \tag{6}$$

the sum on $\gamma$ is over the various shell model configurations that may be present in the wave function of the target nucleus and which can be excited in the two-nucleon transfer reaction. The factor $g^{\gamma}$ expresses the exchange symmetry of the two nucleons in the transferred pair. If the pair have a definite symmetry under exchange, then $g^{\gamma} = 1$ if $n_1 \ell_1 j_1 = n_2 \ell_2 j_2$; otherwise $g^{\gamma} = \sqrt{2}$. If the wave function of the pair does not have definite symmetry under exchange (i.e., a neutron-proton configuration without definite isospin), then $g^{\gamma} = 1$.

The factor $\beta^{\gamma}_{LSJT}$ is analogous to the same term in Eq. (2) for a single-nucleon transfer reaction and is the two-nucleon parentage factor, which gives the overlap between initial and final nuclear states. To be specific, in a pickup reaction, $\beta^{\gamma}_{LSJT}$ measures the extent to which the final nucleus plus two nucleons in the state $\gamma(n_1\ \ell_1,\ n_2\ \ell_2)$ resembles the ground state of the target nucleus. Formulas expressing parentage factors for the transfer of two nucleons from general target nuclei are given below. Assuming harmonic oscillator wave functions for the two nucleons in the state $\gamma$, they can be readily transformed to relative (r) and center of mass coordinates (R) using the Talmi coefficients, numerical

tables of which have been prepared by Brody and Moshinsky.[29] This transformation has the form

$$[\phi_{n_1\ell_1}(r_1)\ \phi_{n_2\ell_2}(r_2)]_L = \sum_{n\lambda N\Lambda} \langle n\lambda,\ N\Lambda;\ L|n_1\ell_1,\ n_2\ell_2;\ L\rangle [\phi_{n\lambda}(r)\ \Phi_{N\Lambda}(R)]_L \tag{7}$$

where $\phi_{n\lambda}(r)$ represents the relative motion of the two nucleons and $\Phi_{N\Lambda}(R)$ is their center of mass motion. With the usual simplifying assumption that the light particle is purely spherically symmetric ($^2S_{1/2}$), then only $\lambda = 0$ states of relative motion are possible (the ground state wave function of A=3 is known to be at least 94% $^2S_{1/2}$, with a 6% $^4D_{1/2}$ admixture),[30] which accounts for only a $\lambda = 0$ term in the Moshinsky bracket of Eq. (6). The relative motion of the two nucleons in the nucleus-$\phi_{n\lambda}(r)$- must overlap with the motion of the same pair in the light nuclide, which is assumed to be gaussian, and this overlap is denoted in Eq. (6) by $\Omega_n$. The important thing to note is that the nuclear structure factors ($G_{NLSJT}$) are a <u>coherent sum</u> over all the amplitudes shown (Eq. (6)).

Unlike single-nucleon transfer reactions, where the spectroscopic factor is merely multiplicative, one cannot, in general, deduce the "spectroscopic factor" in a two-nucleon transfer reaction by a comparison between DWBA and experiment. This is due to the fact that there is no unique way to combine the three factors of Eq. (6) and moreover this structure factor is also coherent with the distorted wave amplitude ($B^M_{NL}$) through the sum on N. However, if the nuclear wave functions of initial and final states are available, say from a shell model calculation, then the parentage factor and the nuclear structure factor ($G_{NLSJT}$) can be calculated. One must then regard the theory as a test of the nuclear wave functions being used rather than as a means for the extraction of "spectroscopic factors". Due to the coherent effects mentioned above, the two-nucleon transfer reaction is, in principle, sensitive to small impurities in the wave functions used to describe the initial and final nuclear states. A more stringent test of the accuracy of such wave functions, other than just fitting experimental angular distributions, is a comparison of relative cross sections and several calculations of this kind have now been reported.[6,16,31-33]

2. Selection Rules

The general selection rules of other two-nucleon transfer reactions have been reviewed elsewhere,[2,3,34] and only those pertinent to (p,t) and (p,$^3$He) reactions will be considered here. In all direct reactions, the total angular momentum (J) transferred in the reaction is related to the angular momentum of the initial state ($J_i$) and the angular momentum of the final state ($J_f$) by

$$\bar{J} = \bar{J}_i - \bar{J}_f = (\bar{\ell}_i - \bar{\ell}_f) + (\bar{s}_i - \bar{s}_f) = \bar{L} + \bar{S}$$

where $\ell$ and s refer to the orbital and spin angular momentum, respectively, in the incident (i) and exit (f) channels and L and S refer to the total orbital and spin angular momentum transferred in the reaction, respectively. The main difference in the selection rules between a one and a two-nucleon transfer reaction is due to the relative motion present in the pair of nucleons. Thus, if L is the transferred orbital angular momentum in, for example, a (d,p) reaction, then $J = L \pm 1/2$ and the parity change[35,36] in the reaction is given by $\Delta\pi = (-1)^L$. In a two-nucleon transfer reaction, however, the orbital angular momentum transfer $L = \bar{\Lambda} + \bar{\lambda}$, where $\bar{\Lambda}$ refers to the center-of-mass motion of the pair (and is the only term present in a (d,p) reaction) and $\bar{\lambda}$ refers to the relative motion of the pair. (As described earlier, any two single particle wave functions, $|n_1 \ell_1\rangle$ and $|n_2 \ell_2\rangle$, can be readily transformed into relative and center-of-mass coordinates, and if harmonic oscillator wave functions have been chosen for the single particle states, then this transformation can be written in closed form).[29]

In general, then, for a two-nucleon transfer reaction

$$\bar{J} = \bar{L} + \bar{S} = \bar{\Lambda} + \bar{\lambda} + \bar{S} \quad \text{and} \quad \Delta\pi = (-)^{\lambda + \Lambda}$$

However, as previously discussed, the relative motion of a pair of nucleons in the target (in a pickup reaction) must overlap with the motion of the same pair in the light nuclide (here triton or helium-3), so that under the assumption of a pure $^2S_{1/2}$ state for the triton or helium-3 ground state, only $\lambda = 0$ states of relative motion are possible in the transferred pair. Thus,

$$\bar{J} = \bar{\Lambda} + \bar{S} = \bar{L} + \bar{S} \quad \text{and} \quad \Delta\pi = (-1)^L$$

in complete analogy with the theory of single nucleon transfer reactions.[2]

It must be borne in mind that the $\lambda = 0$ selection rule is not rigorous and is based on the assumption that the ground state of the triton or helium-3 wave function is purely spherically symmetric ($^2S_{1/2}$). The small $^4D_{1/2}$ admixture expected to be present [30] could introduce some $\lambda = 2$ component into the selection rules just discussed. Thus the parity change would no longer be simply related to the center-of-mass angular momentum transfer ($\Lambda = L$) and this could have the result, for example, of allowing the formation of "unnatural parity" states in (p,t) reactions on $[0^+]$ targets.

3. <u>The Effect of a Spin-Dependent Force on the Cross Section</u>

The factor $C_{ST}^2$ in the expression for the cross section (Eq. (1)) is given, for a pickup reaction, by

$$C_{ST}^2 = b_{ST}^2 \langle t_f m_f T M_T | t_i m_i \rangle$$

The Clebsch-Gordon coefficient has been defined before. The factor $b_{ST}^2$ is a spectroscopic overlap integral involving the spin-isospin wave functions of the transferred pair and the $A = 3$ ground state wave function. When generalized to include the effect of a spin-dependent force, this overlap can be written as

$$b_{ST}^2 = \begin{cases} a_0^2(\delta_{S0}\delta_{T1}) & (p,t) \\ 1/2[a_0^2(\delta_{S0}\delta_{T1}) + a_1^2(\delta_{S1}\delta_{T0})] & (p,{}^3He) \end{cases} \tag{8}$$

where $a_0^2$ and $a_1^2$ arise from the spin-exchange properties of the two-nucleon force, as described in more detail below.

Transfer of a pair of nucleons in the spin state $S$ involves the matrix element

$$\langle \chi^{\sigma_a \tau_a}_{1/2\ 1/2}(3)\ \chi^{M_S M_T}_{ST}(1,2)\,|V_{13}(r_{13}) + V_{23}(r_{23})|\,\chi^{\sigma_b \tau_b}_{1/2\ 1/2}(1,2,3)\rangle$$

$$\equiv C^{1/2\ S\ 1/2}_{\sigma_a\ M_S\ \sigma_b}\ \sqrt{2S+1}\ b_{ST} \tag{9}$$

where, in these reactions, channel a represents the incident proton (with spin, isospin projections $\sigma_a \tau_a$) and channel b represents the outgoing triton or helium-3. The transferred pair is represented by the wave function $\chi_{ST}$ with projection quantum numbers $M_S$ and $M_T$ and the Clebsch-Gordon coefficient couples the channel spins by the spin transfer (S) in the reaction. $V_{ij}$ is the two-body interaction potential between the incident proton (particle 3) and either one of the nucleons (particles 1,2) in the transferred pair, which in general may be transferred in either an S=0, T=1 state ($^{13}S$) or in an S=1, T=0 state ($^{31}S$). In this work, the singlet-even strength of the two-body potential ($V_{ij}$) will be represented by $A^S$ and the triplet-even strength by $A^T$. Then the dependence of the matrix element (9) on these potentials for transfer of the pair in singlet or triplet spin states is given,[37] respectively, by

$$\begin{aligned} a_0 &= 3/4\ A^T + 1/4\ A^S \\ -a_1 &= 1/4\ A^T + 3/4\ A^S \end{aligned} \tag{10}$$

For the (p,t) reaction, only the $a_0(S=0)$ term will contribute; for the (p,$^3$He) reaction, however, both the $a_0(S=0)$ and $a_1(S=1)$ terms are important. Writing Eq. (9) in terms of $a_0$ and $a_1$ and expressing the overlap in terms of a fractional parentage expansion of the three-nucleon wave function (which introduces a factor of 1/2) and performing an incoherent sum of squares (as required by the previous assumption of a zero spin-orbit force in the optical model) yields the result given in Eq. (8).

The intrinsic ratio of $a_0^2$ to $a_1^2$ depends upon the nature of the nucleon-nucleon force. Evidence that the tensor force influences nucleon-nucleon scattering[38,39] as well as evidence from model-dependent

central-force calculations of S-wave scattering[40] and the bound state of the deuteron leads one to expect some spin dependence in these pickup reactions. Moreover, a variety of shell model calculations indicate that the tensor force is strong[41,42] and that the ratio of the singlet-even ($A^S$) strength to the triplet-even ($A^T$) strength should be about 0.6/1.[41,43] The later calculations suggest use of a more strongly spin-dependent interaction than this, and the ratio $A^S = 0.3\ A^T$ is used. If the nucleon-nucleon interaction were spin-independent, then $A^S = A^T$ and $a_0^2/a_1^2 = 1.0$, and there would be equal probability of transferring either S=0 or S=1 in the (p,$^3$He) reaction. However, this is no longer true for the case of a spin-dependent interaction and for the particular choice made ($A^S = 0.3\ A^T$), $a_0^2/a_1^2 = 3.0$, so that for a given L transfer, the S=0 transfer is enhanced by a factor of three over the S=1 transfer.

4. Cross Section Ratio for Mirror (p,t) and (p,$^3$He) Transitions

In comparing (p,t) and (p,$^3$He) reactions to mirror final states, which will be discussed later, it is of interest to calculate the theoretical cross section ratio expected for these transitions based on the limit of a pure S=0 transfer for the (p,$^3$He) reaction:

$$\left.\frac{\sigma(p,t)}{\sigma(p,{}^3He)}\right\}_{S=0} = \frac{C_{ST}^{\ 2}(p,t)}{C_{ST}^{\ 2}(p,{}^3He)} \cdot \frac{\sum_{JM}\left|\sum_N G_{NJT}\ B_{NL}^M\right|^2}{\sum_{JM}\left|\sum_N G_{NJT}\ B_{NL}^M\right|^2} \tag{11}$$

Experimental results for (p,t) and (p,$^3$He) transitions from T=1/2 to T=3/2 final states--where only a zero spin transfer is allowed--show that the second ratio is essentially unity (within 10%), both in the 1p shell[18] and in the 2s-1d shell.[44,45] (One would also expect this ratio to be unity for single-nucleon transfer in the 1p shell and this has been recently verified in the $^{12}C(d,t)^{11}C$ and $^{12}C(d,{}^3He)^{11}B$ reactions).[46] Thus Eq. (11) becomes

$$\left.\frac{\sigma(p,t)}{\sigma(p,{}^3He)}\right\}_{S=0} = \frac{C_{ST}^{\ 2}(p,t)}{C_{ST}^{\ 2}(p,{}^3He)} = \frac{1\cdot|\langle 1/2\ -1/2\ 1\ 1|1/2\ 1/2\rangle|^2}{1/2\cdot|\langle 1/2\ 1/2\ 1\ 0|1/2\ 1/2\rangle|^2} = \frac{4}{1} \tag{12}$$

On the basis of the earlier assumptions, this represents the upper limit[47] that can be expected in comparing (p,t) and (p,$^3$He) cross sections to mirror final states since an incoherent contribution of S=1 transfer in the (p,$^3$He) reaction could only reduce this ratio. The slight effects of the differing kinematic and Coulomb properties in the exit channel will be discussed later.

5. Two-Nucleon Parentage Factors

General two-nucleon parentage factors for odd A and even-even nuclei are given below; complete derivations are presented in the Appendix. This factor is defined as

$$\beta^{\gamma}_{LSJT}(j_1,j_2) = \binom{A+2}{2}^{1/2} \int [\psi_{J_1T_1}(A)\, \phi^{\gamma}_{LSJT}(r_1,r_2)]^*_{J_2T_2}\, \psi_{J_2T_2}(A+2)\, dA\, dr_1\, dr_2 \tag{12}$$

where the square bracket denotes vector coupling and the combinatorial factor $\binom{A+2}{2}^{1/2}$ denotes the number of possible ways a pair can be removed from the target. These parentage factors are constructed from a neutron-proton formalism of initial and final states, so that this statistical factor is replaced by the product

$$\binom{A+2}{2} \rightarrow \binom{N+\nu}{\nu}\binom{Z+\pi}{\pi}$$

where $\nu$ refers to neutron and $\pi$ to proton and N and Z represent the initial number of neutrons and protons, respectively.

a. For an odd A nucleus. The target has spin j and its wave function can be written in the form

$$|\psi_T\rangle = |(j_a^{n_a})_0\ (j_b^{n_b})_0,\ j;j\rangle$$

(1) For a pair of like nucleons added or taken out of a given shell - say $j_b$ - where $n_b$ is even, the final state wave function has the form

$$|\psi_F\rangle = |(j_a^{n_a})_0,\ (j_b^{n_b-2})_J,\ j;J_f\rangle$$

The parentage factor relating initial and final state configurations for a particular total angular momentum transfer J and a particular final state spin $J_f$ is

$$\beta^{\gamma}(j_b{}^2)_J = \left(\frac{n_b(n_b-1)}{2}\right)^{1/2} ((j_b{}^{n_b-2})_{vJ}(j_b{}^2)_J;\ 0|\}(j^{n_b})_0)\left(\frac{2J_f+1}{(2J+1)(2j+1)}\right)^{1/2} \tag{14}$$

Explicit expressions for the two-nucleon coefficients of fractional parentage, $(\cdot|\})$, are found in the Appendix.

(2) For a pair of nucleons transferred across shells or a pair of non-identical nucleons (a neutron-proton pair) transferred within the same shell, the final state wave function has the form

$$|\psi_F\rangle = |[(j_a^{n_a-1})_{j_a}\ (j_b^{n_b-1})_{j_b}]_J, j; J_f\rangle$$

where the square bracket again denotes vector coupling and $n_a$ and $n_b$ are even. The parentage factor relating this configuration to the initial state by the total angular momentum transfer J is given by

$$\beta^{\gamma}(j_a, j_b)_J = (n_a\ n_b)^{1/2}\left(\frac{2J_f+1}{(2j_a+1)(2j_b+1)(2j+1)}\right)^{1/2} \tag{15}$$

b. <u>For an even-even nucleus.</u>[48] The target has spin zero and the wave function can be written in the form

$$|\psi_T\rangle = |(j_a^{n_a})_0\ (j_b^{n_b})_0; 0\rangle$$

where $n_a$ and $n_b$ are even.

(1) For a pair of like nucleons added or taken out of a given shell, say $j_b$, then the final state wave function has the form

$$|\psi_F\rangle = |(j_a^{n_a})_0\ (j_b^{n_b-2})_J; J_f = J\rangle$$

and the parentage factor is

$$\beta^{\gamma}(j_b{}^2)_J = \left(\frac{n_b(n_b-1)}{2}\right)^{1/2} ((j_b{}^{n_b-2})_{vJ}\ (j_b{}^2)_J;0|\}\ (j_b{}^{n_b})_0) \tag{16}$$

Explicit values for the two-nucleon coefficients of fractional parentage, ($|\}$), may be found in the Appendix.

(2) For a pair of nucleons transferred across shells or a pair of unlike nucleons transferred within the same shell, then the final state wave function has the form

$$|\psi_F\rangle = |[(j_a{}^{n_a-1})_{j_a}(j_b{}^{n_b-1})_{j_b}]_J;J_f = J\rangle$$

and the parentage factor is given by

$$\beta^{\gamma}(j_a j_b)_J = (n_a n_b)^{1/2}\left(\frac{2J+1}{(2j_a+1)(2j_b+1)}\right)^{1/2} \tag{17}$$

Since the angular distribution of a two-nucleon transfer reaction is characterized by the orbital angular momentum transfer (L) and not the total angular momentum transfer (J), then it is more instructive to express the parentage factor in LS coupling. This is accomplished by the following jj-LS transformation coefficient:

$$\beta^{\gamma}(\ell_1\ell_2)_{LSJ} = \begin{bmatrix} \ell_1 & s_1 & j_1 \\ \ell_2 & s_2 & j_2 \\ L & S & J \end{bmatrix} \beta^{\gamma}(j_1 j_2)_J$$

where $\begin{bmatrix} \ell_1 & s_1 & j_1 \\ \ell_2 & s_2 & j_2 \\ L & S & J \end{bmatrix} = \left[(2L+1)(2S+1)(2j_1+1)(2j_2+1)\right]^{1/2} \begin{Bmatrix} \ell_1 & s_1 & j_1 \\ \ell_2 & s_2 & j_2 \\ L & S & J \end{Bmatrix}$

and the curly bracket {} is a 9j symbol.[49]

## B. Core Excitation

Since some transitions to be discussed can be interpreted on the basis of a core-excitation pickup reaction (those "forbidden" on the basis of a direct pickup in the 1p shell), it is worthwhile to include a very brief treatment of the theory of such reactions.

There has been considerable discussion of core-excitation processes populating otherwise j-forbidden transitions in single-nucleon stripping and pickup reactions[46,50,51] but little evidence to date for these effects in two-nucleon transfer reactions. To the extent that two-step processes could contribute in these reactions, the overall general reaction can be represented as shown in Fig. 4. The direct pickup amplitude is represented by $T_1$ and the indirect amplitudes (inelastic scattering plus pickup) are represented by $T_2$ and $T_3$ for the entrance (target excitation) and exit channels, respectively. $J_f$ is the final state nuclear spin, which, in a direct transition, is populated only through the amplitude $T_1$. By a two-step process, it may be excited by a pickup from $J_A'$ which has been excited in the entrance channel, or via inelastic scattering in the exit channel from the level $J_B'$, which may or may not be the ground state of the residual nucleus. For simplicity, only inelastic excitation in the entrance channel will be considered and, further, only a single excited state of the target nucleus will be considered. In order to populate $J_f$ through a core-excitation mechanism, $J_A'$ must be strongly excited in the entrance channel and furthermore the two-nucleon parentage factor between $J_A'$ and $J_f$ must be favorable. In fact, with a strong excitation of $J_A'$ and if the nuclear structure of $J_f$ is more suited to overlap with $J_A'$ than with the target ground state ($J_A$), then the role played by $T_2$ in the overall cross section could be quite important.

The amplitude $T_2$ will be a product of two matrix elements, one representing the inelastic excitation and the other the pickup transition, and in the above simple model can be pictured as having the schematic form

$$T_2 \propto \langle J_f | {}^S L_J | J_A' \rangle \langle J_A' | Y_m^\ell(\hat{r}) | J_A \rangle \qquad (18)$$

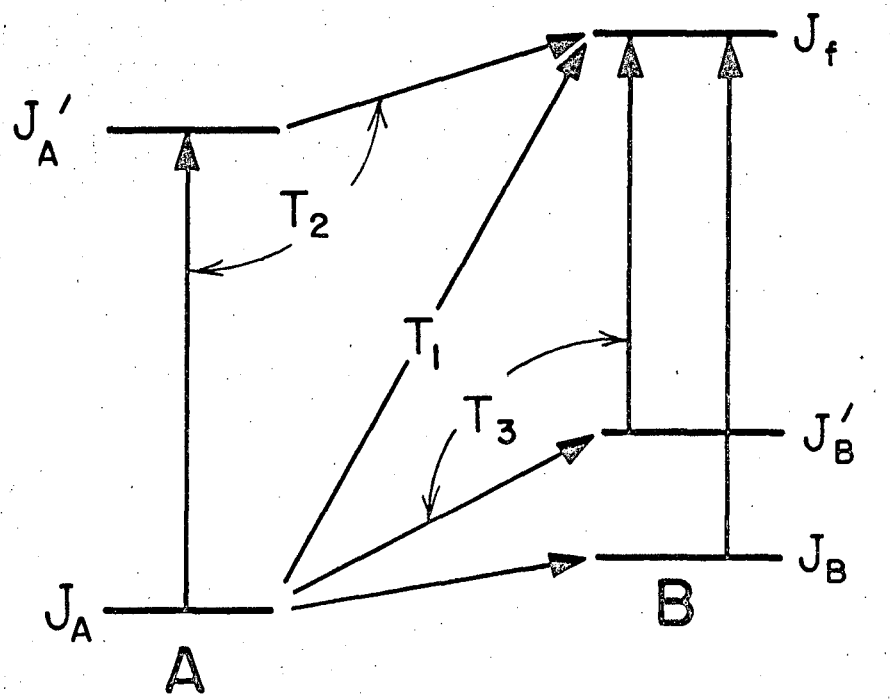


XBL 675-3148

Fig. 4. Various transitions contributing to the population of the final state, $J_f$.

Here $Y_m^\ell(\hat{r})$ characterizes the inelastic scattering step, which in the absence of a "spin-flip", would be a quadrupole excitation. The ${}^S L_J$ represents the angular momenta transferred in the pickup from $J_A'$. Angular momentum selection rules restrict the pickup of two nucleons in this second step to certain allowed values of L,S, and J, just as in a normal direct transition. The shape of the overall angular distribution and the strength of the transition will depend on these two amplitudes in such a way that it is probably not too meaningful to talk about a total angular momentum transfer as characterizing the overall reaction.

## IV. EXPERIMENTAL RESULTS AND NUCLEAR SPECTROSCOPY

In this section the (p,t) and (p,$^3$He) reactions on $^{15}$N and $^{13}$C targets will be studied and the experimental results compared with the predictions of the DWBA theory previously described (see also Ref. 3). The emphasis is strictly on the nuclear spectroscopy that can be learned. In the later discussion of theoretical cross sections, some of the assumptions made in the theory will be tested for consistency with experiment; in particular, a spin-dependence will be incorporated in the nucleon-nucleon interaction in an attempt to account for the observed ratios of mirror (p,t) and (p,$^3$He) cross sections. All of the DWBA treatment to be presented here, however, is calculated with a spin-independent interaction.

### A. $^{15}$N(p,t)$^{13}$N and $^{15}$N(p,$^3$He)$^{13}$C

#### 1. Experimental Results

These reactions were studied at an incident beam energy of 43.7 MeV. Figure 5 presents energy spectra of the $^{15}$N(p,t)$^{13}$N and $^{15}$N(p,$^3$He)$^{13}$C reactions taken at 15° in the laboratory. The excitations shown were obtained in this experiment and for the most part agree with previous values,[52] as shown in Tables I and II. Those levels marked with an asterisk in these tables were used to determine the energy scale and their associated errors (in keV) reflect the overall uncertainties involved in the analysis. In addition, the integrated cross sections are presented in these tables as well as spin and parity assignments, which are later fully explained in the text. An energy level diagram for $^{13}$C and $^{13}$N is presented in Fig. 6. The data in Fig. 5 show that the reaction is very selective, strongly populating only the negative parity states in the mass 13 nuclei. This is expected on the basis of a direct pickup of two nucleons from a $(1p)^{11}$ configuration, which is assumed for the ground state of $^{15}$N. However some positive parity levels are excited relatively strongly and their presence in these spectra will also be discussed. Figure 7 presents energy spectra for the $^{14}$N($^3$He,$\alpha$)$^{13}$N and $^{14}$N(d,$^3$He)$^{13}$C

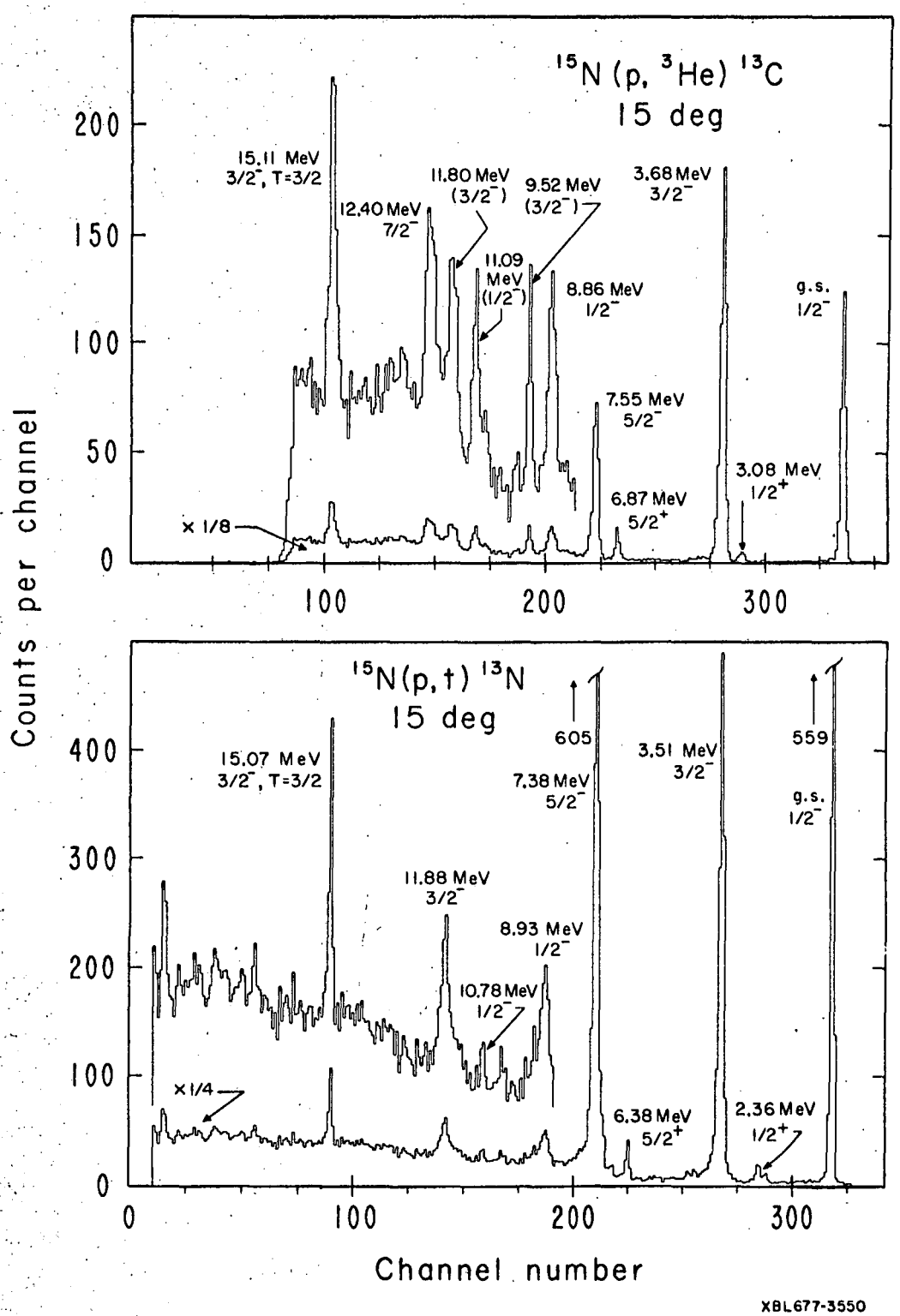


Fig. 5. Energy spectra of the $^{15}N(p,t)^{13}N$ and $^{15}N(p,^{3}He)^{13}C$ reactions.

Table I. Integrated cross sections of the $^{13}N$ levels observed in the $^{15}N(p,t)^{13}N$ reaction and comparison of these states with those previously reported.

| $^{15}N(p,t)^{13}N$ | | | Previously Reported[52] | |
|---|---|---|---|---|
| $J^{\pi}$ | Excitation (MeV) | $\sigma_T$ ($\mu$b) (10-90°, c.m.) | $J^{\pi}$ | Excitation (MeV) |
| $1/2^-$ | *[a]0.0 ± 25[b] | 941 ± 20 | $1/2^-$ | 0.0 |
| $1/2^+$ | 2.36 ± 30 | very weak | $1/2^+$ | 2.366 ± 2 |
| $3/2^-$ | *3.51 ± 30 | 652 ± 25 | $3/2^-$ | 3.510 ± 2 |
| $5/2^+$ | 6.38 ± 30 | 63 ± 7 | $5/2^+$ | 6.382 |
| $5/2^-$ | *7.38 ± 20 | 1271 ± 44 | $5/2^-$ | 7.385 ± 8 |
| $1/2^-$ | 8.93 ± 50 | 130 ± 16 | $1/2^-$ | 8.90 |
| | not observed | | $3/2^-$ | 9.48 |
| $1/2^-$ | 10.78 ± 60 | 17.6 ± 4 | not reported | |
| $3/2^-$ | 11.88 ± 40 | 93 ± 9 | $3/2^-$[c] | 11.85 |
| $3/2^-$ | *15.07 ± 20 | 115 ± 11 | $3/2^-$ | 15.068 ± 8 |
| [T = 3/2] | | | [T = 3/2] | |

[a]Levels marked with an asterisk were considered known in the energy analysis.

[b]Errors are given in keV.

[c]Spin and parity assigned in Refs. 53 and 54.

Table II. Integrated cross sections of the $^{13}C$ levels observed in the $^{15}N(p,^{3}He)^{13}C$ reaction and comparison of these states with those previously reported.

| $^{15}N(p,^{3}He)^{13}C$ | | | Previously Reported[52] | |
|---|---|---|---|---|
| $J^{\pi}$ | Excitation (MeV) | $\sigma_T(\mu b)$ (10-90°, c.m.) | $J^{\pi}$ | Excitation (MeV) |
| $1/2^-$ | *[a]0.0 ± 15[b] | 308 ± 18 | $1/2^-$ | 0.0 |
| $1/2^+$ | 3.08 ± 20 | very weak | $1/2^+$ | 3.086 ± 3 |
| $3/2^-$ | *3.68 ± 5 | 573 ± 20 | $3/2^-$ | 3.681 ± 3 |
| $5/2^+$ | *6.87 ± 12 | 42 ± 5 | $5/2^+$ | 6.866 ± 7 |
| $5/2^-$ | 7.55 ± 20 | 270 ± 18 | | 7.55 ± 15 |
| $1/2^-$ | 8.86 ± 60 | 61 ± 9 | $1/2^-$ | 8.86 ± 20 |
| $(3/2^-)$ | 9.52 ± 30 | 71 ± 12 | | 9.503 ± 15 |
| $(1/2^-)$ | 11.09 ± 50 | 52 ± 7 | | 11.078 ± 20 |
| $(3/2^-)$ | 11.80 ± 30 | 137 ± 14 | | 11.721 ± 30 |
| $7/2^-$ | 12.40 ± 50 | 100 ± 10 | $(1/2^-)$ | 12.45 |
| $3/2^-$ | *15.11 ± 20 | [c]88 ± 7 | $3/2^-$ | 15.113 ± 5 |
| [T = 3/2] | | | [T = 3/2] | |

[a]Levels marked with an asterisk were considered known in the energy analysis.

[b]Errors are given in keV.

[c]Integrated to 65°, c.m.

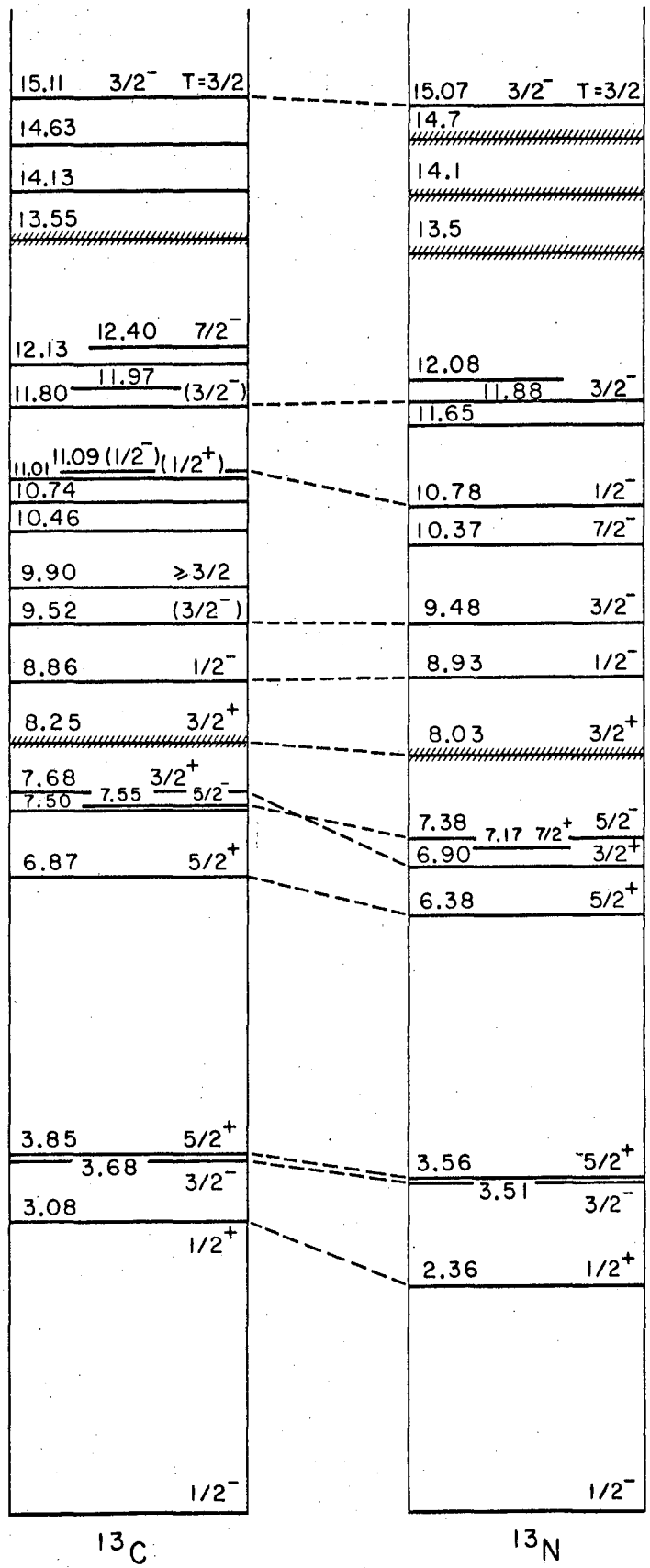


XBL677-3549

Fig. 6. Energy level diagrams of $^{13}C$ and $^{13}N$.

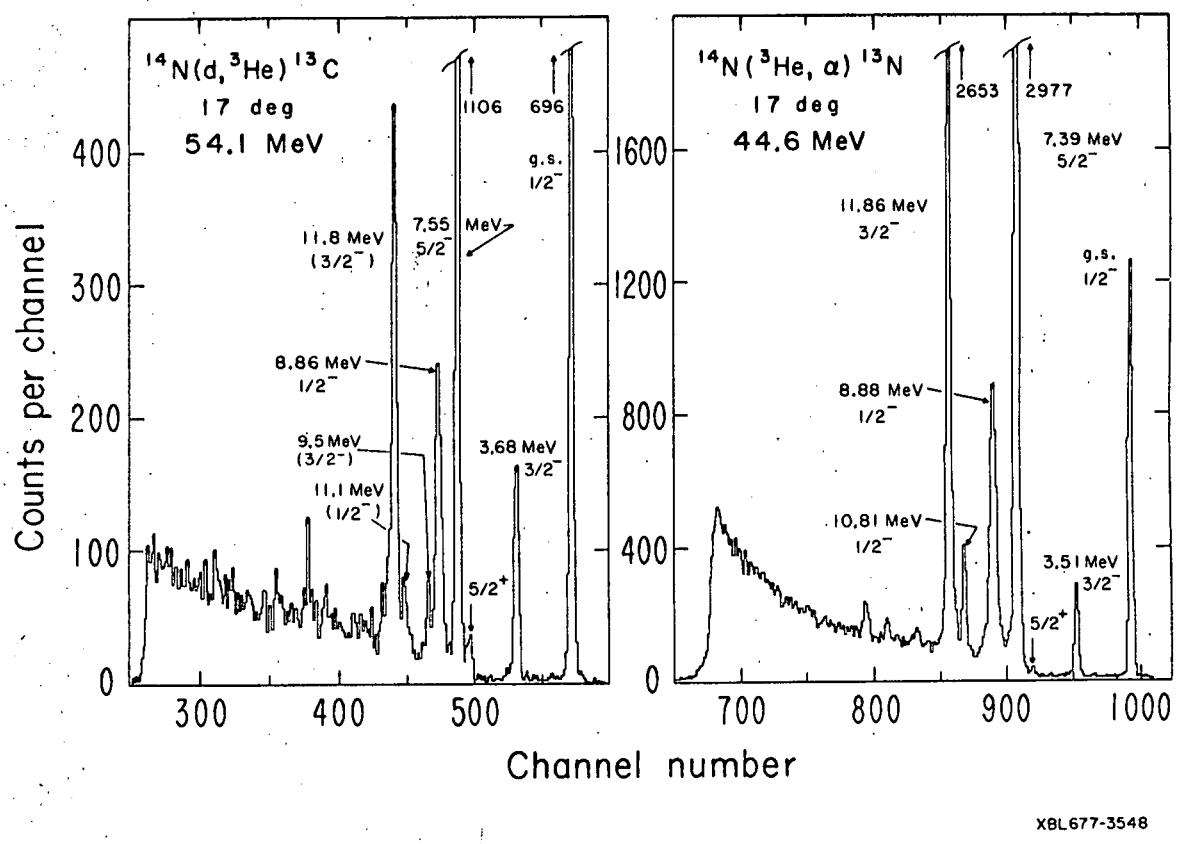


Fig. 7. Energy spectra of the $^{14}N(d,^3He)^{13}C$ and $^{14}N(^3He,\alpha)^{13}N$ reactions.

reactions[53] taken at a laboratory angle of 17°, which will be used to support some of the later discussion. Similar data on single-nucleon transfer reactions populating states in $^{13}N$ has been obtained in $^{14}N(p,d)^{13}N$ experiments.[54]

Angular distributions for levels excited in the $^{15}N(p,t)^{13}N$ and $^{15}N(p,^{3}He)^{13}C$ reactions are shown in Figs. 8-13; the statistical errors are contained within the points unless explicitly indicated. The total integrated cross sections for these reactions are presented in Tables I and II. The absolute errors on the large transitions are expected to be $\leq$ 10 percent. Representative relative errors for all states are given in these tables. Of later interest will be Figs. 14 and 15 which present (p,t) L=0 and L=2 angular distributions obtained on a variety of light nuclei. These are remarkably similar in shape, considering the range of particle energy involved. Hintz and co-workers[12] have observed similar effects with (p,t) reactions on heavier nuclei.

2. Optical Model Parameters

Since appropriate elastic scattering data were not available, in either the entrance or the exit channel, the optical model parameters used in this study were obtained from an examination of the "best fit" parameters available in the literature. There are only a few reports of higher energy (40-50 MeV) optical model fits for proton scattering on light nuclei[55-57] and most of these[55,57] have employed a spin-orbit term in the optical model. Although the DWBA code under discussion does not contain a spin-orbit potential, indications are that the shape of the angular distribution in a nuclear reaction is quite insensitive[58,59] to the inclusion of a spin-orbit potential and consequently some of the parameters in Refs. 55 and 57 were tried directly. However, whereas a real well depth is employed which is consistent with the value given in these references, the absorptive potential had to be increased considerably in order to fit the data. The proton real and imaginary potentials that proved to give the best overall fit to the data were interpolated from a graph of incident energy vs. optical model potentials given by Bjorklund.[60] The choice of an exit channel potential -- in the absence of elastic scattering data -- is perhaps subject to the most

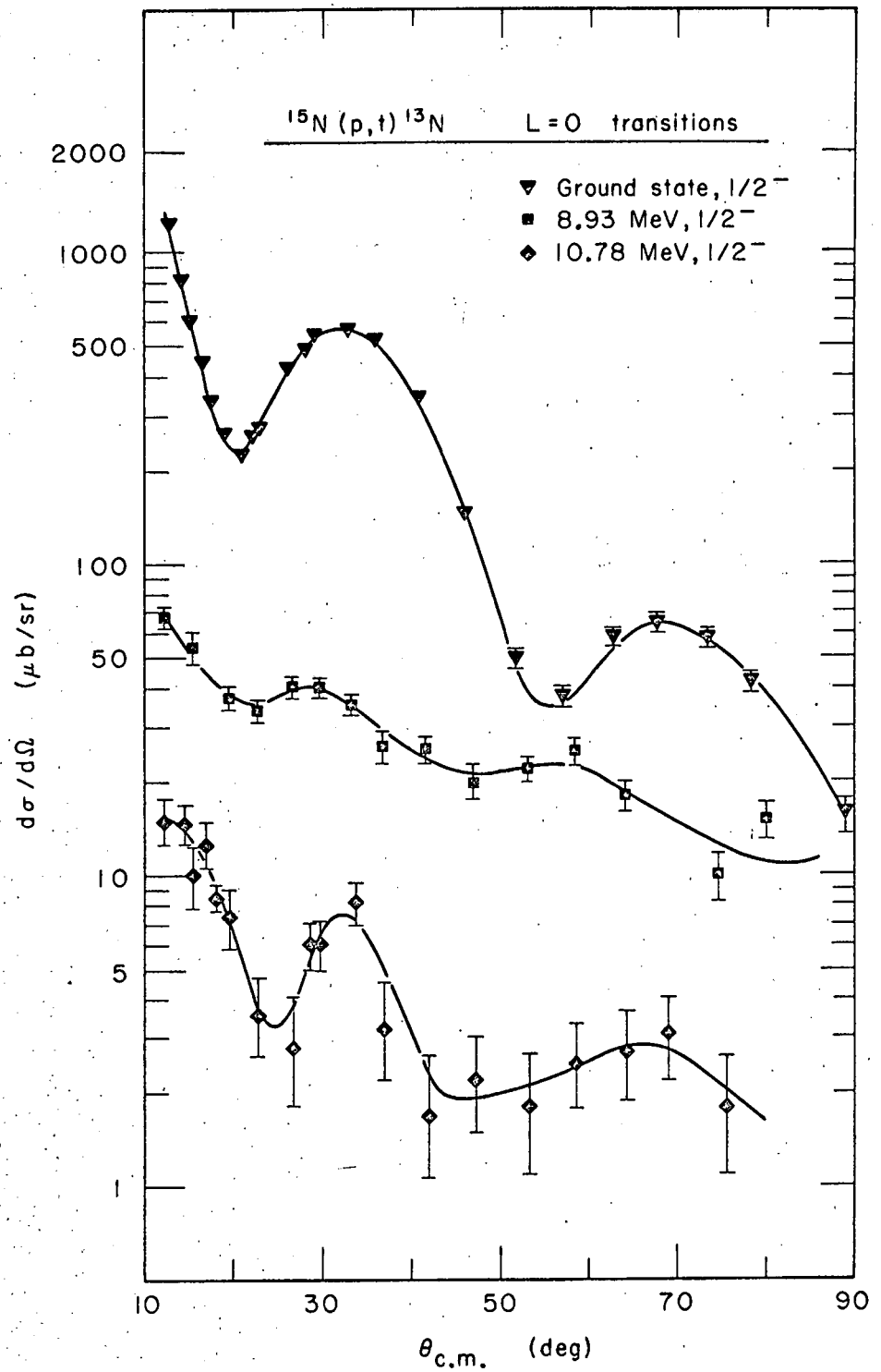


XBL676-3271-A

Fig. 8. Differential cross sections of the (p,t) L=0 transitions on $^{15}N$. The curves have no theoretical significance.

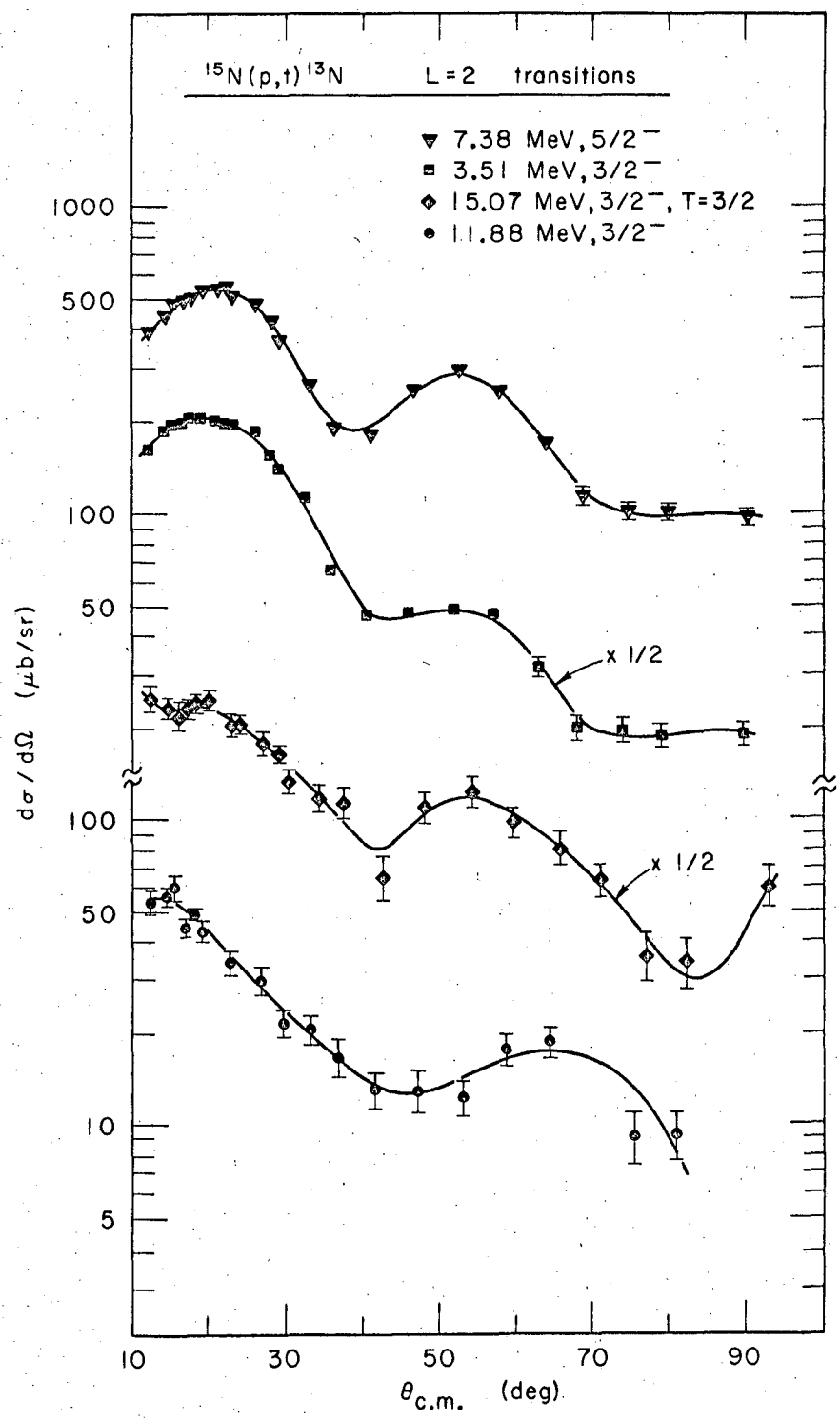


XBL676-3269-A

Fig. 9. Differential cross sections of the (p,t) L=2 transitions on $^{15}N$. The curves have no theoretical significance.

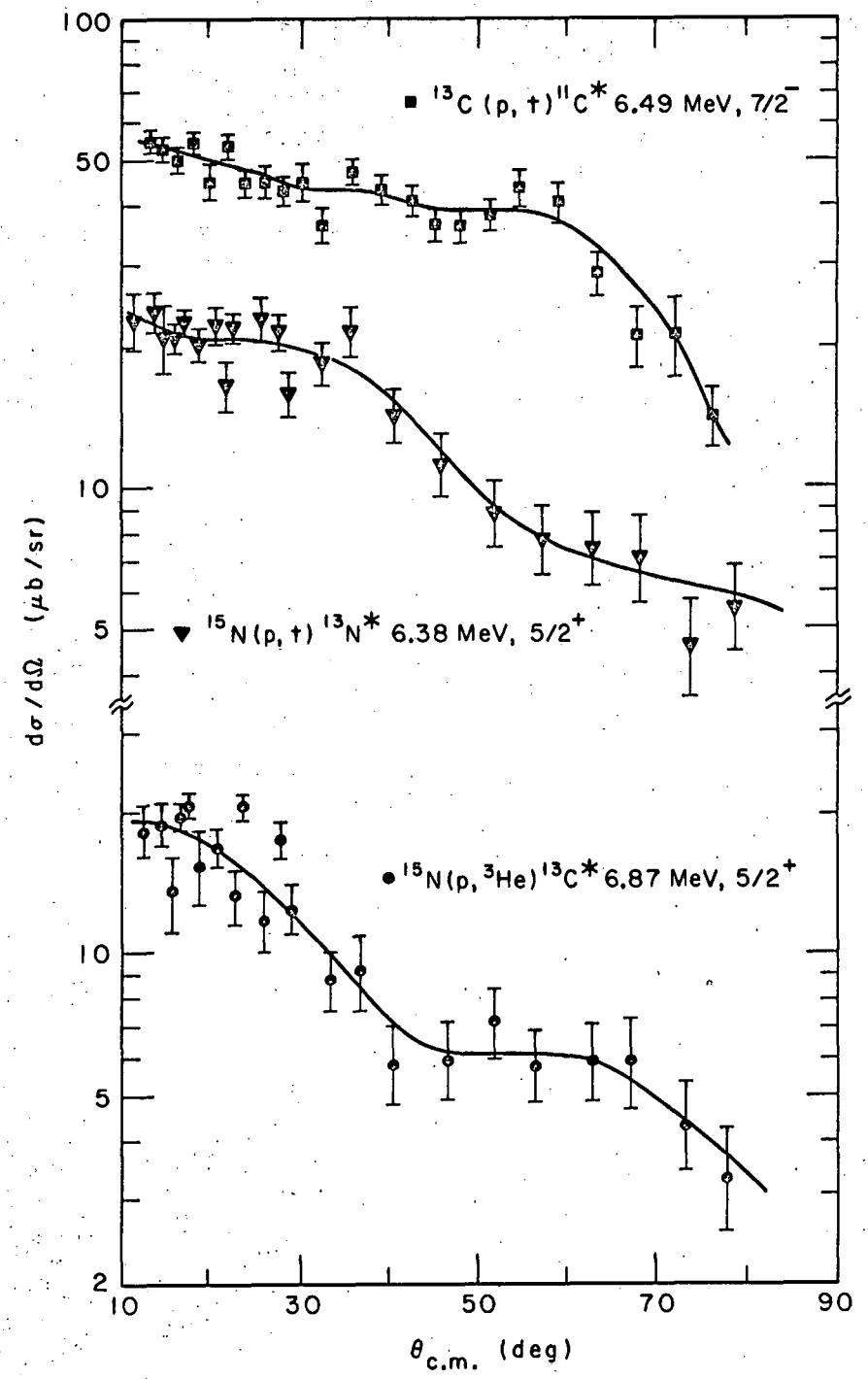


XBL678-3730

Fig. 10. Differential cross sections of some "forbidden" (p,t) and (p,$^3$He) transitions. The curves have no theoretical significance.

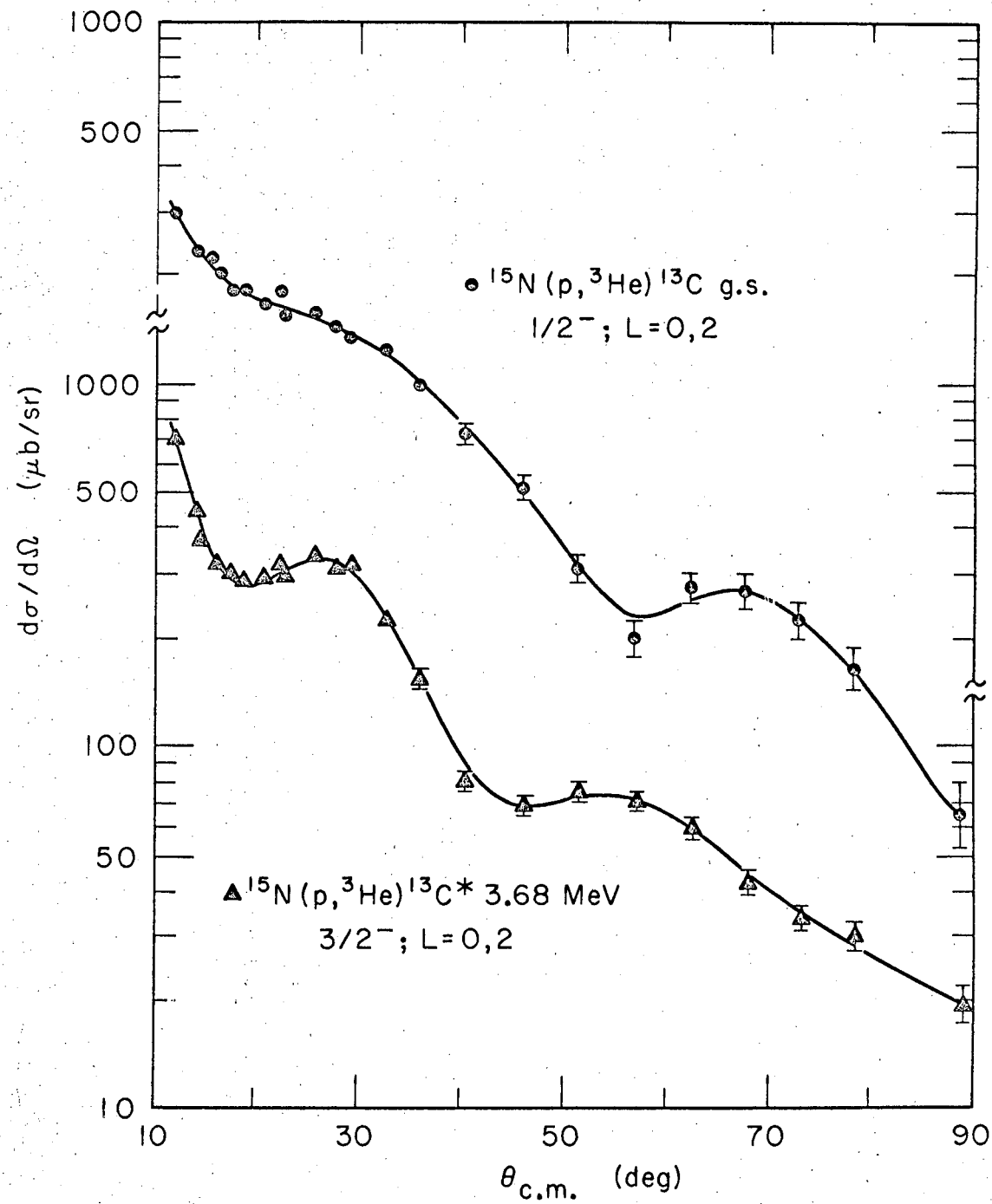


XBL676-3268-A

Fig. 11. Differential cross section of the $^{15}N(p,^{3}He)^{13}C$ g.s. and 3.68 MeV transitions. The curves have no theoretical significance.

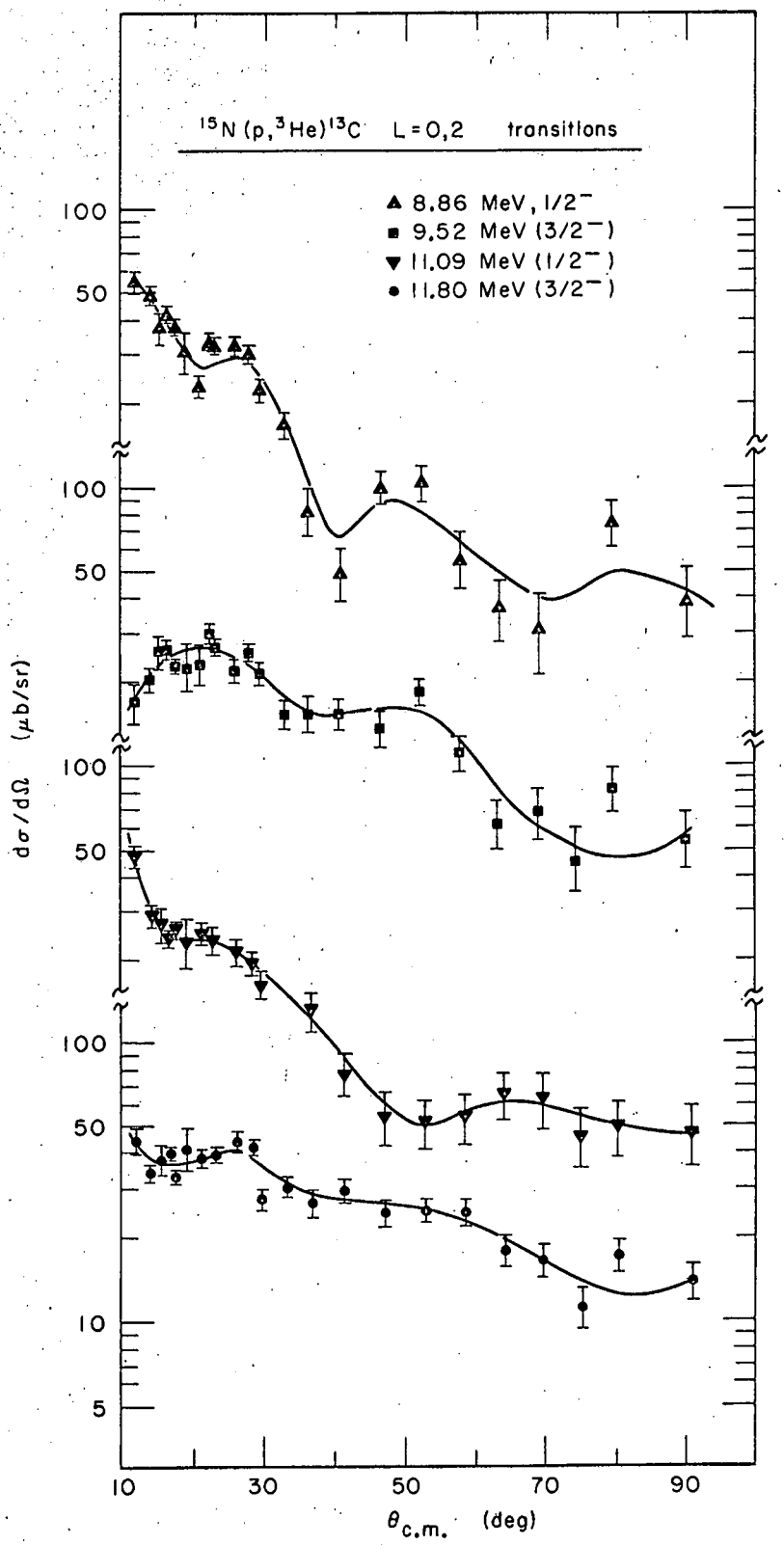


XBL676-3266-A

Fig. 12. Differential cross sections of the $(p,^3He)$ L=0,2 transitions on $^{15}N$. The curves have no theoretical significance.

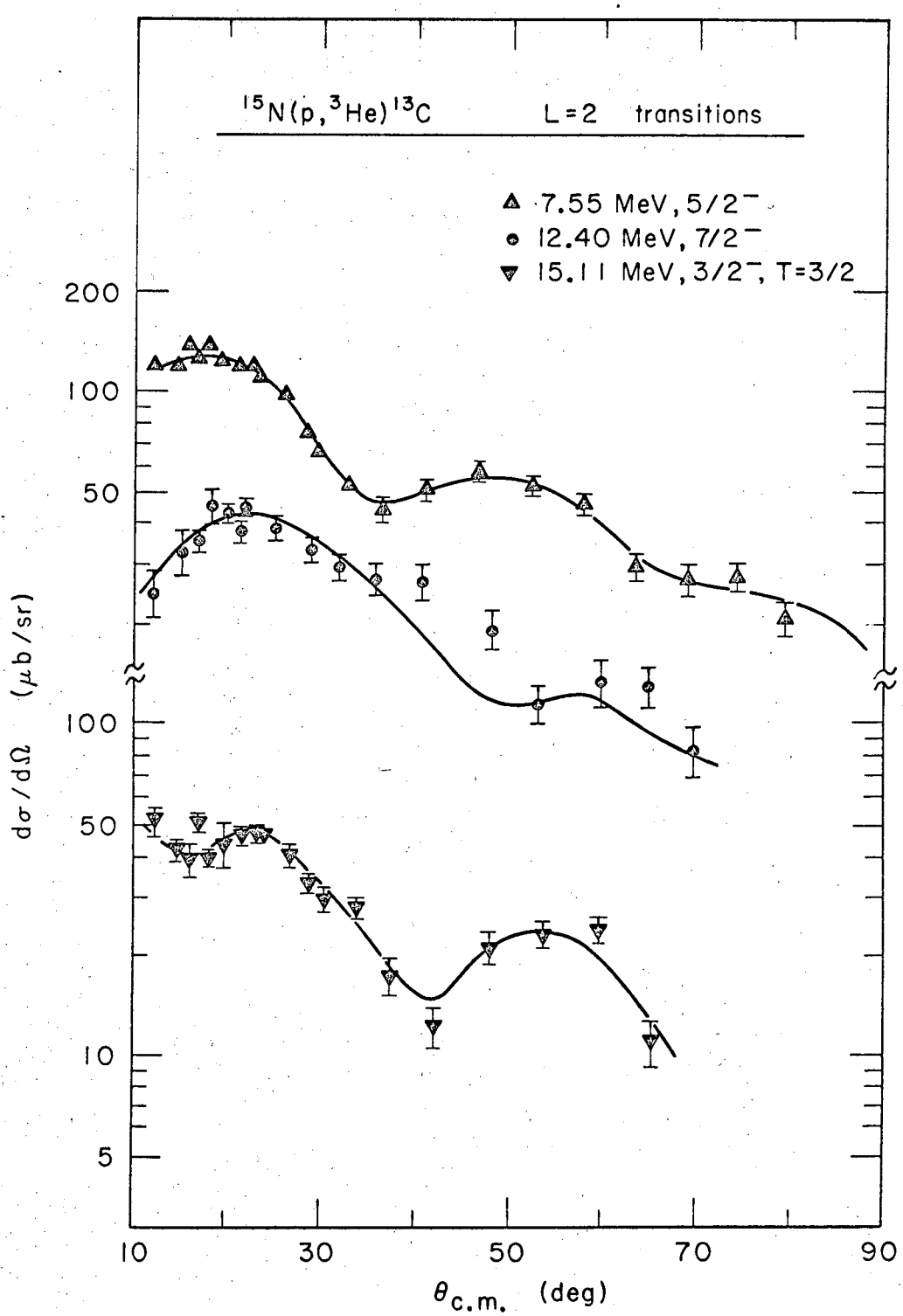


XBL676-3270-A

Fig. 13. Differential cross sections of the $(p,^3He)$ L=2 transitions on $^{15}N$. The curves have no theoretical significance.

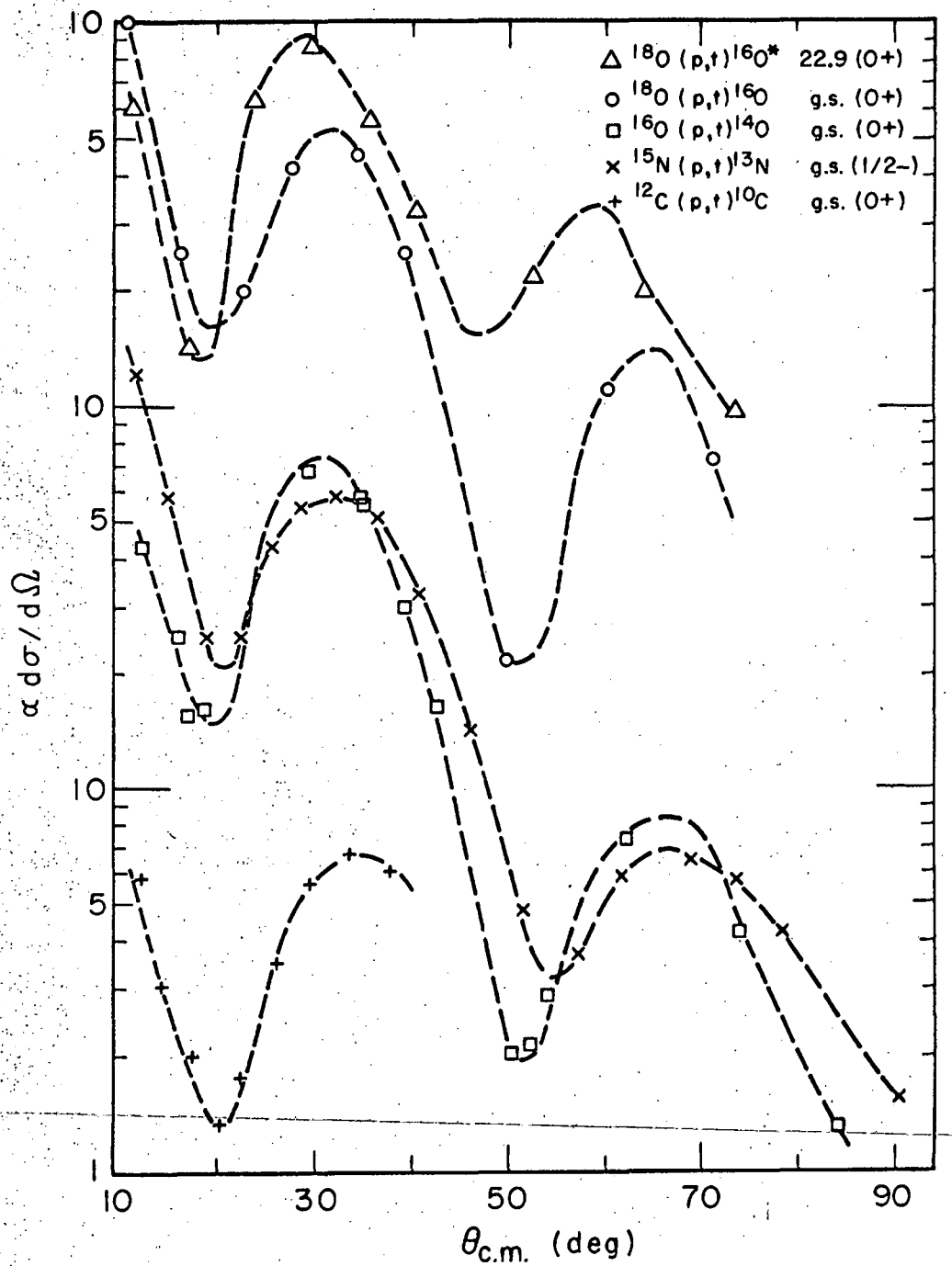


MUB-11572

Fig. 14. Standard (p,t) L=0 angular distributions taken on a variety of light nuclei.

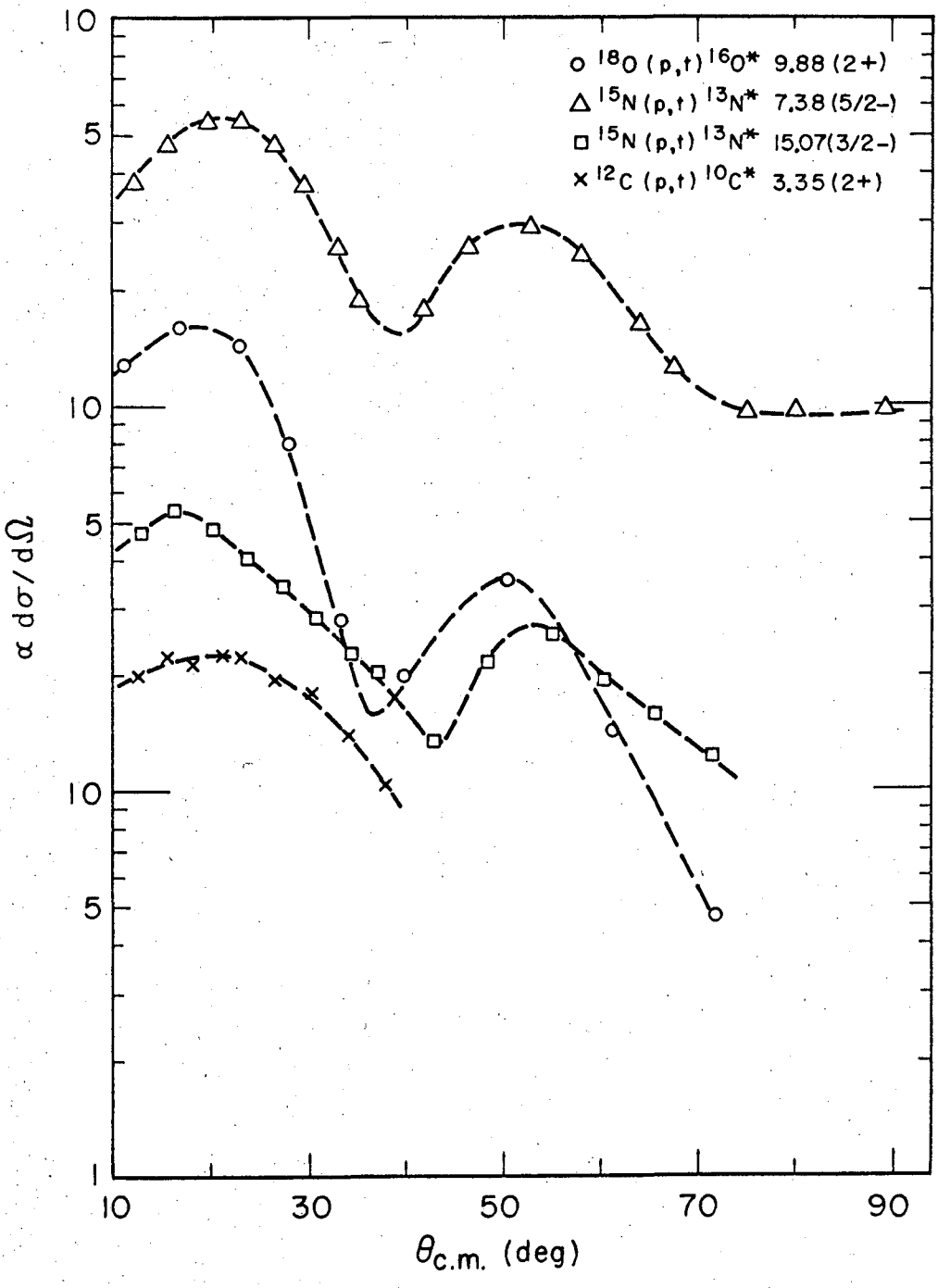


MUB-11571

Fig. 15. Standard (p,t) L=2 angular distributions taken on a variety of light nuclei.

uncertainty. In accord with the hypothesis that in a complex particle one should consider the interaction of each nucleon with the scattering center,[61,62] the triton ($^3$He) optical model parameters used correspond to a sum of single-nucleon potentials. These were obtained from searching the literature for the appropriate low energy (about 10 MeV) nucleon scattering data on light nuclei.[63] Parameters obtained in this way are similar to those found from helium-3 optical model fits[64] in the energy region of this experiment (about 25 MeV), although this reference employs larger radii for the imaginary well. (There are no optical model parameters available for tritons at these energies). The "summed" potential which gave the best overall fit to the $^{15}$N(p,t)$^{13}$N data -- a choice of "best potential" was made from fitting the (p,t) data, since only a single L transfer was allowed -- is shown in Table III (potential X) along with the proton potential[60] mentioned above (potential A). The exit channel parameters were taken to be the same for both tritons and helium-3 and are labelled just by the triton channel in Table III. Earlier work in fitting helium-3 elastic scattering data on light nuclei[65] employed a "shallow" potential for the real well depth, and an average of the parameters given in Ref. 65 is shown in Table III (potential Y). In addition, Table III contains a potential found from 30 MeV helium-3 scattering on $^{12}$C [32] (potential Z) and the proton potential from Ref. 56 (potential B), which gave a fit to 40 MeV proton scattering on $^{12}$C. The combination that produced the best overall results -- over 15 MeV of excitation -- was AX. Although the proton potential was relatively insensitive to the choice of volume or surface (derivative Saxon-Wood) absorption, the triton potential in the AX combination gave better overall fits to the data with surface absorption.

DWBA fits to the data are compared in Figs. 16 and 17 for the $^{15}$N(p,t)$^{13}$N ground state (L=0) and $^{15}$N(p,t)$^{13*}$N 7.38 MeV (L=2) transitions, respectively, utilizing the potentials AX, AY, and AZ of Table III. The fits have all been arbitrarily normalized to the data, at 32° for the ground state transition (Fig. 16) and at 20° for the 7.38 MeV transition (Fig. 17). These are the two strongest states in the spectrum, so that they should be good tests for the correctness of the optical model wave functions. The ground state transition (L=0) is best fit with potential

Table III. Optical model potentials

$$-U(r) = Vf(r) + iWf(r) + 4aiW_D f'(r) - V_c(r)$$

| Channel | V (MeV) | W (MeV) | $W_D$ (MeV) | $a_V$ (f) | $a_W$ (f) | $a_{W_D}$ (f) | $r_V$ (f) | $r_{W,W_D}$ (f) | $r_c$ (f) |
|---|---|---|---|---|---|---|---|---|---|
| $^{15}$N+p (A) | 34.0 | | 22.0 | 0.65 | | 0.50 | 1.25 | 1.25 | 1.30 |
| $^{13}$N+t (X) | 153.0 | | 16.0 | 0.65 | | 0.54 | 1.25 | 1.25 | 1.30 |
| $^{13}$N+t (Y) | 63.4 | 62.8 | | 0.58 | 0.58 | | 1.61 | 1.61 | 1.30 |
| $^{13}$N+t (Z) | 220.0 | 23.8 | | 0.53 | 0.99 | | 1.22 | 1.80 | 1.30 |
| $^{15}$N+p (B) | 33.0 | 5.9 | | 0.65 | 0.65 | | 1.31 | 1.31 | 1.30 |
| $^{31}$P+p | 41.7 | 11.1 | | 0.70 | 0.70 | | 1.20 | 1.20 | 1.30 |
| $^{29}$P+t | 153.0 | | 16.0 | 0.65 | | 0.54 | 1.25 | 1.50 | 1.30 |

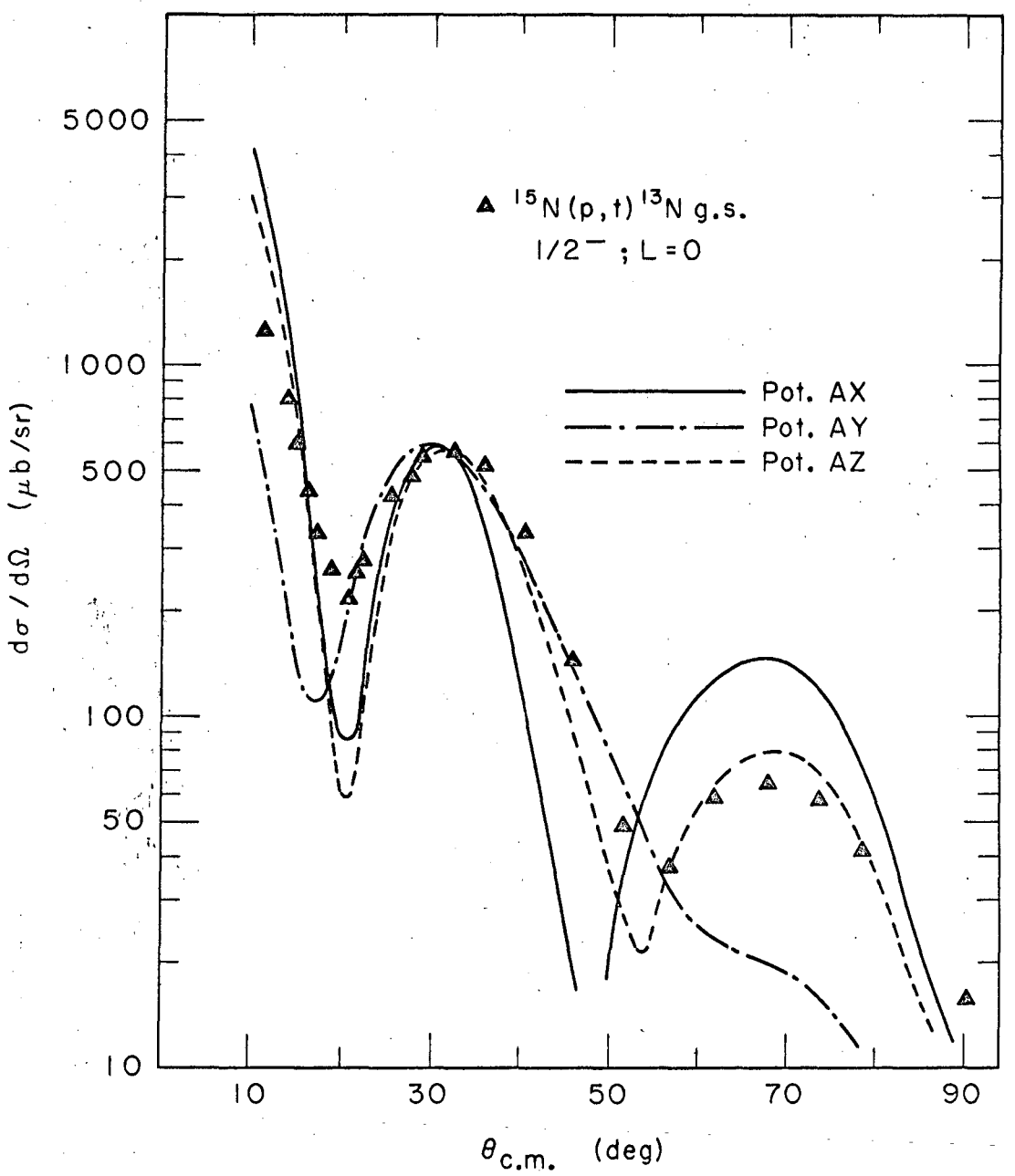


XBL676-3273

Fig. 16. Normalized DWBA fits to the $^{15}N(p,t)^{13}N$ g.s. (L=0) transition, utilizing the AX, AY and AZ optical model potentials of Table III.

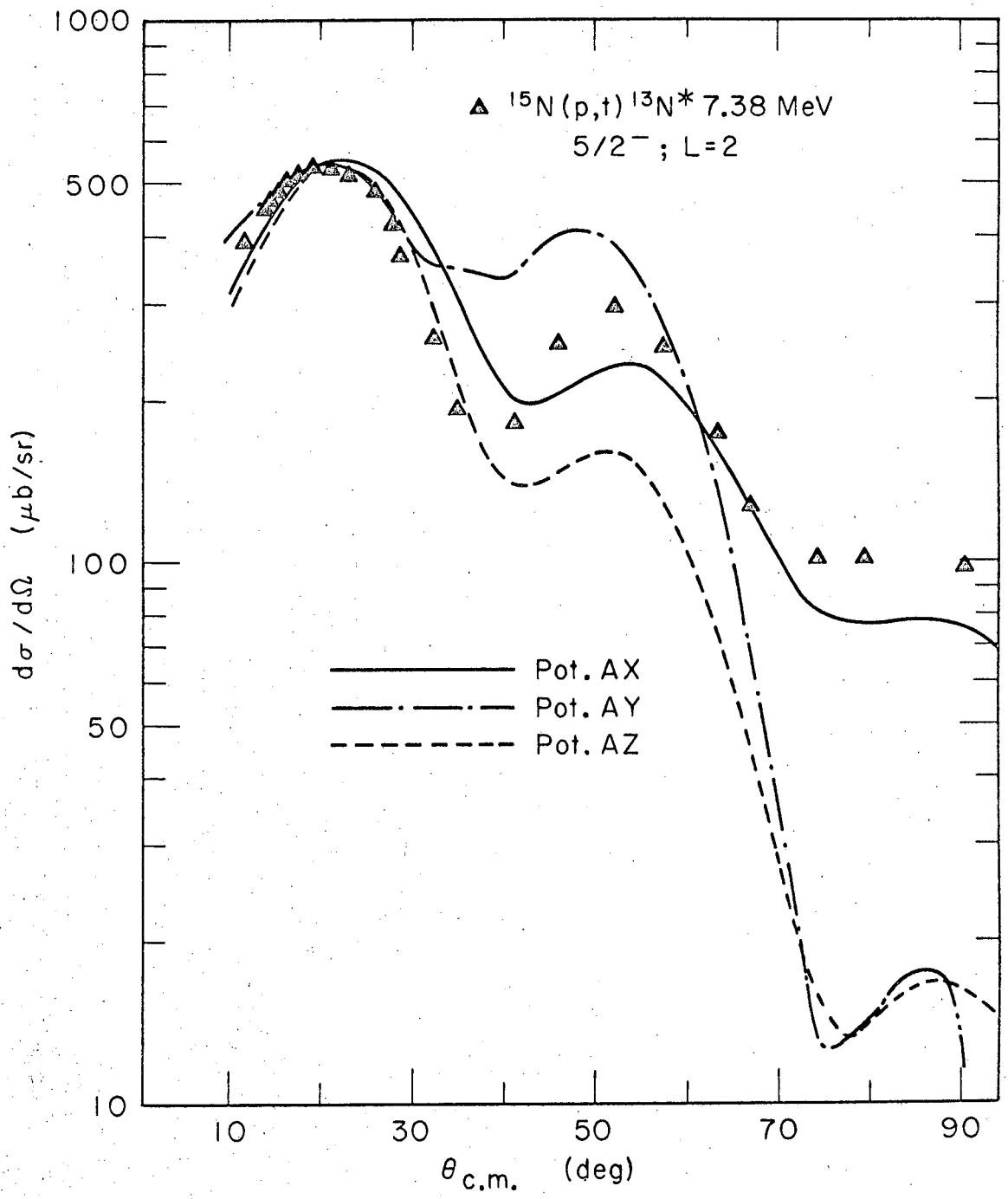


XBL676-3277-A

Fig. 17. Normalized DWBA fits to the $^{15}N(p,t)^{13}N^*$ 7.38 MeV (L=2) transition, utilizing the AX, AY and AZ optical model potentials of Table III.

AZ while the 7.38 MeV (L=2) transition is better fit with potential AX. For both transitions, the "shallow" potential AY gives relatively poor fits to the data. The original choice for the proton parameters was B and the potentials BX, BY and BZ are compared in Figs. 18 and 19 for these these same transitions. Potential B is taken directly from Ref. 56 (without spin-orbit coupling) for proton scattering on $^{12}C$ and corresponds quite closely to recent proton potentials which include spin-orbit coupling.[55,57] As such, it might be expected to give a better fit than the A potentials. Of these three, potential BZ gives the best fit to the ground state (L=0) transition and none are able to fit the 7.38 MeV (L=2) transition. The A proton potential, with a much deeper imaginary well than the B potential, gave consistently better fits to all the (p,t) transitions. Of the A potentials, AY gives the poorest fits; AX gives a better fit to the 7.38 MeV state than does AZ and moreover AX fits all the other transitions in the $^{15}N(p,t)^{13}N$ reaction better than AZ does. Attempts to improve the DWBA fits to excited states by introducing an energy dependence in the triton potential, thru a reduction of the real well depth as a linear function of excitation,[66] were not successful; the DWBA results continued to look better with the AX potential fixed for all excited states. All of the (p,t) and (p,$^3$He) fits discussed in the following pages have been calculated with the potential AX.

## 3. Intermediate Coupling Theory and Nuclear Structure Calculations

Considerable theoretical interest has been concentrated on nuclei in the 1p shell within the framework of the intermediate coupling shell model. The early calculations of Inglis[67] and Lane[68] were followed by those of Kurath,[7] Boyarkina[8] and Barker.[9] In all of these calculations the nucleon-nucleon interaction was taken to be purely central and the ratio "a/k", where "a" is the strength of the spin-orbit potential and "k" is the value of the two-body exchange integral, was left as a parameter to be determined by a comparison with experiment. More recently, Halbert et al.[69] reported a calculation similar to those above but using the Hamada-Johnston potential[39] for the nucleon-nucleon interaction, rather than a simple central interaction. An alternative approach is the "effective interaction" treatment of the problem, where the nucleon-nucleon

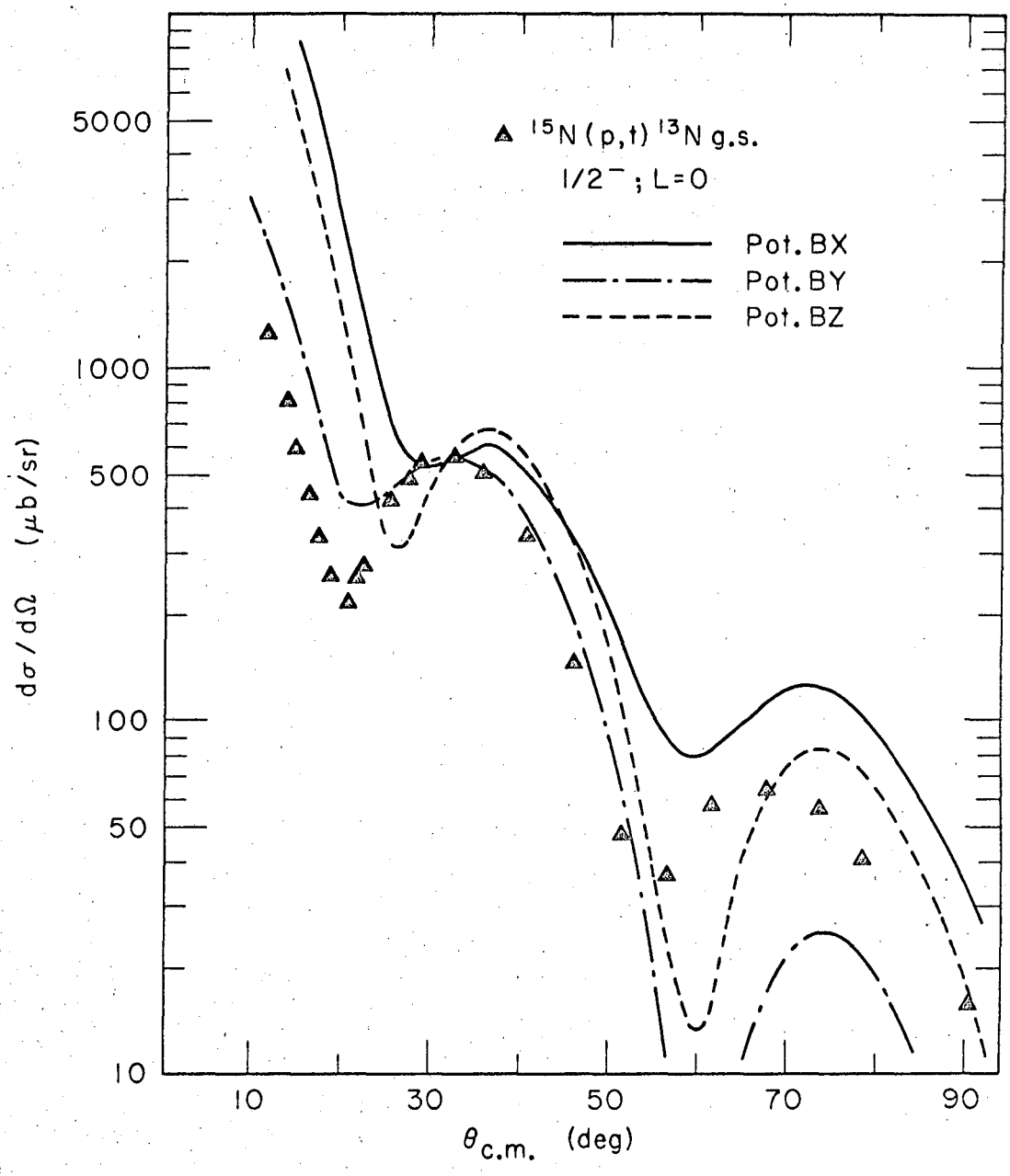


XBL676-3276

Fig. 18. Normalized DWBA fits to the $^{15}N(p,t)^{13}N$ g.s. (L=0) transition, utilizing the BX, BY and BZ optical model potentials of Table III.

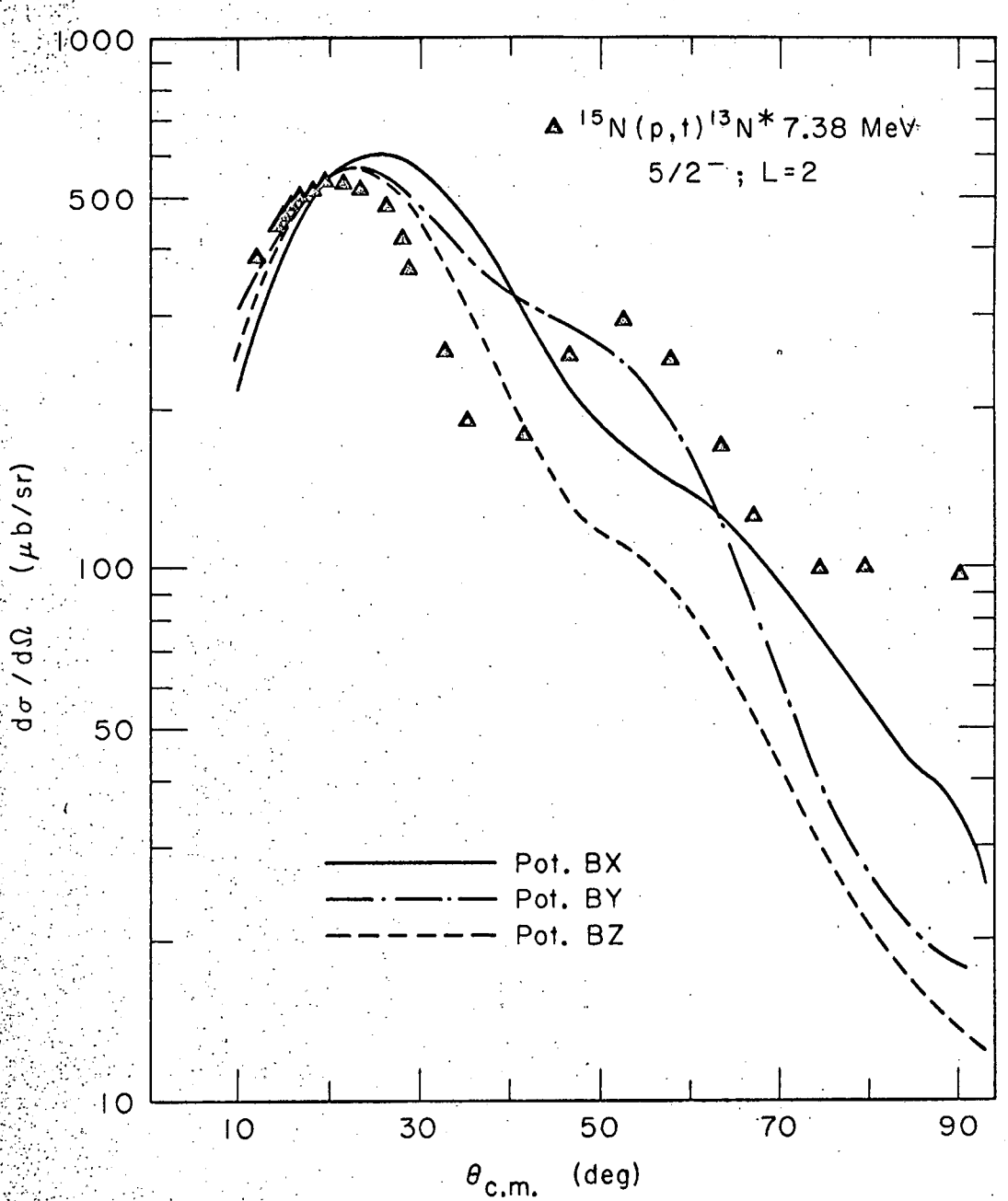


XBL676-3275

Fig. 19. Normalized DWBA fits to the $^{15}N(p,t)^{13}N^*$ 7.38 MeV (L=2) transition, utilizing the BX, BY and BZ optical model potentials of Table III.

potential is not explicitly defined and the matrix elements of the two-body interaction are left as parameters to be determined by experiment. Calculations of this kind have recently been reported by Cohen and Kurath[70] and Barker.[71] In Table IV, which will be referred to in the following discussion, are shown the predictions of these calculations (Refs. 7-9, 69, 70) for the levels in mass 13, along with the experimental assignments.

As mentioned earlier, the two-nucleon transfer theory[3] requires a separate calculation of nuclear structure factors ($G_{NLSJT}$) which are then used in the DWBA calculation. These factors have been calculated using coefficients of fractional parentage derived from Cohen and Kurath's complete intermediate coupling wave functions[70] the major amplitudes of which, for the states of interest, are presented in Table V. For comparative purposes, these structure factors have also been calculated for most of the states assuming pure jj wave functions. Table VI shows the major nuclear structure factors (multiplied by $C_{ST}$) for $^{15}N(p,t)^{13}N$ and $^{15}N(p,^{3}He)^{13}C$ transitions to mirror final states for both of these cases. (Those calculated from the wave functions in Table V are denoted by CK). Harmonic oscillator wave functions are assumed for the single particle states and the oscillator parameter $\nu$ is taken to be 0.32 $F^{-2}$, which is the same value that True employed for the 1p levels in his shell model calculation of $^{14}N$.[72]

## 4. Spectroscopy of Individual Transitions

In the following discussion of individual levels, the normalized DWBA fits for the $^{15}N(p,t)^{13}N$ and $^{15}N(p,^{3}He)^{13}C$ transitions were calculated only from the CK nuclear structure factors of Table VI, which were derived from the intermediate coupling wave functions of Ref. 70. Using pure jj wave functions for the final state -- which would only affect the $(p,^{3}He)$ angular distributions -- gave normalized DWBA fits which were, in most cases, essentially the same as those obtained using intermediate coupling wave functions. As one would expect, however, the predictions of relative cross sections of the (p,t)[73] transitions are in much better agreement with experiment using the intermediate coupling wave functions, and this will be noted later.

Table IV. Intermediate coupling predictions compared with experimental assignments for the mass 13 levels.

| $J^{\pi}$ | $^{13}N$ (MeV) | $^{13}C$ (MeV) | Kurath[7] a/k=5.5 | Boyarkina[8] a/k=4.2 | Barker[9] a/k=3.5 | Halbert[69] et al. | Cohen and[70] Kurath |
|---|---|---|---|---|---|---|---|
| $1/2^-$ | 0.0 | 0.0 | 0.0 | 0.0 | 0.0 | 0.0 | 0.0 |
| $3/2^-$ | 3.51 | 3.68 | 3.7 | 3.7 | 3.93 | 3.5 | 3.7 |
| $5/2^-$ | 7.38 | 7.55 | 5.3 | 6.1 | 7.11 | 7.0 | 7.4 |
| $1/2^-$ | 8.93 | 8.86 | 10.7 | 10.4 | 9.3 | 9.0 | 9.0 |
| $1/2^-$ | 10.78 | 11.09 | 12.5 | 12.4 | 11.3 | - | 13.8 |
| $3/2^-$ | 11.88 | 11.80 | 11.3 | 11.6 | 10.2 | 10.2 | 10.4 |
| $7/2^-$ | - | 12.40 | 12.0 | 12.3 | 13.5 | - | 11.1 |
| $3/2^-$ | 15.07 | 15.11 | 14.5 | 14.5 | 13.2 | 15.0 | 14.8 |
| [T=3/2] | | | | | | | |
| $3/2^-$ | | | | 15.2 | | | 14.0 |
| $5/2^-$ | | | | 16.4 | | | 13.2 |
| $1/2^-$ | | | | 22.2 | | | 17.4 |

Table V. Dominant configurations of the intermediate coupling wave functions of Cohen and Kurath[a] for the states in mass 13.

| $J^{\pi}$ | $^{13}N$ (MeV) | $^{13}C$ (MeV) | Theory (MeV) | Dominant Configurations |
|---|---|---|---|---|
| $1/2^-$ | 0.0 | 0.0 | 0.0 | $.187(p_{3/2})^6_1(p_{1/2})^3_{1/2}-.501(p_{3/2})^6_0(p_{1/2})^3_{1/2}-.837(p_{3/2})^8_0p_{1/2}$ |
| $3/2^-$ | 3.51 | 3.68 | 3.7 | $.376(p_{3/2})^7_{3/2}(p_{1/2})^2_1+.450(p_{3/2})^5_{3/2}(p_{1/2})^4_0-.733(p_{3/2})^7_{3/2}(p_{1/2})^2_0$ |
| $5/2^-$ | 7.38 | 7.55 | 7.4 | $.177(p_{3/2})^6_3(p_{1/2})^3_{1/2}+.313(p_{3/2})^6_2(p_{1/2})^3_{1/2}-.929(p_{3/2})^7_{3/2}(p_{1/2})^2_1$ |
| $1/2^-$ | 8.93 | 8.86 | 9.0 | $-.151(p_{3/2})^6_0(p_{1/2})^3_{1/2}+.328(p_{3/2})^6_1(p_{1/2})^3_{1/2}-.921(p_{3/2})^7_{3/2}(p_{1/2})^2_1$ |
| $1/2^-$ | 10.78 | 11.09 | 13.8 | $+.411(p_{3/2})^5_{1/2}(p_{1/2})^4_0-.509(p_{3/2})^8_0p_{1/2}+.647(p_{3/2})^6_0(p_{1/2})^3_{1/2}$ |
| $3/2^-$ | 11.88 | 11.80 | 10.4 | $-.200(p_{3/2})^6_2(p_{1/2})^3_{1/2}+.287(p_{3/2})^7_{3/2}(p_{1/2})^2_0+.917(p_{3/2})^7_{3/2}(p_{1/2})^2_1$ |
| $7/2^-$ | | 12.40 | 11.1 | $-.329(p_{3/2})^5_{7/2}(p_{1/2})^4_0+.945(p_{3/2})^6_3(p_{1/2})^3_{1/2}$ |
| $3/2^-$ [T=3/2⁻] | 15.07 | 15.11 | 14.8 | $.159(p_{3/2})^6_2(p_{1/2})^3_{1/2}-.237(p_{3/2})^5_{3/2}(p_{1/2})^4_0+.958(p_{3/2})^7_{3/2}(p_{1/2})^2_0$ |

[a]See Ref. 70. I am indebted to Dr. Kurath for providing me with these wave functions.

Table VI. Major nuclear structure factors ($C_{ST}G_{NLSJT}$) for the states in mass 13.

| $J^{\pi}$ | $^{13}N$ (MeV) | $^{13}C$ (MeV) | $^{15}N(p,t)^{13}N$ | | | $^{15}N(p,{}^{3}He)^{13}C$ | | |
|---|---|---|---|---|---|---|---|---|
| | | | $G_{NLSJT}$ | pure (jj) | mixed (CK) | $G_{NLSJT}$ | pure (jj) | mixed (CK) |
| $1/2^-$ | 0 | 0 | 20001 | .408 | .579 | 20110 | .117 | .151 |
| | | | | | | 20001 | .201 | .284 |
| | | | | | | 12110 | .523 | .462 |
| $3/2^-$ | 3.51 | 3.68 | 12021 | .373 | .565 | 20110 | .403 | .522 |
| | | | | | | 12110 | .224 | .177 |
| | | | | | | 12021 | .184 | .278 |
| | | | | | | 12120 | .226 | .380 |
| $5/2^-$ | 7.38 | 7.55 | 12021 | 1.00 | 1.11 | 12120 | .601 | .562 |
| | | | | | | 12021 | .494 | .546 |
| | | | | | | 12130 | - | .151 |
| $1/2^-$ | 8.93 | 8.86 | 20001 | - | .0103 | 20110 | .269 | .328 |
| | | | | | | 20001 | - | .00506 |
| | | | | | | 12110 | .150 | .172 |
| $1/2^-$ | 10.78 | 11.09 | 20001 | - | .0972 | 20110 | - | .0530 |
| | | | | | | 20001 | - | .0488 |
| | | | | | | 12110 | - | .185 |
| $3/2^-$ | 11.88 | 11.80 | 12021 | .500 | .256 | 20110 | .300 | .153 |
| | | | | | | 12110 | .168 | .0921 |
| | | | | | | 12021 | .247 | .127 |
| | | | | | | 12120 | .302 | .471 |
| $7/2^-$ | - | 12.40 | | | | 12130 | .980 | .933 |
| $3/2^-$ [ T=3/2 ] | 15.07 | 15.11 | 12021 | .527 | .560 | 12021 | .520 | .552 |

a. 0 MeV, [$^{13}$N and $^{13}$C], $1/2^-$. Two nucleon transfer selection rules restrict this transition to a pure L=0 transfer for the (p,t) reaction but allow both L=0 and L=2 for the (p,$^3$He) reaction. The DWBA fits are shown in Fig. 20 and are arbitrarily normalized -- the (p,t) independently of the (p,$^3$He). The theoretical (p,t) cross section is overpredicted at back angles but otherwise gives a reasonably good account of the data. The (p,$^3$He) fit, which gives a good representation of the envelope of the angular distribution, does not completely account for the forward angle behavior of the data. A better fit can be obtained through the inclusion of a strongly spin-dependent force, which enhances the L=0 component of the transition, as is later discussed.

b. 3.51 MeV [$^{13}$N] and 3.68 MeV [$^{13}$C], $3/2^-$. Two-nucleon transfer selection rules now restrict the (p,t) transition to be pure L=2 while the (p,$^3$He) is again a mixture of L=0 and L=2. The DWBA fits to these data,[74] normalized separately and independently of the ground state transition, are shown in Fig. 21. The (p,t) transition is well predicted by the theory; the (p,$^3$He) fit does not completely reproduce the back angle structure, although it gives a good account of the forward angle behavior.

c. 7.38 MeV [$^{13}$N] and 7.55 MeV [$^{13}$C], $5/2^-$. Early $^{12}$C plus proton scattering results by Shute et al.[75] indicated that the parity of this level (in $^{13}$N) should be positive ($5/2^+$, $7/2^+$), in agreement with the results of other workers.[76] Barker,[77] from analysis of $^{12}$C(p,p'$\gamma$) results, agreed that the spin of the level was either 5/2 or 7/2, but of negative parity. Based on his intermediate coupling results,[9] reproduced in Table IV, Barker assigned this level to be $5/2^-$. Similar calculations by both Kurath[7] and Boyarkina[8] predict a $5/2^-$ level at about 6 MeV of excitation (Table IV); further, Gallman et al.[78] show that a value of about 3.5 for a/k, in good agreement with Barker's[9] choice, is required in order to predict a $5/2^-$ level at about 7 MeV of excitation. Nevertheless, recent $^{12}$C(p,p'$\gamma$) experimental results[79] could not clearly distinguish between a $5/2^-$ or a $7/2^-$ assignment.

Transitions to this level are the strongest ones in the $^{15}$N(p,t)$^{13}$N spectra. They show a characteristic L=2 angular distribution (compare

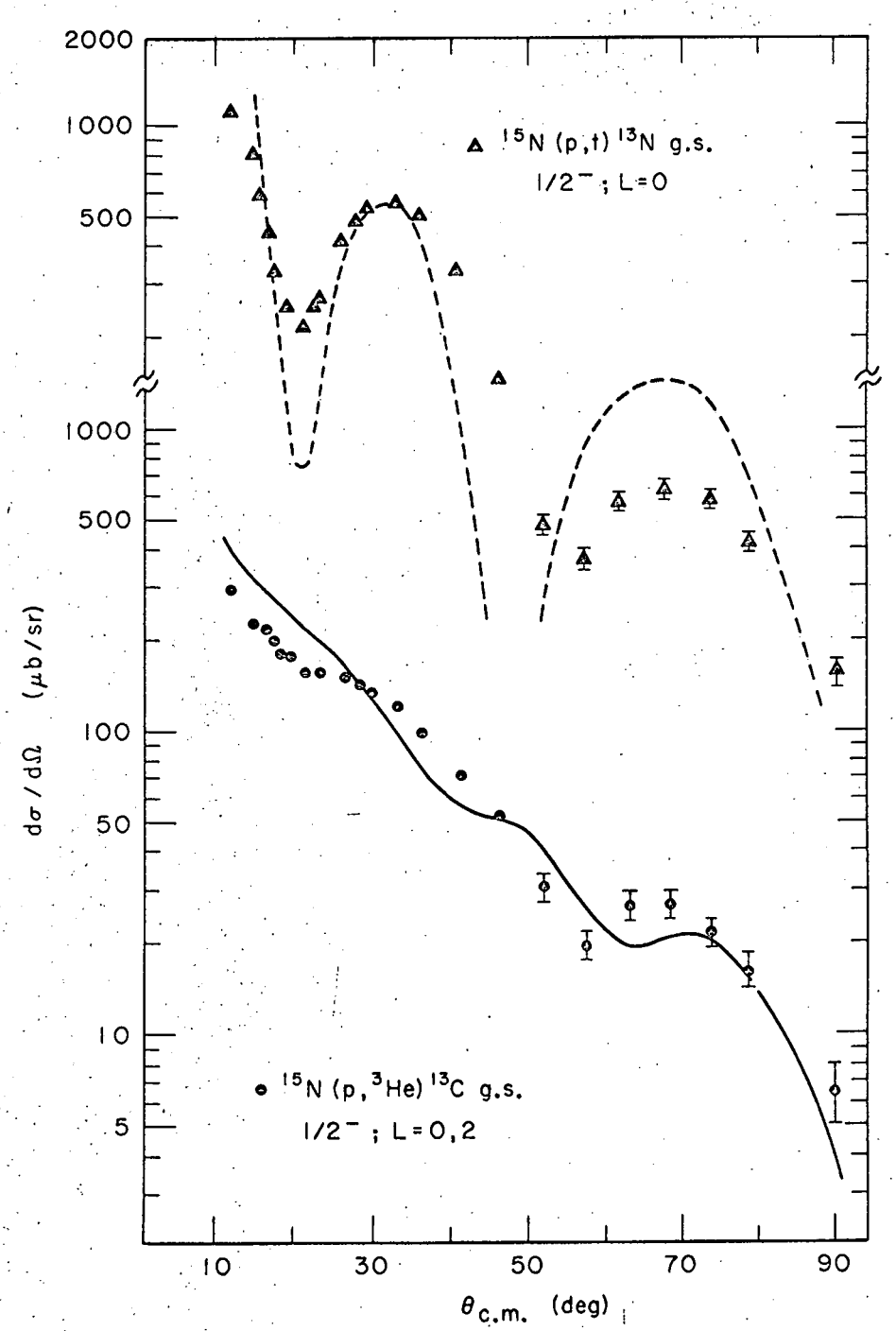


XBL676-3272

Fig. 20. Normalized DWBA fits to the $^{15}N(p,t)^{13}N$ and $^{15}N(p,^{3}He)^{13}C$ ground state transitions.

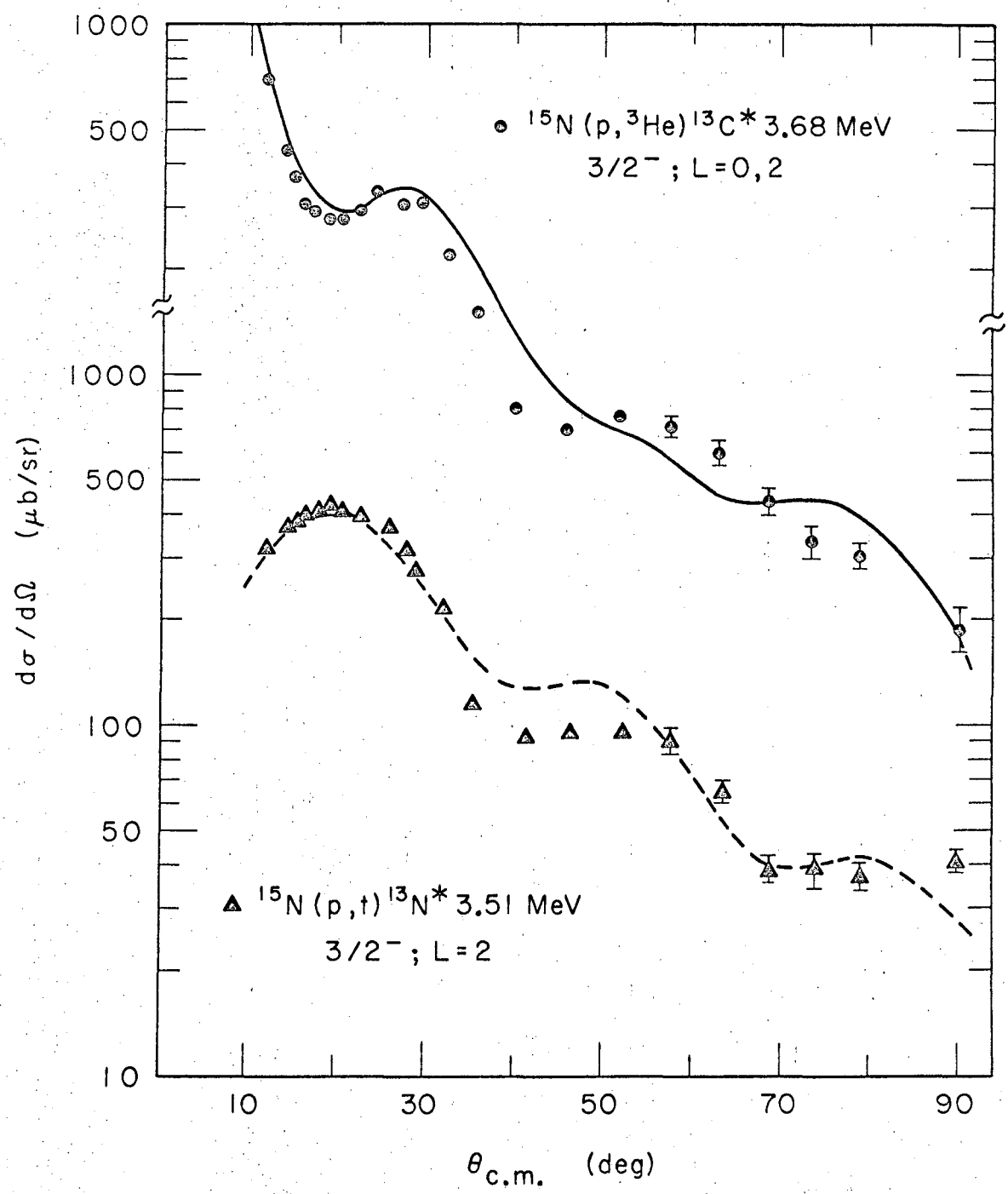


XBL676-3279-A

Fig. 21. Normalized DWBA fits to the $^{15}N(p,t)^{13}N^*$ 3.51 MeV and $^{15}N(p,^3He)^{13}C^*$ 3.68 MeV transitions.

Fig. 9 with Figs. 14 and 15) which requires either a $3/2^-$ or a $5/2^-$ assignment, and $3/2^-$ seems unlikely in view of the evidence presented above. This, and the relative cross sections discussed later, can be taken as confirmation that the level in question is $5/2^-$, a conclusion which has also been reached from recent $^{14}N(p,d)^{13}N$ analyses.[54] The mirror level is observed at 7.55 MeV in $^{13}C$ via the $(p,^3He)$ reaction. Unlike the ground state and first excited states, however, the $(p,^3He)$ transition is now restricted by angular momentum selection rules to a pure L=2 transfer. Consequently, these (p,t) and $(p,^3He)$ $5/2^-$ transitions are expected to have similar angular distributions. The DWBA fits for these transitions are shown in Fig. 22. The theory gives a very good account of the shape of the (p,t) angular distribution and a reasonable fit to the $(p,^3He)$ data, although it has not been able to account for the shift of the first maximum toward smaller angles observed in the $(p,^3He)$ angular distribution. Nevertheless, the angular distribution is well enough characterized to confirm a $5/2^-$ assignment to the 7.55 MeV level in $^{13}C$.

d. <u>8.93 MeV [$^{13}N$] and 8.86 MeV [$^{13}C$], $1/2^-$</u>. This level has been strongly excited in $^{13}N$ via proton scattering on $^{12}C$,[75] by a p-wave resonance and a spin-parity of $1/2^-$ has been assigned. It is also strongly excited in the $^{14}N(^3He,\alpha)^{13}N$ reaction (Fig. 7) and the $^{14}N(p,d)^{13}N$ reaction,[54] confirming its negative parity assignment. The analysis of the 8.93 MeV level observed in the $^{15}N(p,t)^{13}N$ reaction (its width is known[52,75] to be 230 keV) yields a reaonsable L=0 angular distribution (Fig. 8), in agreement with its $1/2^-$ assignment. A level at 8.86 MeV in $^{13}C$, which is probably the mirror of the 8.93 MeV level in $^{13}N$, is populated in the $^{15}N(p,^3He)^{13}C$ reaction. It has an angular distribution fairly similar to the (p,t) transition even though both L=0 and L=2 are allowed by two-nucleon selection rules. This, however, is understandable on the basis of the nuclear structure calculation; as shown in Table VI, the L=0 strength in the cross section is expected to be about a factor of three stronger than the L=2 strength. As expected, a level at this excitation (8.8 MeV) is strongly excited in the $^{14}N(d,^3He)^{13}C$ reaction (Fig. 7), consistent with its earlier[52,80] $1/2^-$ assignment. Intermediate coupling predictions for the appearance of a second $1/2^-$ level in this energy region are generally in very good agreement with experiment (see Table IV).

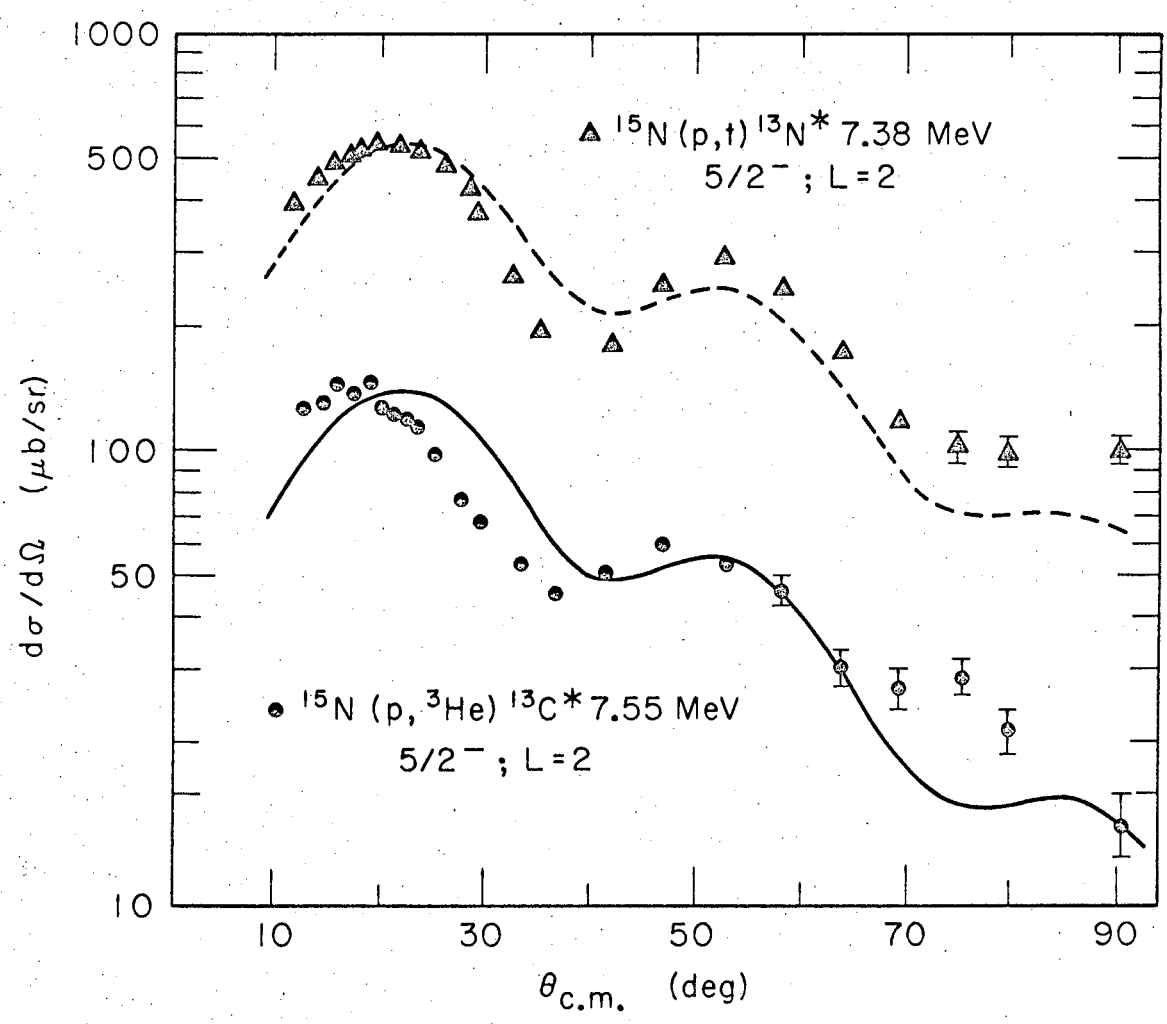


XBL676-3274-A

Fig. 22. Normalized DWBA fits to the $^{15}N(p,t)^{13}N^*$ 7.38 MeV and $^{15}N(p,^3He)^{13}C^*$ 7.55 MeV transitions.

The DWBA predictions for the angular distributions to these levels are shown in Fig. 23, again normalized independently. These fits are of poor quality compared to the ones previously presented. In addition, as is later discussed, the relative cross section for this 8.93 MeV ($1/2^-$) transition is underpredicted in a DWBA calculation by a factor of 600, whereas agreement to within a factor of two is obtained for all the other (p,t) transitions. However, the cross sections predicted from $^{14}N(p,d)^{13}N$ DWBA analysis[54] for this level agree with the data to better than a factor of two. This enormous discrepancy in the (p,t) reaction is difficult to understand and will be later discussed.

e. 9.48 MeV [$^{13}N$] $3/2^-$, and 9.52 MeV [$^{13}C$], ($3/2^-$). This level was originally assigned $3/2^-$ in $^{13}N$ from proton scattering results on $^{12}C$ [75] and until recently was thought to correspond to the second $3/2^-$ level predicted by intermediate coupling theory (Table IV). However, it is virtually absent in the $^{15}N(p,t)^{13}N$ spectrum (Fig. 5) and it is not observed in the $^{14}N(p,d)^{13}N$ [54] or $^{14}N(^3He,\alpha)^{13}N$ reactions (Fig. 7). The single nucleon pickup data are particularly interesting since coefficients of fractional parentage for these reactions[70] show that a second $3/2^-$ level, predicted to lie at about 10 MeV of excitation, should be strongly populated. Furthermore, the CK structure factors shown in Table VI from the Cohen and Kurath work[70] indicate that the second $3/2^-$ level populated in the (p,t) reaction should be roughly only a factor of five weaker than the first $3/2^-$ level (3.51 MeV). This would imply a peak angle cross section of roughly 80 μb, and thus should be about as strong as the T=3/2 level (15.07 MeV, $3/2^-$), which is clearly seen in the spectrum (Fig. 5). This, and the evidence presented above, seems to indicate overwhelmingly that the 9.48 MeV ($3/2^-$) level in $^{13}N$ is not primarily composed of a $(1p)^9$ configuration, and is therefore not the second $3/2^-$ level predicted by intermediate coupling theory. This interpretation is supported further by the data of McPherson et al.,[81] who studied the beta decay of $^{13}O$. The log ft value for this decay (and also for the beta decay of the mirror $^{13}B$ nucleus[82]) is in good agreement with intermediate coupling calculations,[70] except for the transition to the 9.48 MeV ($3/2^-$) level in $^{13}N$. In fact, it is possible

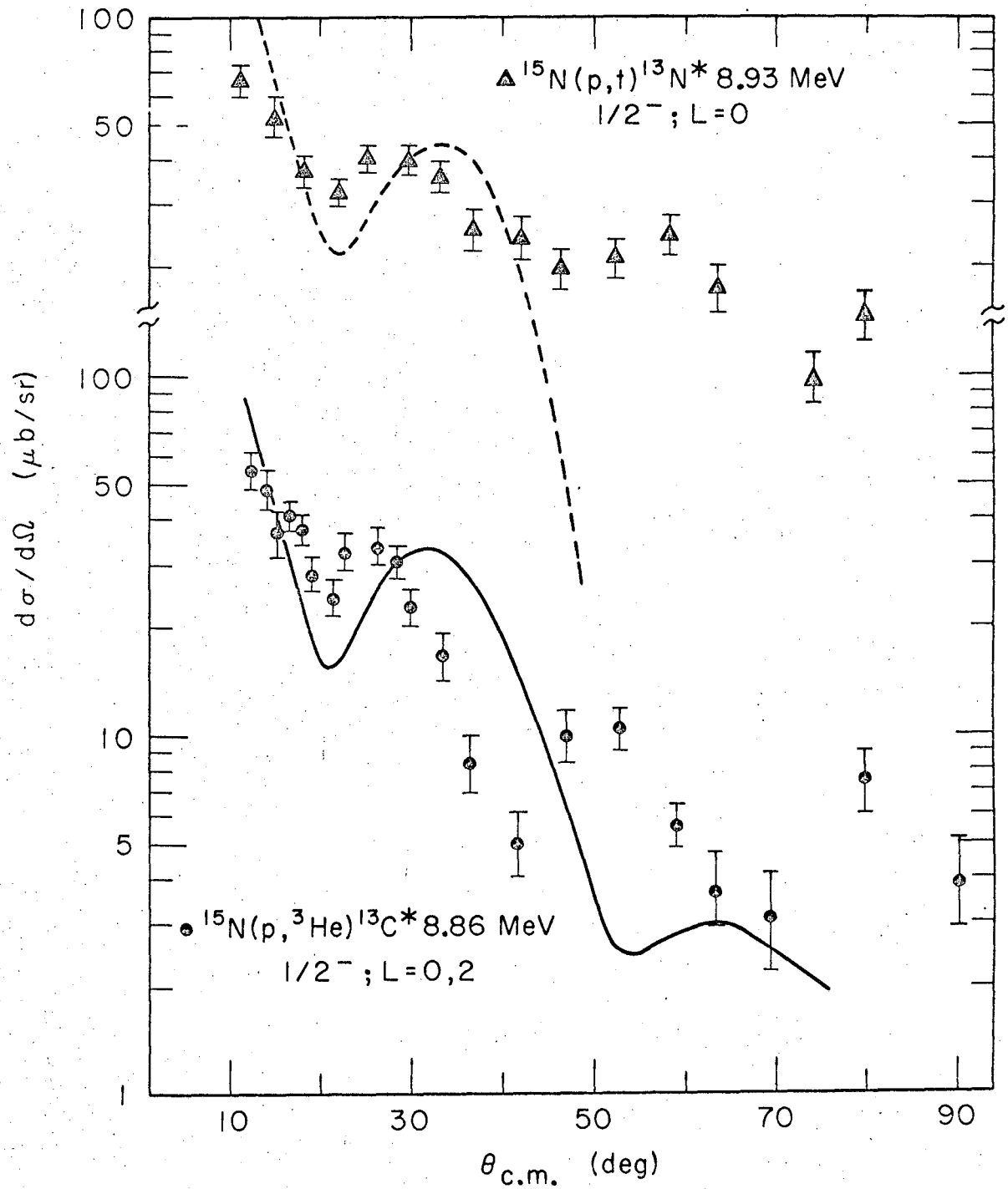


XBL676-3281-A

Fig. 23. Normalized DWBA fits to the $^{15}N(p,t)^{13}N^*$ 8.93 MeV and $^{15}N(p,^3He)^{13}C^*$ 8.86 MeV transitions.

that this particular level contains appreciable $(2s,1d)^2$ admixtures.[70] Such configurations could not be excited in the beta decay of $^{13}O$, nor would they be expected to be appreciably excited in these nuclear reactions. The second $3/2^-$ level predicted by theory is found to lie at 11.9 MeV, as discussed below.

However, a level at 9.52 MeV is excited in the $^{15}N(p,^3He)^{13}C$ reaction which is relatively strong in comparison to the other levels in this region (Fig. 5 and Table II). A level at this excitation has also been observed in the $^{14}N(d,^3He)^{13}C$ reaction (Fig. 7) which, although weakly populated is excited stronger than any of the positive parity levels of $^{13}C$. This is a good indication that the 9.52 MeV level in $^{13}C$ is of negative parity and one might consider it to be the $3/2^-$ mirror of the 9.48 MeV $(3/2^-)$ level in $^{13}N$.[54] The angular distribution (Fig. 12) seems to be predominantly L=2 (compare Figs. 14 and 15) which is consistent with a $3/2^-$ assignment. The puzzling aspect about this $(p,^3He)$ transition is its appreciable cross section (Table II), especially relative to the missing mirror (p,t) transition. Both of these levels -- the 9.48 MeV $(3/2^-)$ level in $^{13}N$ and the 9.52 MeV level in $^{13}C$ -- can be expected to mix with neighboring $3/2^-$ levels, the nearest being the 11.90 MeV level, which is discussed below. This latter level has strong components of quartet spin states[8] which would be "S forbidden" in the (p,t) reaction (see Ref. 10). Such components mixed into the 9.5 MeV $(3/2^-)$ level could favor the $(p,^3He)$ transition.

f. <u>10.78 MeV [$^{13}N$] $1/2^-$, and 11.09 MeV [$^{13}C$], $(1/2^-)$</u>. A new level in the $^{13}N$ spectrum possessing a small cross section (less than that to the 6.38 MeV $5/2^+$ level) is observed at 10.78 MeV; tritons from this level exhibit an angular distribution sharply peaked forward at small angles (Fig. 8). A level at this excitation is also weakly excited in the $^{14}N(^3He,\alpha)^{13}N$ reaction (Fig. 7) although here it is much more strongly populated than any of the positive parity levels. The relative strength with which the 10.78 MeV level is populated in the $(^3He,\alpha)$ reaction indicates a level of negative parity and its L=0 angular distribution (compare Figs. 14 and 15) in the (p,t) reaction (albeit with very poor statistics) indicates a probable spin and parity of $1/2^-$.

In contrast to the (p,t) data, the (p,$^3$He) transition to a level at 11.09 MeV in $^{13}$C, which is probably the mirror of the one above, is more strongly populated. Although only a few angles were taken, the $^{14}$N(d,$^3$He)$^{13}$C reaction (Fig. 7) excites a level at 11.1 MeV, in good agreement with the value obtained in the (p,$^3$He) reaction. There are two known levels in this region of $^{13}$C,[52] at 11.01 and 11.08 MeV, and it would appear from the energy analysis that the second one is populated in the $^{15}$N(p,$^3$He) $^{13}$C reaction. (The level at 11.01 MeV has been tentatively assigned as $1/2^+$,[52] which would not be appreciably excited in the (p,$^3$He) reaction).

The angular distribution of this $^{15}$N(p,$^3$He)$^{13}$C transition is presented in Fig. 12 and indicates a mixture of L=0 and L=2 transfers, which would be consistent with either a $1/2^-$ or a $3/2^-$ assignment. Assuming that the 10.78 MeV level in $^{13}$N and the 11.09 MeV level in $^{13}$C correspond to the third $1/2^-$ state predicted by theory (Table IV) produced the DWBA fits shown in Fig. 24. The L=0 shape of the (p,t) transition is well reproduced over the peak and, as is later discussed, the relative cross section of this level is in much better agreement for this choice than with a $3/2^-$ (L=2) assignment. The (p,$^3$He) angular distribution is also reasonably well fit for a level at this high excitation. An assignment of $1/2^-$ is consistent with the above fits and a complete DWBA analysis of the $^{14}$N($^3$He,$\alpha$)$^{13}$N data[53] confirms this conclusion.

g. <u>11.88 MeV [$^{13}$N] $3/2^-$, and 11.80 MeV [$^{13}$C], ($3/2^-$)</u>. These levels have recently been observed in single nucleon transfer reactions on $^{14}$N [53,54] (Fig. 7) through a p 3/2 pickup. An analysis of the intermediate coupling wavefunctions for the various final states[70] in $^{13}$N shows that the $5/2^-$, 7.38 MeV level; the $1/2^-$, 8.93 MeV level; and a $3/2^-$ level should all have the same dominant configuration, $|(p_{1/2})^2_1,(p_{3/2})^{-1};J\rangle$ and consequently these would all be expected to be strongly excited in single nucleon transfer reactions on $^{14}$N. All three are indeed strongly excited, in good agreement with Cohen and Kurath's spectroscopic factors,[70] and on this basis a $3/2^-$ assignment was made for the level at about 11.9 MeV in $^{13}$N.[53,54] A level at 11.88 MeV is observed in the $^{15}$N(p,t)$^{13}$N reaction and one at 11.80 MeV in the $^{15}$N(p,$^3$He)$^{13}$C reaction - this latter level

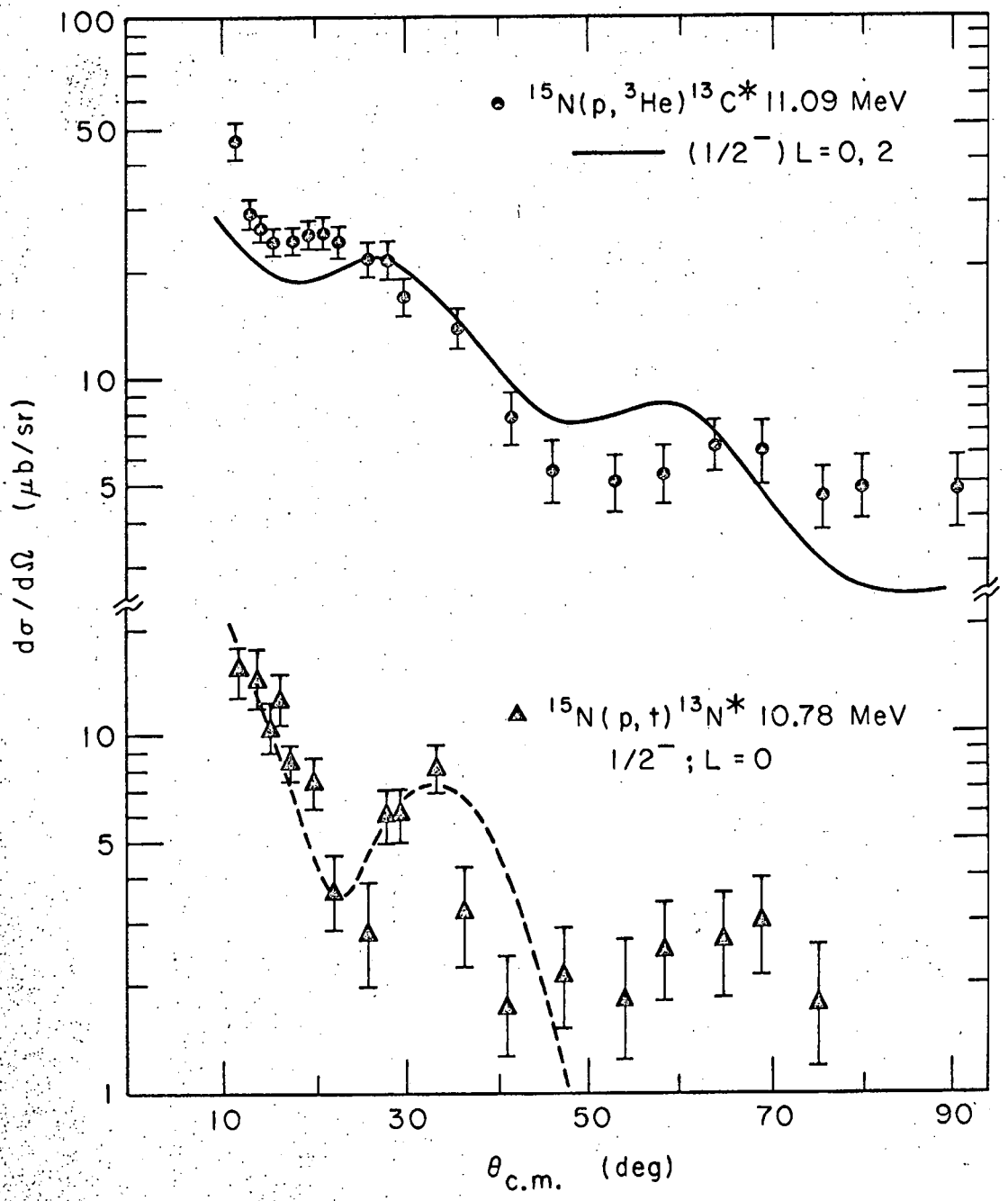


XBL676-3282A

Fig. 24. Normalized DWBA fits to the $^{15}N(p,t)^{13}N^*$ 10.78 MeV and $^{15}N(p,{}^3He)^{13}C^*$ 11.09 MeV transitions

most likely being the mirror of the one in $^{13}N$. This $^{13}C$ level has also been observed in $^{14}N(d,^3He)^{13}C$ (Fig. 7) and $^{13}C(^3He,^3He)^{13}C$ reactions[53] and similar excitations have been found. The (p,t) reaction populating a $3/2^-$ level is restricted by two-nucleon transfer selection rules to a pure L=2 transfer and the angular distribution of the 11.88 MeV transition is shown in Fig. 9. It has the general structure of other pure L=2 transitions, although the first maximum is shifted sharply inward. The $(p,^3He)$ transition, on the other hand, can be populated by both L=0 and L=2 components and its angular distribution is given in Fig. 12.

The DWBA fits for these levels, using intermediate coupling wave functions for the second predicted $3/2^-$ level, are given in Fig. 25. For the (p,t) reaction, both a representative L=0 transition at this excitation and an L=2 transition are compared with the data. It can be seen that L=2 gives a decidedly better fit, which is consistent with a $3/2^-$ assignment for the 11.88 MeV level in $^{13}N$. The DWBA calculation is, however, unable to account for the small angle behavior observed. This shift of the most forward maximum to smaller angles with increasing excitation has been observed in other (p,t) transitions (Figs. 14 and 15). The theory, on the other hand, exhibits a slight shift outward in angle with increasing excitation. The $^{15}N(p,t)^{13}N^*$ 7.38 MeV (L=2) transition gave a slight indication of this effect, although not so drastic as observed here. The $(p,^3He)$ fit, on the other hand, is quite good, especially for such a highly excited state. Both the structure and the envelope of the cross section are well predicted by the theory, which gives a good indication for a $3/2^-$ assignment to the 11.80 MeV level in $^{13}C$.

h. <u>12.40 MeV [$^{13}C$], $7/2^-$</u>. A level at 12.40 MeV in $^{13}C$ was excited fairly strongly in the $^{15}N(p,^3He)^{13}C$ reaction, although its counterpart in the $^{15}N(p,t)^{13}N$ spectrum was completely absent. A previously reported level at 12.44 MeV excitation in $^{13}C$ has been tentatively assigned as $1/2^-$.[52] This level at 12.40 MeV had a width consistent with the recently reported value of 90 keV,[52,83] in contrast with other reports on the width of a level at this excitation of about 300 keV.[84] Other levels are also observed in this region in the $^{15}N(p,^3He)^{13}C$ reaction, at about 12.2 and 12.6 MeV, and these could be the cause of the

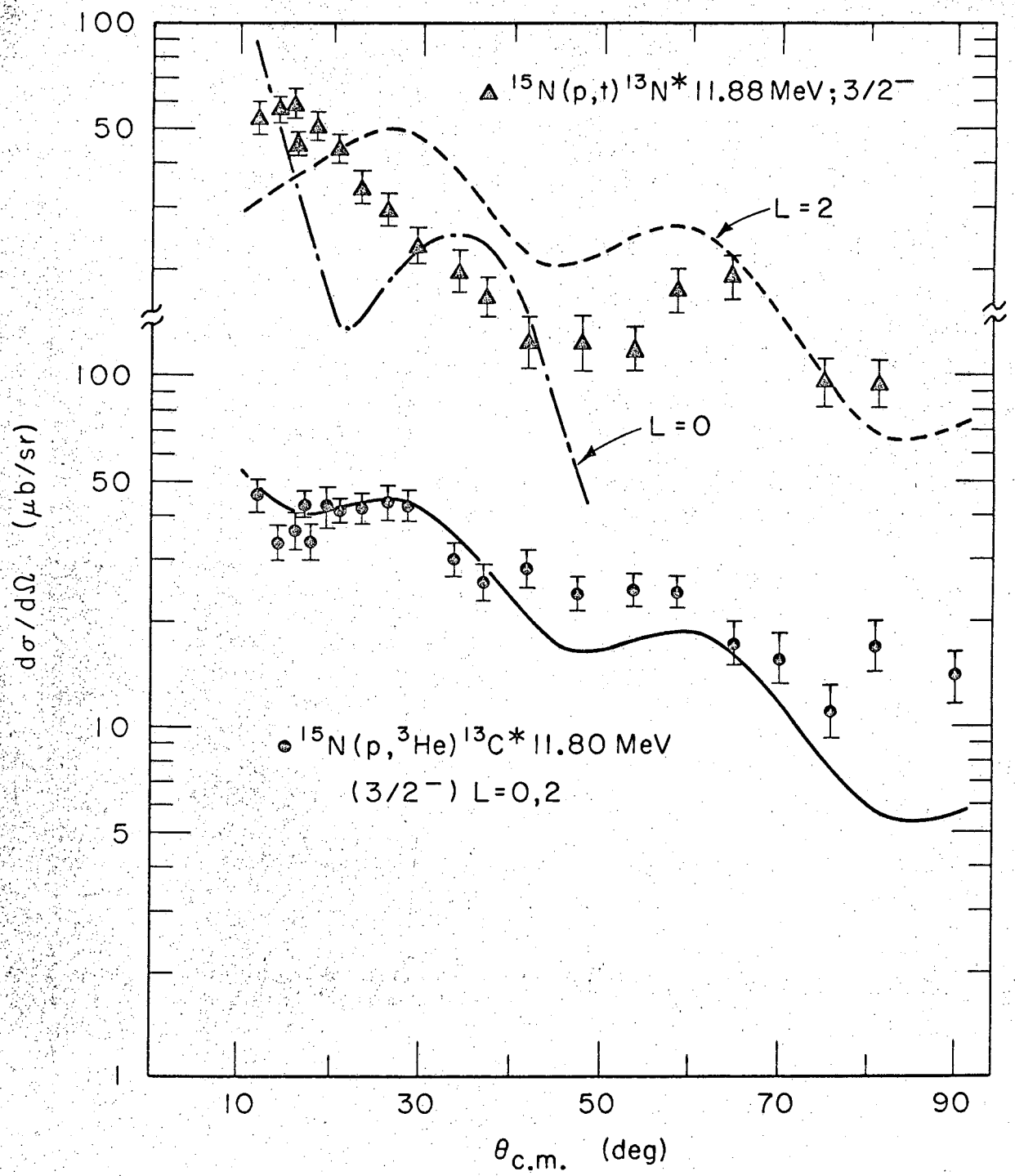


XBL676-3280-A

Fig. 25. Normalized DWBA fits to the $^{15}N(p,t)^{13}N^*$ 11.88 MeV and $^{15}N(p,^3He)^{13}C^*$ 11.80 MeV transitions.

differing widths reported for this state. Although the 12.40 MeV level was not well resolved at most angles from these other peaks, its angular distribution was extracted and is shown in Fig. 13.

The angular distribution for this level has a reasonably pure L=2 shape (compare Figs. 12-15) which would imply that this was a transition to a $5/2^-$ or $7/2^-$ final state, rather than to a $1/2^-$ state. Intermediate coupling theory (Table IV) would argue for a $7/2^-$ assignment. Most importantly, this state is absent in the $^{15}N(p,t)^{13}N$ spectrum and there is no evidence for a level in this range of excitation in either the $^{14}N(^3He,\alpha)^{13}N$ or $^{14}N(d,^3He)^{13}C$ reactions (Fig. 7) or in the $^{14}N(p,d)^{13}N$ reactions.[54] A $7/2^-$ assignment is the only one consistent with these observations since of the allowed 1p - shell pickup final states for this $(p,^3He)$ reaction ($1/2^-$, $3/2^-$, $5/2^-$, $7/2^-$) only the $7/2^-$ state is J (or j) forbidden in all the other reactions. The DWBA fit based on a $7/2^-$ assignment[85] (L=2) is shown in Fig. 26. The theory gives a satisfactory account of the data, predicting quite well the envelope of the cross section. For these reasons, then, the assignment of this state as $7/2^-$ rather than the earlier $1/2^-$ seems warranted. (Curiously, the original assignment[86] for this level was $7/2^-$ rather than $1/2^-$).

i. <u>15.07 MeV [$^{13}N$] and 15.11 MeV [$^{13}C$], $3/2^-$, T=3/2</u>.

The (p,t) and $(p,^3He)$ reactions on T=1/2 targets are able to populate both T=1/2 and T=3/2 states in the final nucleus. For transitions to T=3/2 levels, the $(p,^3He)$ reaction is restricted to a pure $^{13}S$ spin-isospin transfer of the neutron-proton pair (whereas, as previously discussed, both $^{13}S$ and $^{31}S$ transfers are allowed in transitions to T=1/2 final states). In such cases then, both the (p,t) and $(p,^3He)$ reactions are transitions from the same initial to identical final states. Within the framework of charge independence of nuclear forces, identical cross sections are to be expected for (p,t) and $(p,^3He)$ transitions populating T=3/2 final states. This can be seen as follows: writing Eq. (1) as a ratio,

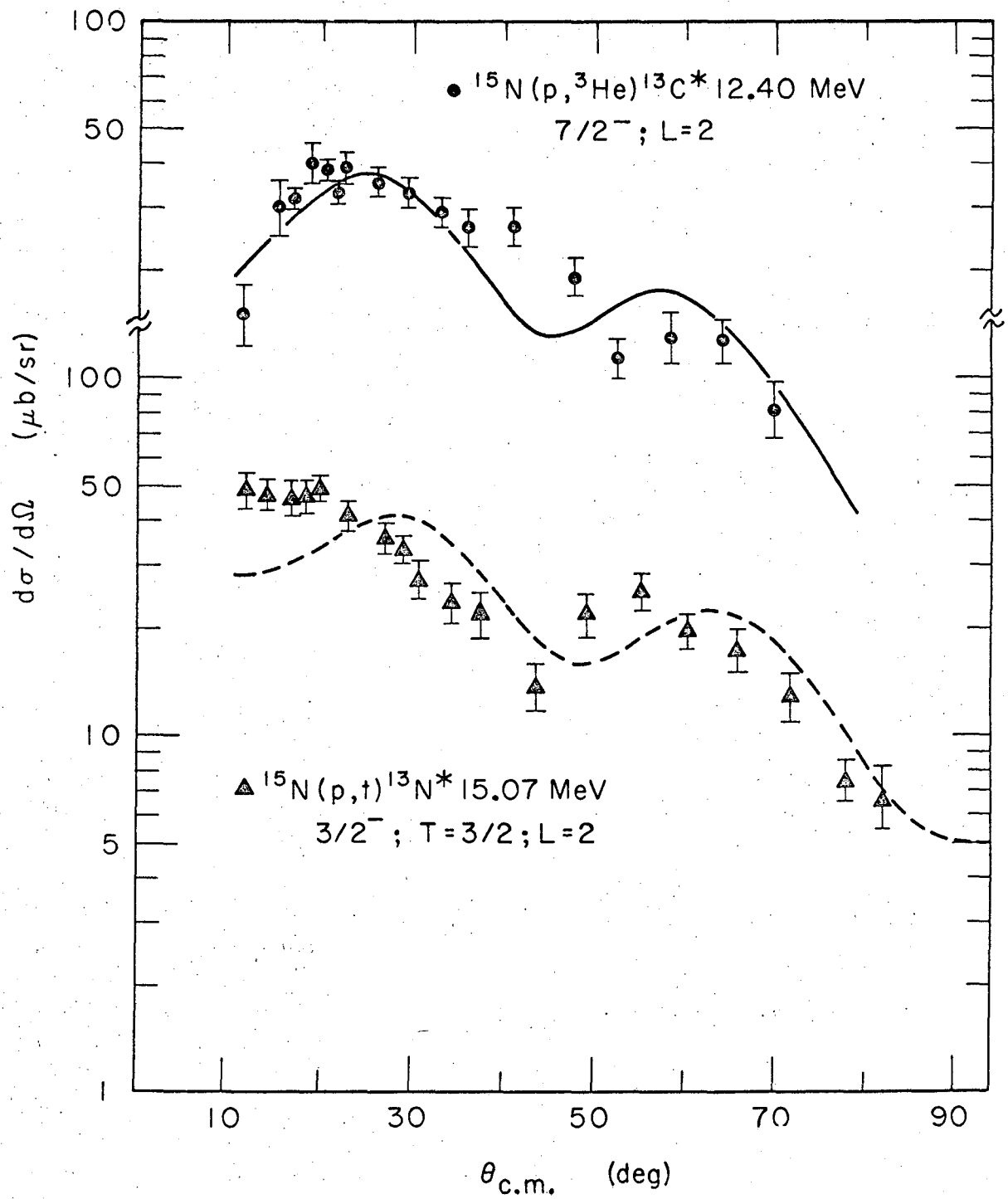


XBL676-3283-A

Fig. 26. Normalized DWBA fits to the $^{15}N(p,^3He)^{13}C^*$ 12.40 MeV and $^{15}N(p,t)^{13}N^*$ 15.07 MeV (T=3/2) transitions.

$$\frac{\sigma(p,t)}{\sigma(p,{}^3He)} = \frac{k_t}{k_{{}^3He}} \cdot \frac{C^2_{ST}(p,t)}{C^2_{ST}(p,{}^3He)} \cdot \left| \frac{\sum_N G_{NLSJT}\, B^M_{NL}(k_p,k_t)}{\sum_N G_{NLSJT}\, B^M_{NL}(k_p,k_{{}^3He})} \right|^2$$

Thus if nuclear forces are charge independent, then the third ratio should be unity (the different binding energies of the transferred pair and the different Coulomb potential for triton and helium-3 in the optical model make a negligible difference to the ratios of these cross sections, as is later indicated). Thus

$$\left.\frac{\sigma(p,t)}{\sigma(p,{}^3He)}\right\}_{T=3/2} = \frac{k_t}{k_{{}^3He}} \cdot \frac{C^2_{ST}(p,t)}{C^2_{ST}(p,{}^3He)}$$

From Eqs. (3) and (8), $C^2_{ST}(p,t) = |\langle 3/2\text{-}1/2\ 1\ 1|1/2\ 1/2\rangle|^2 = 1/6$

$$C^2_{ST}(p,{}^3He) = 1/2\times|\langle 3/2\ 1/2\ 1\ 0|1/2\ 1/2\rangle|^2 = 1/2\times 1/3 = 1/6$$

Hence the second ratio in the above expression is also unity, so that the ratios of (p,t) and (p,$^3$He) T=3/2 transitions should just be given by the phase-space factor, $k_t/k_{{}^3He}$ .

The lowest T=3/2 states in $^{13}$N and $^{13}$C are expected to lie near 15.3 MeV of excitation, as calculated from the $^{13}$B mass after corrections for Coulomb energy and neutron-hydrogen atom mass differences. This prediction is in good agreement with the observed excitations of the 15.07 and 15.11 MeV levels in $^{13}$N and $^{13}$C, respectively. As such, these states should be members of the lowest isobaric multiplet in mass 13 with a spin and parity of $3/2^-$, since this is the measured value of the $^{13}B(T_Z = +3/2)$ ground state.[82] Two-nucleon selection rules would then restrict the (p,t) and (p,$^3$He) transitions populating these levels to pure L=2 transfers. The experimental angular distributions are shown in Fig. 27, with the (p,$^3$He) multiplied by the phase space factor, 0.924. Comparing the shapes of these angular distributions with those shown in Figs. 8 and 9 and in Figs. 11 thru 15 shows that they are indeed L=2 transfers, consistent with their $3/2^-$ spin and parity assignment. These levels have also been observed in the $^{11}B(^3He,p)^{13}C$ [87] and $^{11}B(^3He,n)^{13}N$ [88] reactions and the T=3/2 state in $^{13}$N has been seen as a "twice-forbidden" resonance in the $^{12}$C plus proton reaction.[89]

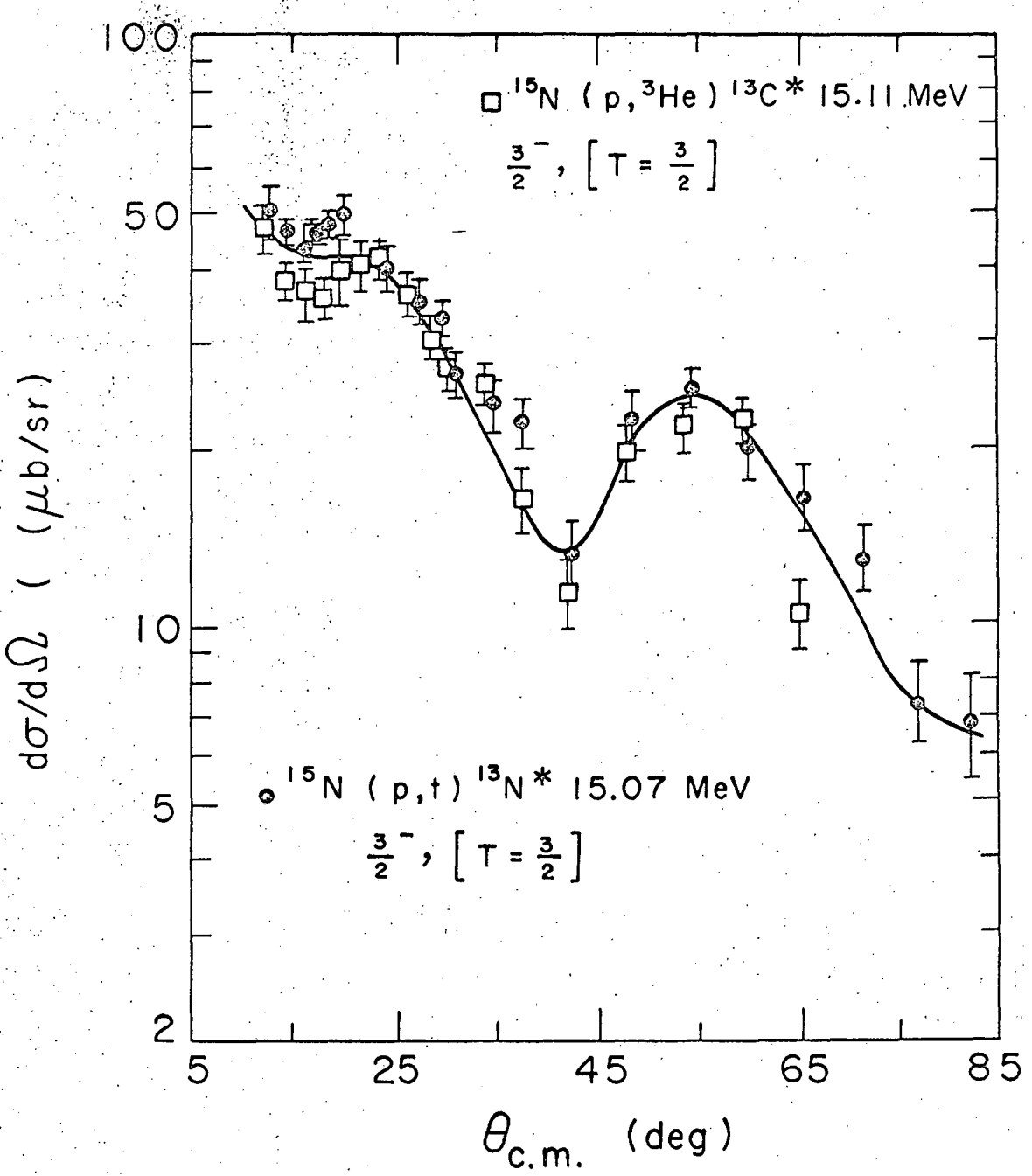


XBL678-5115

Fig. 27. Differential cross sections of the $^{15}N(p,t)^{13}N$ and $^{15}N(p,^{3}He)^{13}C$ T=3/2 transitions. The (p,$^{3}$He) cross section has been multiplied by the phase space factor 0.924.

The above analogue states are "sharp" in the (p,t) and (p,$^3$He) spectrum, with a resolution comparable to that of their respective ground state transitions. This long lifetime is consistent with their being the lowest T=3/2 states in $^{13}$N and $^{13}$C since there are no T=3/2 channels energetically available for decay. The cross sections of the $^{15}$N(p,t)$^{13}$N$^*$ 15.07 MeV (3/2$^-$, T=3/2) and $^{15}$N(p,$^3$He)$^{13}$C$^*$ 15.11 MeV (3/2$^-$, T=3/2) transitions are expected from the charge independence of nuclear forces to be identical. The differential cross sections shown in Fig. 27 are indeed almost identical and the integrated cross sections (10-65°, c.m.) are in the ratio of 1.09/1, with the (p,t) being the larger. It would be difficult, however, to interpret this difference as a measure of the expected isospin admixtures[90] in the nuclear states involved (T=3/2 admixtures in the $^{15}$N ground state and/or T=1/2 admixtures in the T=3/2 states) because these are very highly excited states with relatively low cross sections, so that background corrections could conceivably contribute a large fraction of their cross section differences.

The intermediate coupling predictions for the energies of the lowest T=3/2 states in these nuclei (Table IV) are generally in good agreement with the observed values, except for the results of Barker,[9] which place them about two MeV too low. The (p,t) DWBA fit (the (p,$^3$He) fit was virtually the same) is presented in Fig. 26, along with the DWBA fit to the $^{13}$C$^*$ 12.40 MeV (7/2$^-$) transition disucssed earlier. The same effect appears in this T=3/2 transition which occurred in the 11.88 MeV (3/2$^-$) transition; namely, the data are peaking toward smaller angles and the peak angle is consequently shifted inward with respect to the theoretical fit. Nevertheless, considering that this is such a highly excited level, the DWBA fit is still reasonable.

j. 6.38 MeV [$^{13}$N] and 6.87 MeV [$^{13}$C], 5/2$^+$. Insofar as the ground state of $^{15}$N can be represented by a pure $(1p)^{11}$ configuration, then the direct pickup of two nucleons can only excite negative parity states in the final nucleus. Hence, the population of positive parity levels must be due to other effects, such as $(2s,1d)^2$ impurities in the $^{15}$N ground state or an additional mechanism such as core excitation or knockout. (Compound nucleus contributions are expected to be negligible at these high bombarding energies). Only two positive parity levels could be con-

sistently observed in both the (p,t) and (p,$^3$He) spectra; the first $1/2^+$ level at 2.37 and 3.09 MeV in $^{13}$N and $^{13}$C, respectively, and the second $5/2^+$ level at 6.38 and 6.87 MeV, respectively. In both spectra, the $5/2^+$ transition is much stronger and angular distributions populating it are shown in Fig. 10. Also of interest, in an attempt to interpret the population of these $5/2^+$ states, is the $^{13}$C(p,t)$^{11}$C $7/2^-$ transition, which is later discussed in detail; it is J-forbidden (see later discussion) on the basis of a two neutron pickup reaction on a pure $(1p)^9$ $^{13}$C target, but is populated relatively strongly. Its angular distribution is also shown in Fig. 10. (In the following discussion, a knockout mechanism has been disregarded, in view of the relative population of the $1/2^+$ and $5/2^+$ levels and since this mechanism has recently been shown to be inadequate in a treatment of "forbidden" (d,p) reactions,[91] where its influence might be expected to be greater than in the (p,t) reaction).

Although the shape of the $^{13}$N $5/2^+$ angular distribution[92] is not what is normally observed for an L=3 transfer,[13,93] as would be required for a pickup from a $(1d)^2$ impurity in the $^{15}$N ground state, it is possible to obtain a reasonable fit to the data. In Fig. 28, are shown DWBA fits to this transition as well as to the $^{13}$C(p,t)$^{11}$C* ($7/2^-$) transition. Two curves are shown for each transition, corresponding to differenct choices of the oscillator parameter for the bound state wave function; $\nu$=0.32 (the standard one) and 0.40 for the $5/2^+$ transition and $\nu$=0.32, 0.46 for the $7/2^-$ transition. The larger values of $\nu$ correspond to different radii for matching the Hankel function tail at the nuclear surface. (This procedure is discussed in more detail later). Since it is not clear how to treat the bound state wave function for a (1d,1p) L=3 or a (1p,1f) L=4 transition (a problem which also arises in the theory[94] of single nucleon transfer reactions), these larger values of $\nu$ are perhaps not unreasonable and their use does result in improved fits to the data.

Under these assumptions and using the configurations predicted from weak coupling calculations[95] for the $^{13}$N $5/2^+$ state, about a 15 ± 5% admixture of $(d5/2)^2$ in the $^{15}$N ground state would be necessary to account for the relative strength of the observed transition. The relative

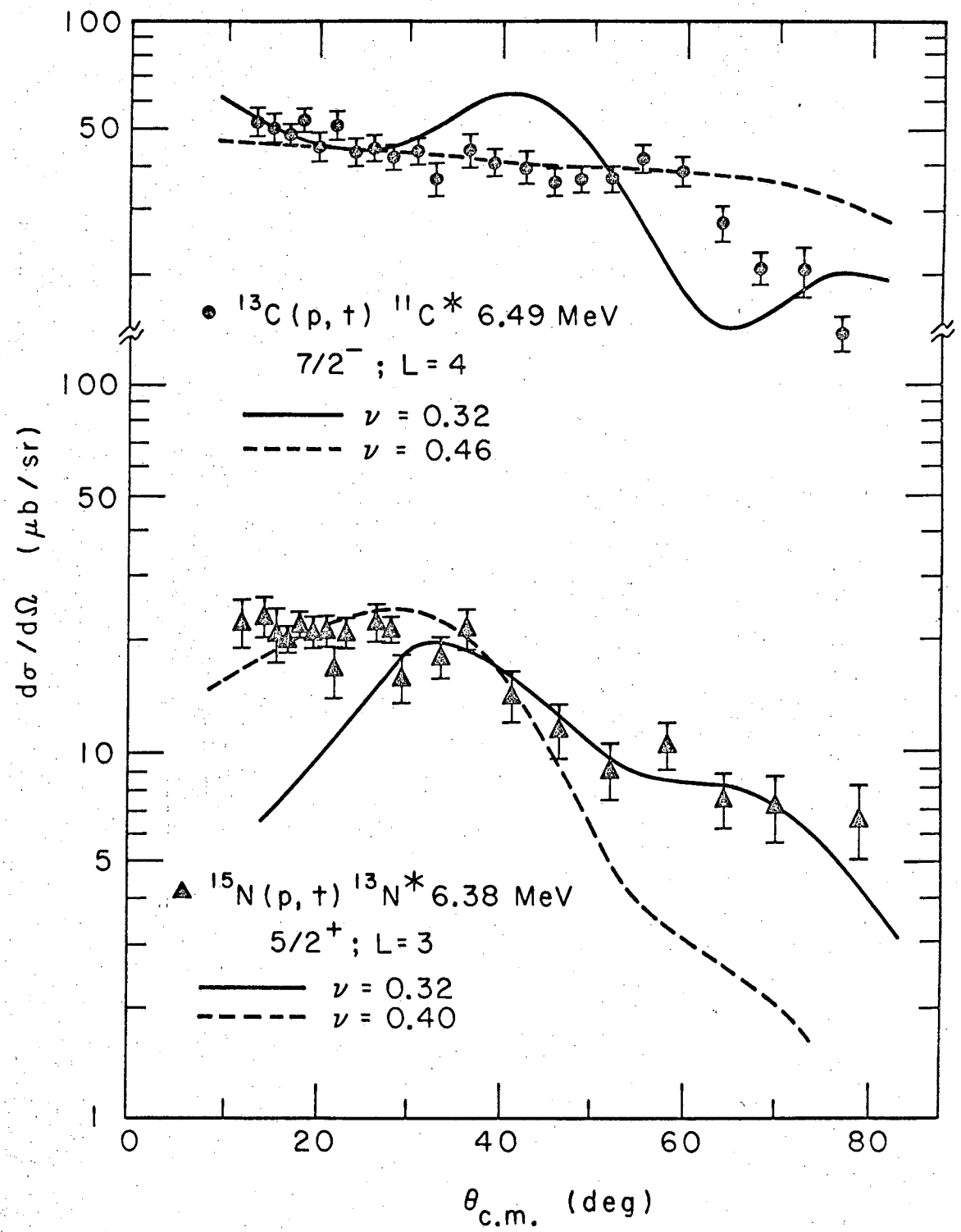


XBL 677-3547

Fig. 28. Normalized DWBA fits to the $^{15}N(p,t)^{13}N^*$ 6.38 MeV and $^{13}C(p,t)^{11}C^*$ 6.49 MeV transitions.

population of the 6.38 MeV ($5/2^+$) and 2.37 MeV ($1/2^+$) levels in $^{13}N$ can be understood through a larger amount of $(d5/2)^2$ than of $(s1/2)^2$ in the $^{15}N$ ground state - a conclusion consistent with an analysis of negative parity states populated in the $^{15}N(^3He,\alpha)^{14}N$ reaction[53] and with the excitation of the $^{15}N^*$ 5.28 MeV ($5/2^+$) level in the $^{16}O(d,^3He)^{15}N$ reaction.[64]

However, the relative population of the $1/2^+$ and $5/2^+$ levels can also be understood on the basis of a core-excitation pickup reaction. The observed angular distribution of the $^{13}N^*$ $5/2^+$ (and the $^{11}C^*$ $7/2^-$) transition is quite similar to that of other transitions where a two-step (core-excitation) reaction mechanism may be applicable.[46,96] As described previously, the two step reaction must have a strong excitation of the parent state via inelastic scattering and a favorable overlap of this state with the configurations of the final state. Bussiere et al.[97] have shown that the $^{15}N^*$ 5.28 MeV ($5/2^+$) level is strongly excited in $(\alpha,\alpha')$ and they interpreted this as due to a single particle promotion of a p1/2 proton to the d5/2 shell. (No similar strong transition to a $1/2^+$ state (promotion to the 2s 1/2 level) was observed). Assuming that this level would also be strongly excited in inelastic proton scattering at 43.7 MeV, then those final state configurations consisting of a $^{12}C$ core coupled to a d5/2 proton could be relatively strongly excited in two-neutron pickup from this $^{15}N^*$ 5.28 MeV level. Such configurations are expected from weak coupling calculations[95] for the 3.56 MeV level and 6.38 MeV $5/2^+$ levels in $^{13}N$. Since the 2.37 MeV ($1/2^+$) level in $^{13}N$ mainly has the configuration of the $^{12}C$ ground state coupled to an s1/2 nucleon,[95] then this state should be relatively weakly excited by this mechanism, as is experimentally observed. Of the two $5/2^+$ levels, the 3.56 MeV one is not resolved, but some population of the mirror $5/2^+$ level at 3.85 MeV in $^{13}C$ can be seen as a slight asymmetry on the side of the allowed 3.68 MeV ($3/2^-$) level. Its cross section, however, is only about 30 μb/sr at forward angles which is about the same as that observed to the 6.87 MeV ($5/2^+$) level of $^{13}C$. Assuming a comparable situation in the (p,t) data would be consistent with the population of the 3.56 and 6.38 MeV ($5/2^+$) states of $^{13}N$ via the chosen core-excitation

route. However, if one assumes a direct pickup, the 3.56 MeV ($5/2^+$) transition is predicted to be much stronger (by a factor of ten) than that to the 6.38 MeV ($5/2^+$) level, and this appears experimentally to be very unlikely. The shape of the angular distribution of the $^{13}N^*$ 6.38 MeV ($5/2^+$) transition, as well as that of the $^{11}C^*$ $7/2^-$ transition and the $^{13}C^*$ ($5/2^+$) transition (Fig. 10) is presumably also consistent with a core-excitation pickup reaction. Clearly much more theoretical work and more extensive experimental data are required in order to determine the significance of core excitation in these reactions.

## B. $^{13}C(p,t)^{11}C$ and $^{13}C(p,^3He)^{11}B$

### 1. Experimental Results

These reactions were studied at incident proton energies of 43.7 and 49.6 MeV. Figure 29 presents energy spectra of the $^{13}C(p,t)^{11}C$ and $^{13}C(p,^3He)^{11}B$ reactions at 49.6 MeV, taken at 22° in the laboratory. The excitations shown were obtained in this experiment and in the majority of cases agree well with previous values.[52,98] Spin and parity assignments consistent with the experimental results are shown on the figure and these also agree well with previous assignments.[52,98] Assuming that $^{13}C$ can be represented by a pure $(1p)^9$ configuration, then the direct pickup of two 1p nucleons could only excite negative parity levels in the mass 11 final nuclei. The data in Fig. 29 do indeed show a selective population of negative parity final states. The only positive parity state that could be clearly identified was the 6.84 MeV ($5/2^+$) level in $^{11}C$, and this was very weakly excited, unlike the $5/2^+$ level previously discussed in the $^{15}N(p,t)^{13}N$ reaction. Since the target was only 94% pure, the $^{12}C$ impurity did present some problems in observing the levels at higher excitation.

The excitations and spins and parities of states observed in these experiments are compared with the results of previous work in Table VII for the $^{11}C$ states and in Table VIII for the $^{11}B$ states. The results are given for two different beam energies, 43.7 and 49.6 MeV; the integrated cross sections are also given in these tables. Those

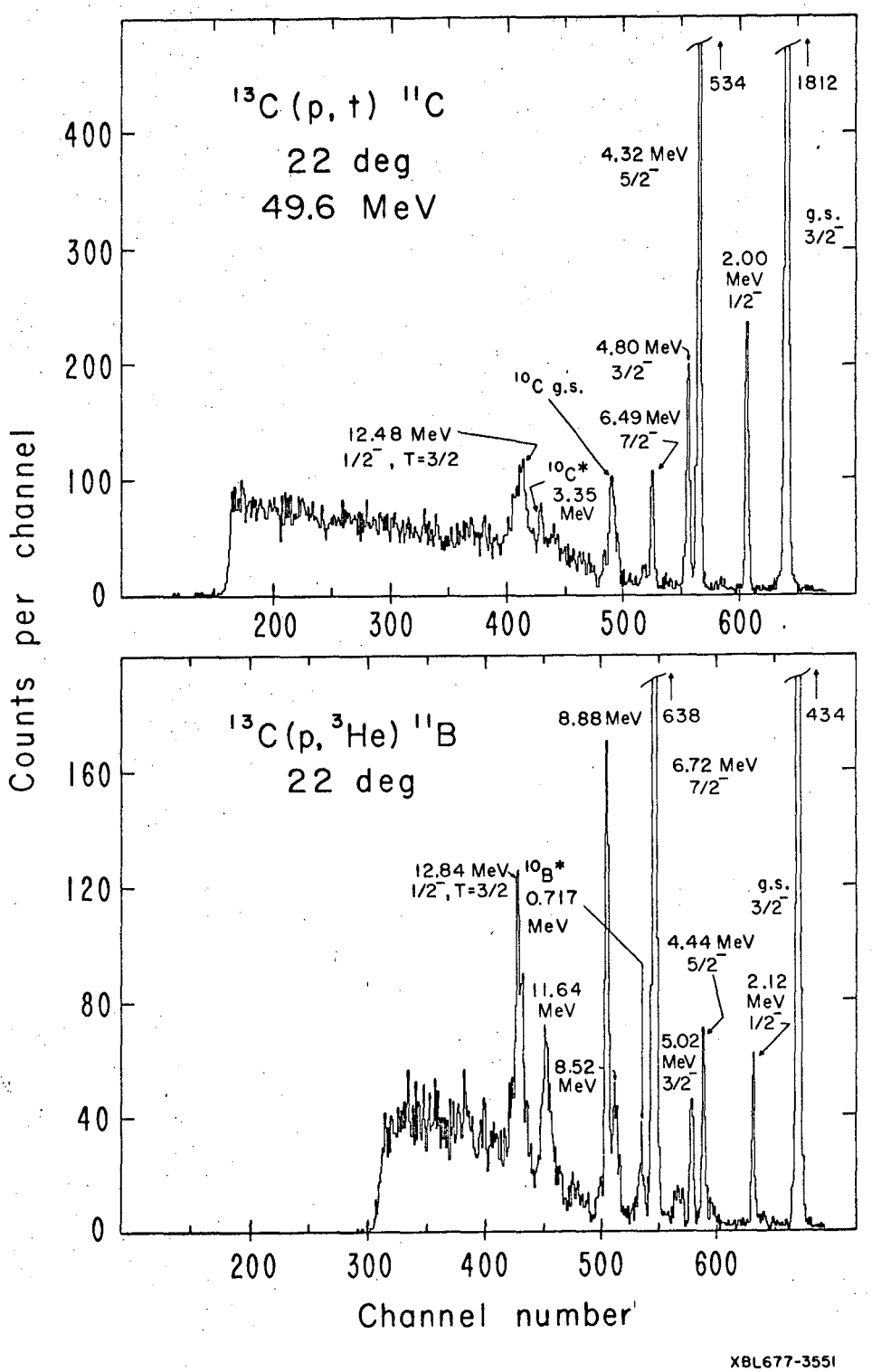


Fig. 29. Energy spectra of the 49.6 MeV (p,t) and (p,$^3$He) reactions on $^{13}$C.

Table VII. Integrated cross sections of the $^{11}C$ levels observed in the $^{13}C(p,t)^{11}C$ reaction and comparison of these states with those previously reported.

| $^{13}C(p,t)^{11}C$ | | | | Previously Reported[52] | |
|---|---|---|---|---|---|
| $J^{\pi}$ | Excitation (MeV) | $\sigma_T(\mu b)$ 43.7 MeV (13-58°,c.m.) | $\sigma_T(\mu b)$ 49.6 MeV (13-77°,c.m.) | $J^{\pi}$ | Excitation (MeV) |
| $3/2^-$ | 0.0[a] | 1156 | 1324 / 1162[d] | $3/2^-$ | 0.0 |
| $1/2^-$ | *[b] 2.00 ± 40[c] | 350 | 310 / 267[d] | $1/2^-$ | 2.00 |
| $5/2^-$ | * 4.32 ± 30 | 333 | 425 / 353[d] | $5/2^-$ | 4.31 |
| $3/2^-$ | * 4.80 ± 40 | 162 | 167 / 140[d] | $3/2^-$ | 4.79 |
| $7/2^-$ | * 6.49 ± 50 | 136 | 167 / 124[d] | $7/2^-$ | 6.48 |
| $5/2^+$ | 6.84 ± 60 | - | 33.2 | $5/2^+$ | 6.90 |
| $1/2^-$ [$T=3/2^-$] | 12.48 ± 70 | 196 | 294 / 196[d] | not reported | |

[a] Not used in the energy scale because these tritons were non linear.

[b] Levels marked with asterisk were used to determine the energy scale.

[c] Errors are given in keV.

[d] Integrated to 58°, c.m.

Table VIII. Integrated cross sections of the $^{11}B$ levels observed in the $^{13}C(p,^{3}He)^{11}B$ reaction and comparison of these states with those previously reported.

| $^{13}C(p,^{3}He)^{11}B$ | | | | Previously Reported[52,98] | |
|---|---|---|---|---|---|
| $J^{\pi}$ | Excitation (MeV) | $\sigma_T(\mu b)$ 43.7 MeV (13-58°, c.m.) | $\sigma_T(\mu b)$ 49.6 MeV (13-77°, c.m.) | $J^{\pi}$ | Excitation (MeV) |
| $3/2^-$ | *[a]0.0 ± 30[b] | 380 | 359<br>309[c] | $3/2^-$ | 0.0 |
| $1/2^-$ | * 2.12 ± 30 | 58.4 | 63.4<br>47.4[c] | $1/2^-$ | 2.12 |
| $5/2^-$ | * 4.44 ± 30 | 63.1 | 90.7<br>65.0[c] | $5/2^-$ | 4.44 |
| $3/2^-$ | * 5.02 ± 30 | 51.7 | 57.8<br>44.4[c] | $3/2^-$ | 5.02 |
| $7/2^-$ | 6.72 ± 50 | 458 | 611<br>529[c] | $7/2^-$ | 6.74 |
| $\leq 5/2^-$ | 8.52 ± 60 | - | 56.4[c] | $\leq 5/2^-$ | 8.57 |
| $\leq 5/2^-$ | 8.88 ± 50 | - | 160[c] | $5/2^-$ | 8.92 |
| $\leq 5/2^-$ | 11.64 ± 60 | - | 92.3[c] | | 11.60 |
| $1/2^-$ [T=3/2] | 12.84 ± 60 | 148[d] | 293<br>195[c] | not reported | |

[a]Levels marked with an asterisk were used to determine the energy scale.
[b]Errors are given in keV.
[c]Integrated to 58°, c.m.
[d]Integrated to 48°, c.m.

levels marked with an asterisk in the tables were used to determine the energy scale and their associated errors (in keV) reflect the overall uncertainty involved in the analysis. The angular distributions for the first five levels (ground state through the $7/2^-$ level) populated in these $^{13}C(p,t)^{11}C$ and $^{13}C(p,^3He)^{11}B$ reactions are shown in Figs. 30 through 34, for the two different beam energies, 43.7 and 49.6 MeV. Error bars reflect counting statistics only. Both the shapes and the magnitudes (also compare integrated cross sections in Tables VII and VIII) of these transitions appear to be relatively insensitive to this 6 MeV increase in the beam energy, although the (p,t) 2.00 MeV ($1/2^-$, L=0) transition is more strongly excited at the lower energy. A dependence of the cross section on incident beam energy for (p,t) L=0 transitions has been noted previously.[99]

2. Optical Model Parameters

The same potentials shown in Table III, which were used in the previous analysis of the $^{15}N(p,t)$ and $(p,^3He)$ reactions, were also tried in analysis of the $^{13}C(p,t)$ and $(p,^3He)$ reactions (only the 49.6 MeV data are considered here). Again the potential that proved to give the best overall fits to the data was AX, although in this case the radius parameter of the imaginary well for the exit potential had to be increased from 1.25 to 1.45. This is the only optical potential used in fitting the data to be presented. No attempt was made to improve the DWBA fits to excited states by introducing an energy dependence in the exit channel. All DWBA fits are arbitrarily and separately normalized to the data.

3. Spectroscopy of Individual Transitions

Unlike the mass 13 states previously discussed, intermediate coupling wave functions for these mass 11 final states were not available. Consequently, nuclear structure factors have been calculated assuming pure jj configurations for the final state. The configurations assumed are the dominant ones expected from the single nucleon coefficients of fractional parentage relating mass 11 to mass 12,[70] and are presented in Table IX. The ground state of $^{13}C$ was also assumed to be described by a pure jj wave function (p1/2 neutron) and the nuclear structure factors calculated on this basis are presented in Table X. Several numerical examples are worked out in the Appendix.

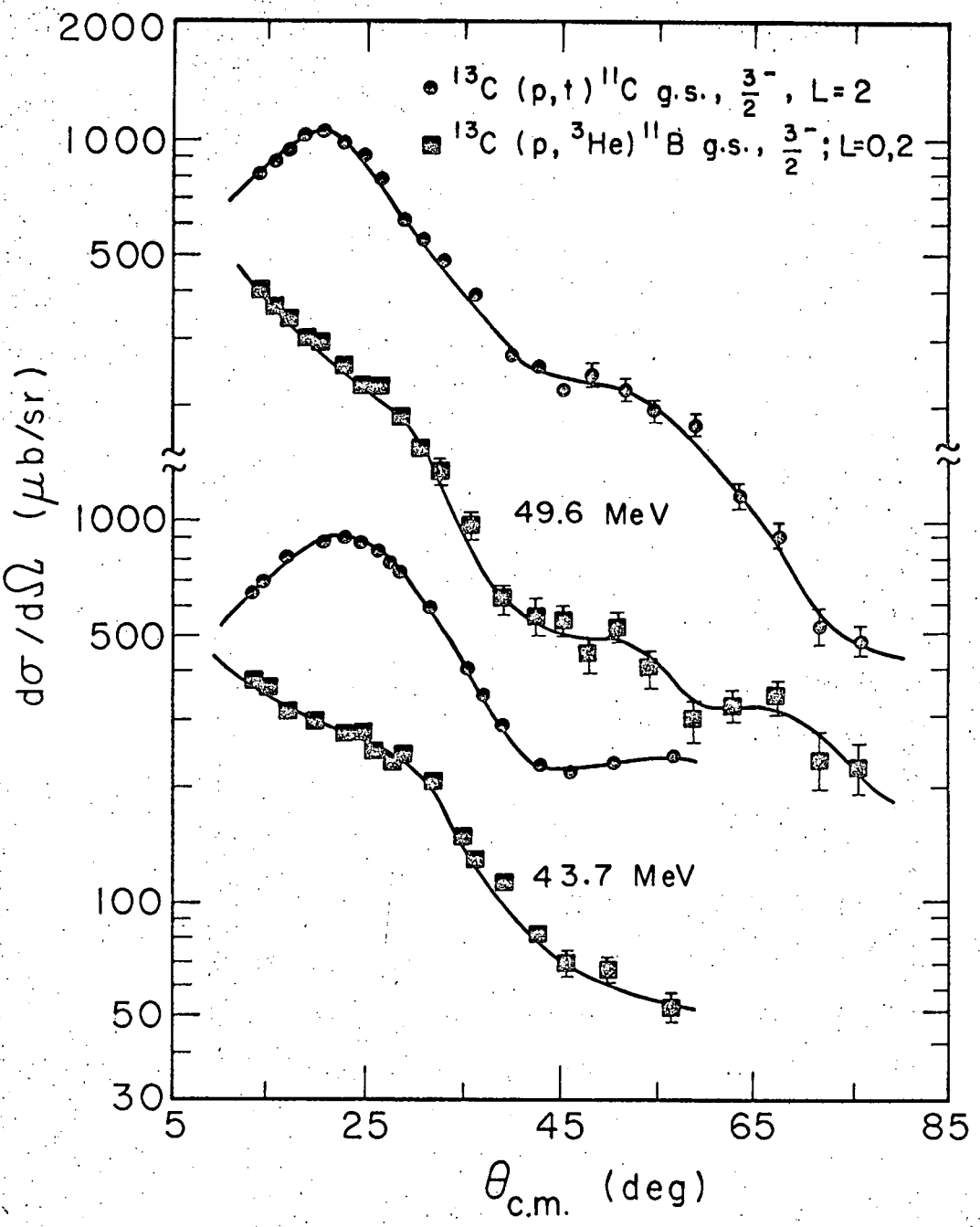


XBL678-3975

Fig. 30. Differential cross sections of the 43.7 and 49.6 MeV $^{13}C(p,t)$ and $(p,^3He)$ ground state transitions. The curves have no theoretical significance.

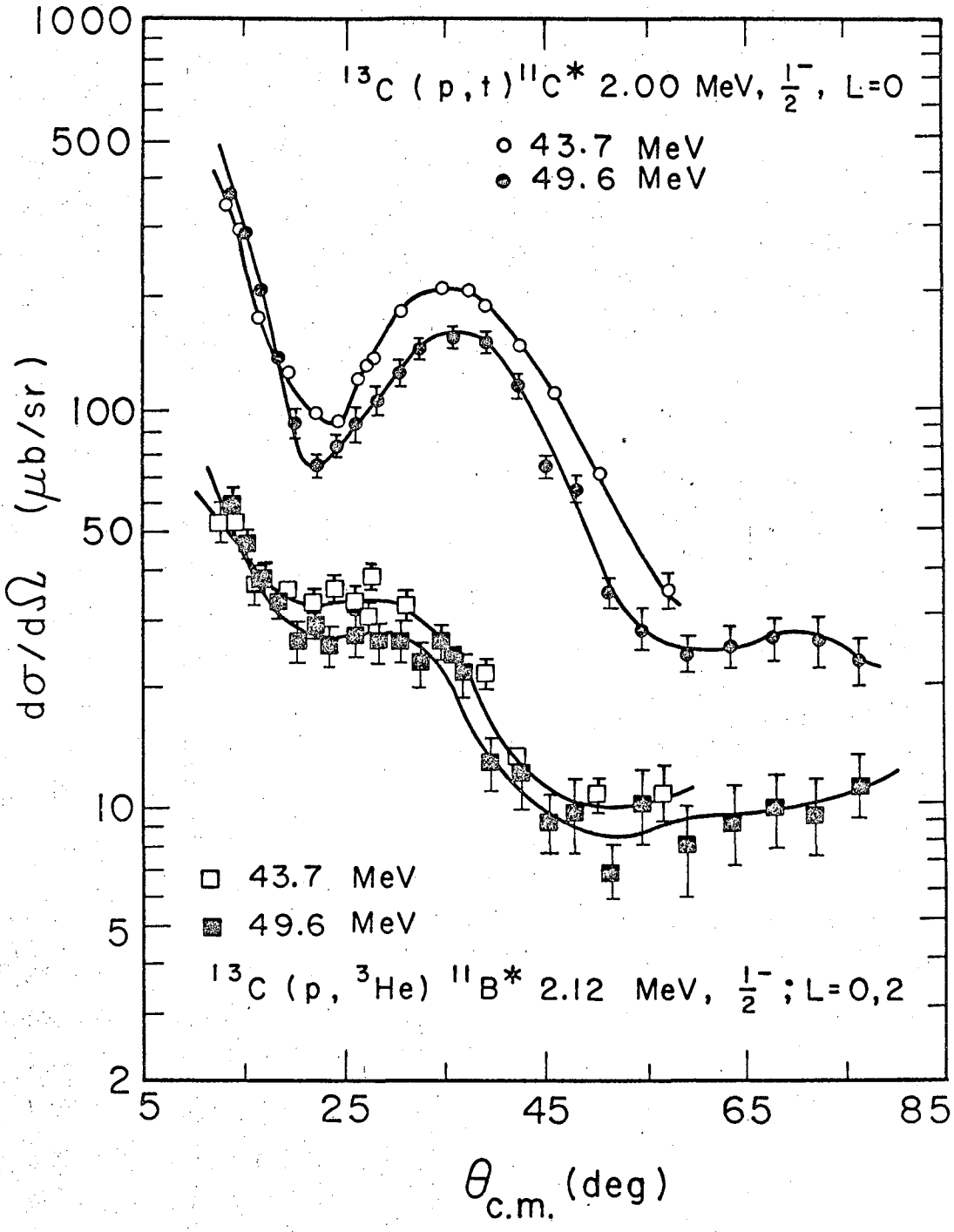


XBL678-3986

Fig. 31. Differential cross sections of the $^{13}C(p,t)^{11}C^*$ 2.00 and $^{13}C(p,{}^3He)^{11}B^*$ 2.12 MeV transitions at 43.7 and 49.6 MeV incident proton energies. The curves have no theoretical significance.

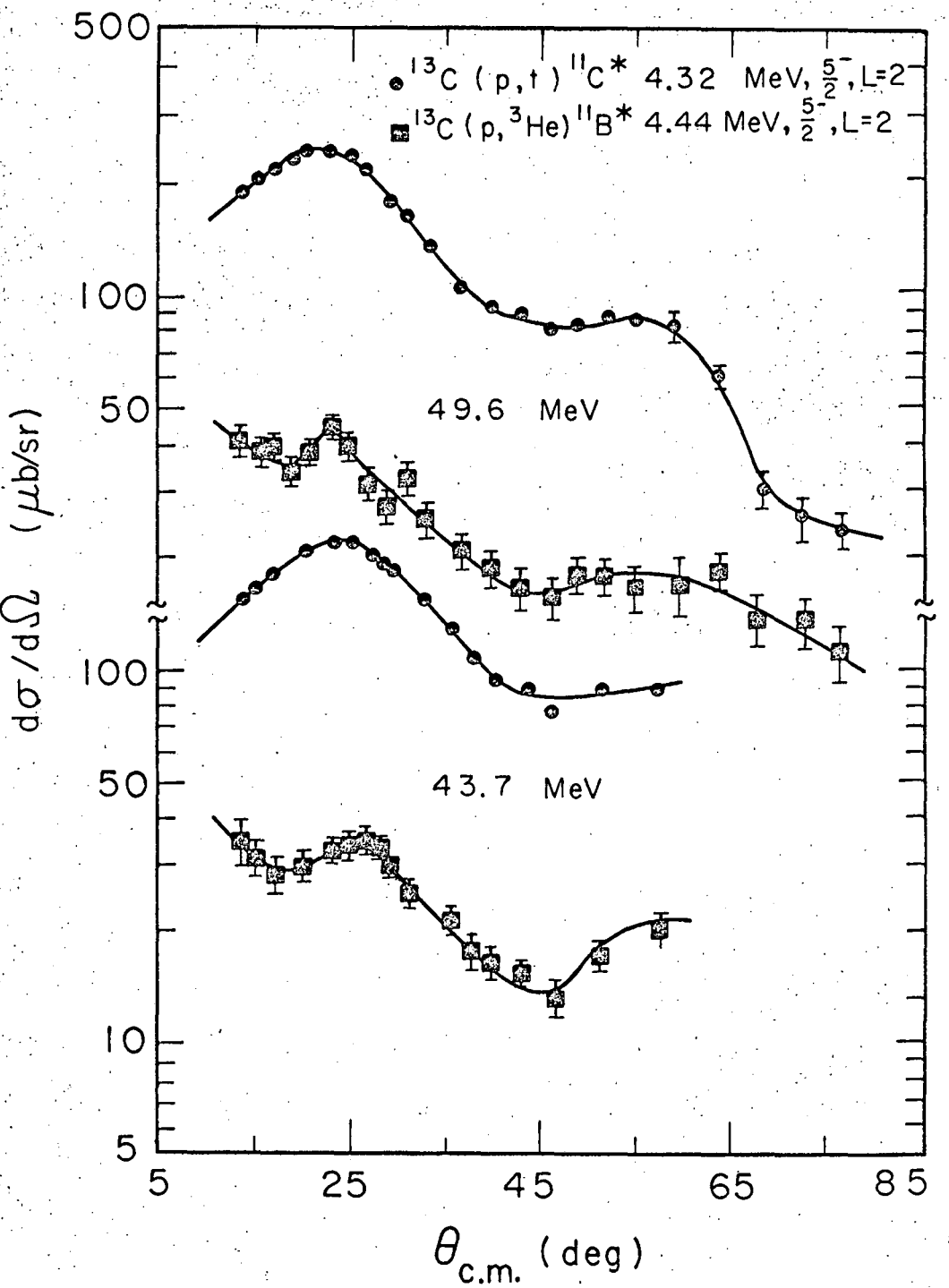


XBL678-3972

Fig. 32. Differential cross sections of the $^{13}C(p,t)^{11}C^*$ 4.32 and $^{13}C(p,^3He)^{11}B^*$ 4.44 MeV transitions at $E_p$ = 43.7 MeV and 49.6 MeV. The curves have no theoretical significance.

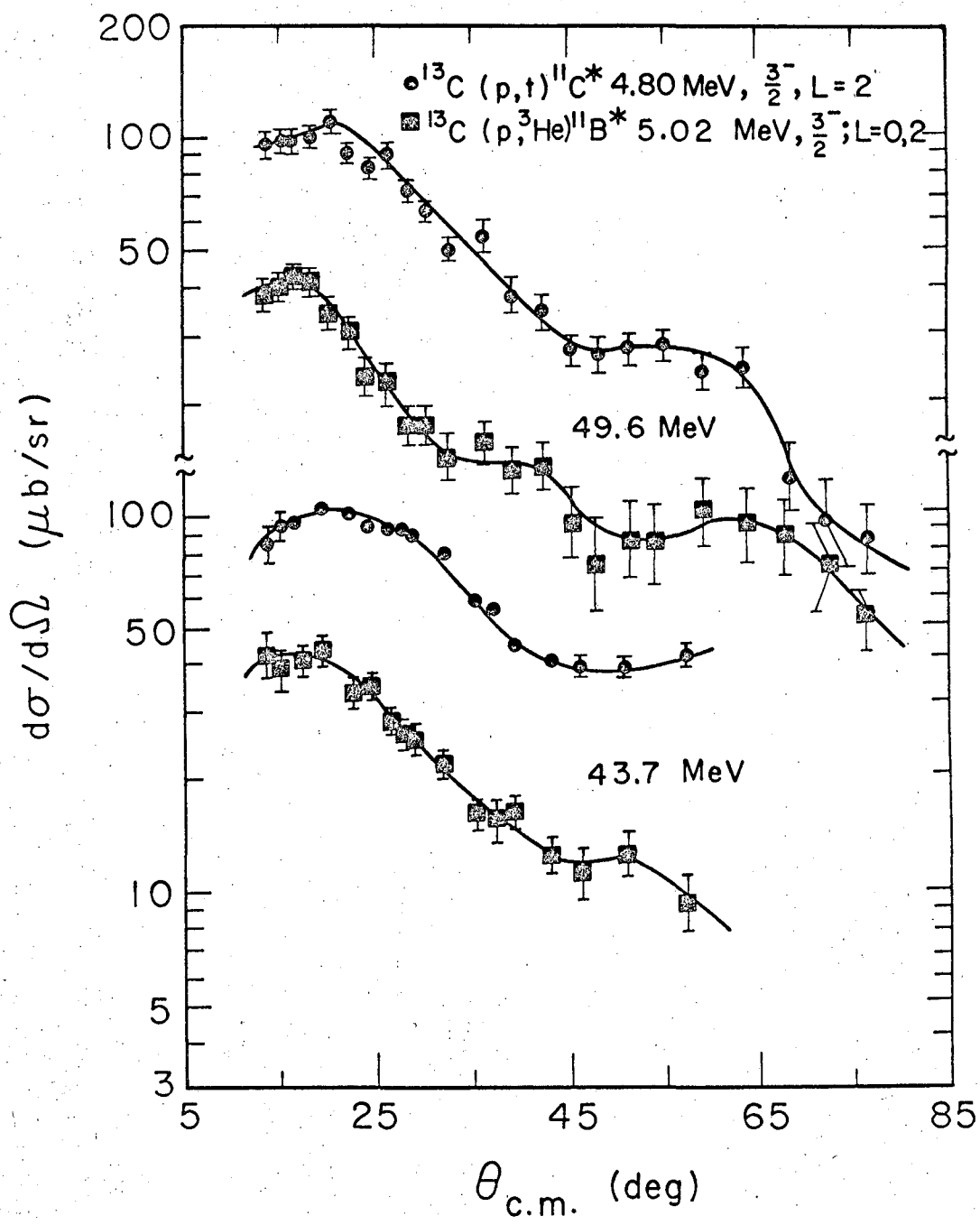


XBL678-3974

Fig. 33. Differential cross sections of the $^{13}C(p,t)^{11}C^*$ 4.80 and $^{13}C(p,^3He)^{11}B^*$ 5.02 MeV transitions at $E_p$ = 43.7 and 49.6 MeV. The curves have no theoretical significance.

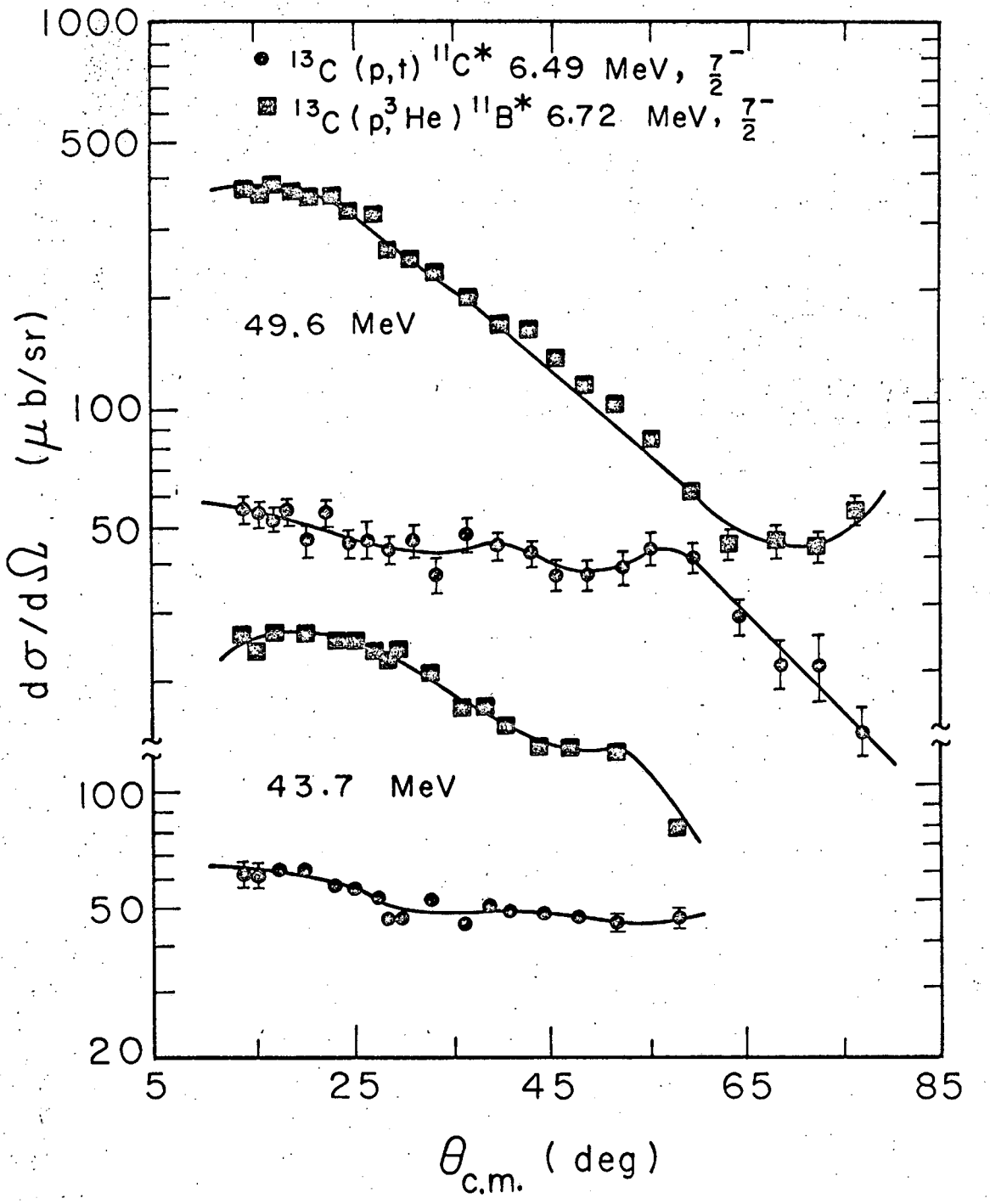


XBL678- 3978

Fig. 34. Differential cross sections of the $^{13}C(p,t)^{11}C^*$ 6.49 and $^{13}C(p,^3He)^{11}B^*$ 6.72 MeV transitions at $E_p$ = 43.7 and 49.6 MeV. The curves have no theoretical significance.

Table IX. Mass 11 levels and assumed jj configurations.

| $J^{\pi}$ | $^{11}C$ (MeV) | $^{11}B$ (MeV) | Configuration |
|---|---|---|---|
| $3/2^-$ | 0.0 | 0.0 | $(p_{3/2})^7_{3/2}$ |
| $1/2^-$ | 2.00 | 2.12 | $(p_{3/2})^6_0\ p_{1/2}$ |
| $5/2^-$ | 4.32 | 4.44 | $(p_{3/2})^6_2\ p_{1/2}$ |
| $3/2^-$ | 4.80 | 5.02 | $(p_{3/2})^6_2\ p_{1/2}$ |
| $7/2^-$ | 6.49 | 6.72 | $(p_{3/2})^6_3\ p_{1/2}$ |
| $1/2^-$ [T=3/2] | 12.48 | 12.84 | $(p_{3/2})^6_0\ p_{1/2}$ |

Table X. Major nuclear structure factors ($C_{ST}G_{NLSJT}$) for the states in mass 11.

| $J^{\pi}$ | $^{11}C$ (MeV) | $^{11}B$ (MeV) | $G_{NLSJT}$ | $^{11}C$ | $^{11}B$ |
|---|---|---|---|---|---|
| | | | 20110 | | .328 |
| $3/2^-$ | 0.0 | 0.0 | 12110 | | .183 |
| | | | 12021 | .915 | .450 |
| | | | 12120 | | .552 |
| | | | 20110 | | .298 |
| $1/2^-$ | 2.00 | 2.12 | 20001 | .473 | .232 |
| | | | 12110 | | .134 |
| $5/2^-$ | 4.32 | 4.44 | 12021 | .577 | .285 |
| | | | 12130 | | .855 |
| | | | 20110 | | .423 |
| $3/2^-$ | 4.80 | 5.02 | 12021 | .478 | .233 |
| | | | 12110 | | .212 |
| $7/2^-$ | 6.49 | 6.72 | 12130 | .0963[a] | .990 |
| $1/2^-$ [T=3/2] | 12.48 | 12.84 | 20001 | .334 | .328 |

[a] Calculated under the assumption of a 5% $(f7/2)^2_0$ admixture in the $^{13}C$ ground state and also assuming an $(f_{7/2}\ p_{1/2})$ pickup.

a. 0 MeV [$^{11}$C and $^{11}$B],3/2$^-$. This transition is restricted by two nucleon selection rules to a pure L=2 transfer for the (p,t) reaction, but both L=0 and L=2 transfers are allowed in the (p,$^3$He) reaction. The DWBA fits to these transitions are shown in Fig. 35 and are independently and separately normalized to the data. The fit to the (p,t) transition is very good; the (p,$^3$He) fit is reasonable, the theory predicting quite well the envelope of the cross section. A better fit to the (p,$^3$He) transition could possibly have been obtained if a complete intermediate coupling wave function had been used to describe the final state. The (p,t) transition, on the other hand, is characterized by only one L transfer and the shape of its angular distribution is insensitive to details of the final state wave function.

b. 2.00 MeV [$^{11}$C] and 2.12 MeV [$^{11}$B], 1/2$^-$. This transition is restricted to an L=0 transfer for the (p,t) reaction while the (p,$^3$He) transition is again a mixture of L=0 and L=2. The DWBA fits to these data, normalized independently of the ground state transition, are shown in Fig. 36. The (p,t) angular distribution is well predicted by calculation out to about 50°, but then shows a deep minimum where the data show little structure. The (p,$^3$He) fit is quite poor, showing almost an identical structure to that of the (p,t) transition, unlike the data. On the basis of the assumed wave functions, however, this similarity in shape can be readily understood by a nuclear structure calculation, as shown in Table X, where the L=0 strength of the (p,$^3$He) transition is expected to be roughly a factor of eight stronger than the L=2 strength.

c. 4.32 MeV [$^{11}$C] and 4.44 MeV [$^{11}$B], 5/2$^-$. Since these are 1/2$^-$ to 5/2$^-$ transitions, both the (p,t) and (p,$^3$He) reactions are restricted to pure L=2 transfers. As such, the angular distributions are expected to be very similar and this is generally found to be the case (Fig. 32), except at forward angles, where the (p,$^3$He) transition exhibits a slight forward angle rise not present in the (p,t) transition. The DWBA calculation for these levels is shown in Fig. 37 and although giving excellent agreement with the data for the (p,t) transition, it gives quite a poor account of the (p,$^3$He) angular distribution; this appears to particularly true at larger angles, although the theory is also unable to account for the observed forward angle rise. Figure 38 presents

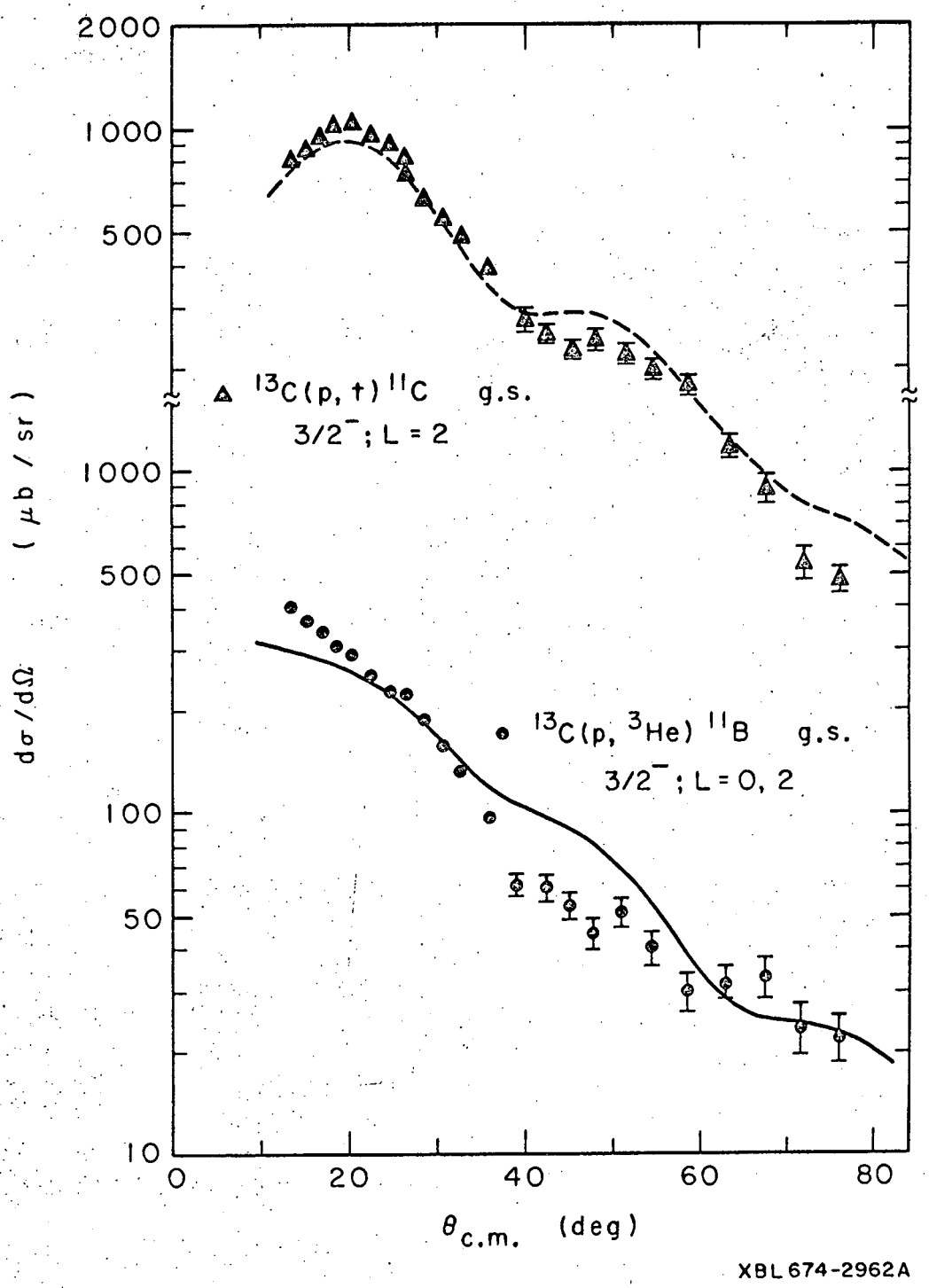


Fig. 35. Normalized DWBA fits to the 49.6 MeV $^{13}C(p,t)^{11}C$ and $^{13}C(p,{}^3He)^{11}B$ ground state transitions.

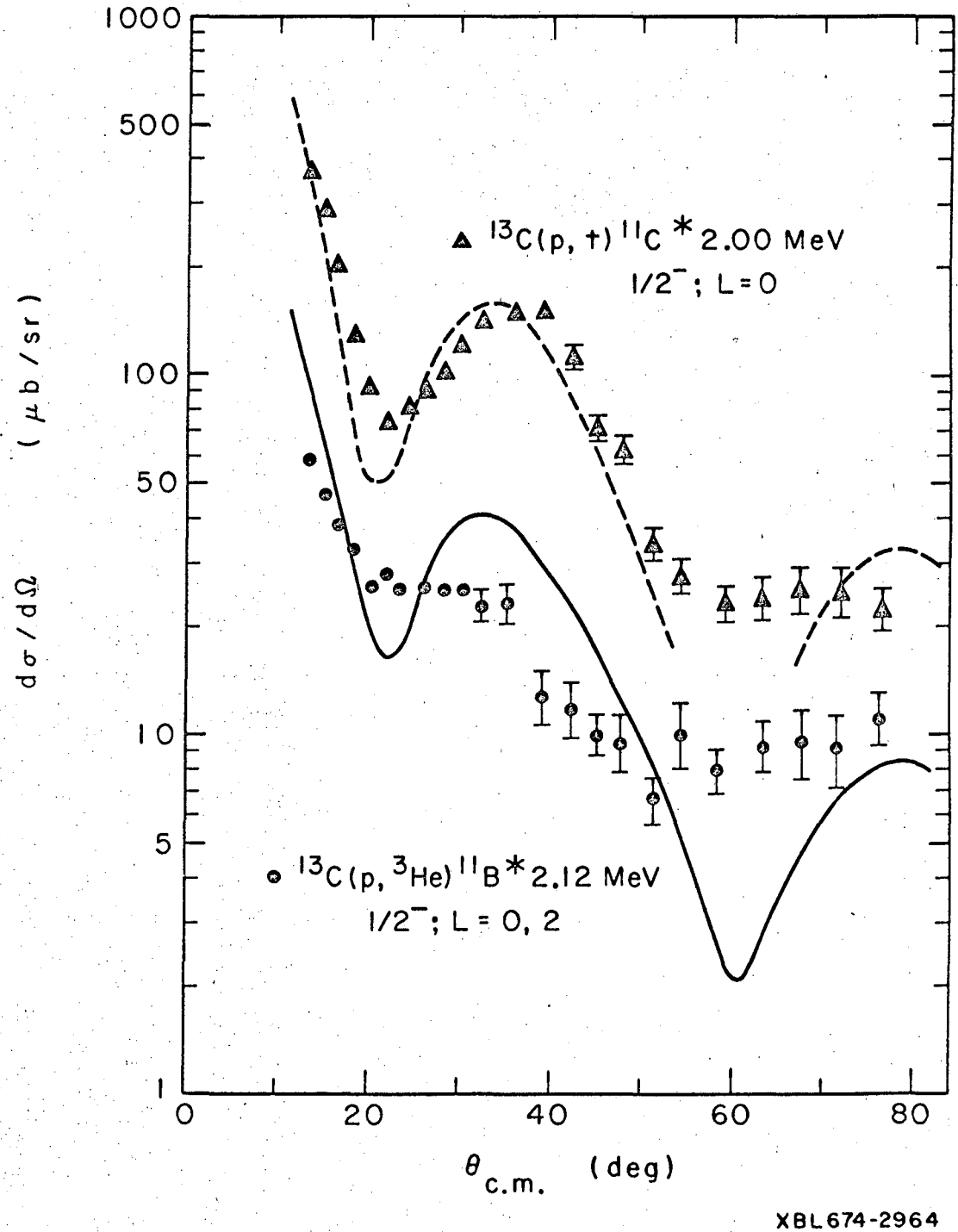


Fig. 36. Normalized DWBA fits to the 49.6 MeV $^{13}C(p,t)^{11}C^*$ 2.00 MeV and $^{13}C(p,^3He)^{11}B^*$ 2.12 MeV transitions.

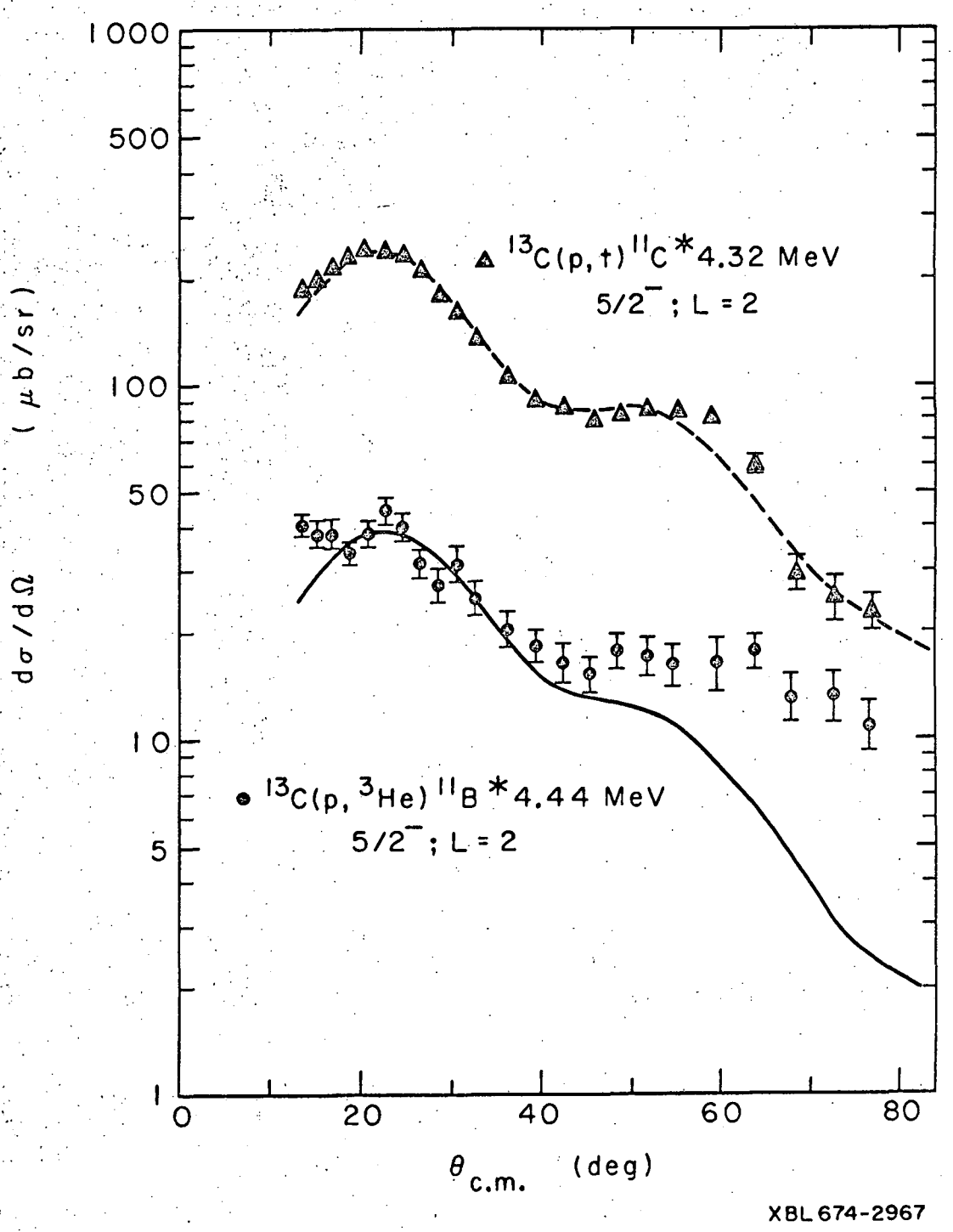


Fig. 37. Normalized DWBA fits to the 49.6 MeV $^{13}C(p,t)^{11}C^*$ 4.32 MeV and $^{13}C(p,^3He)^{11}B^*$ 4.44 MeV transitions.

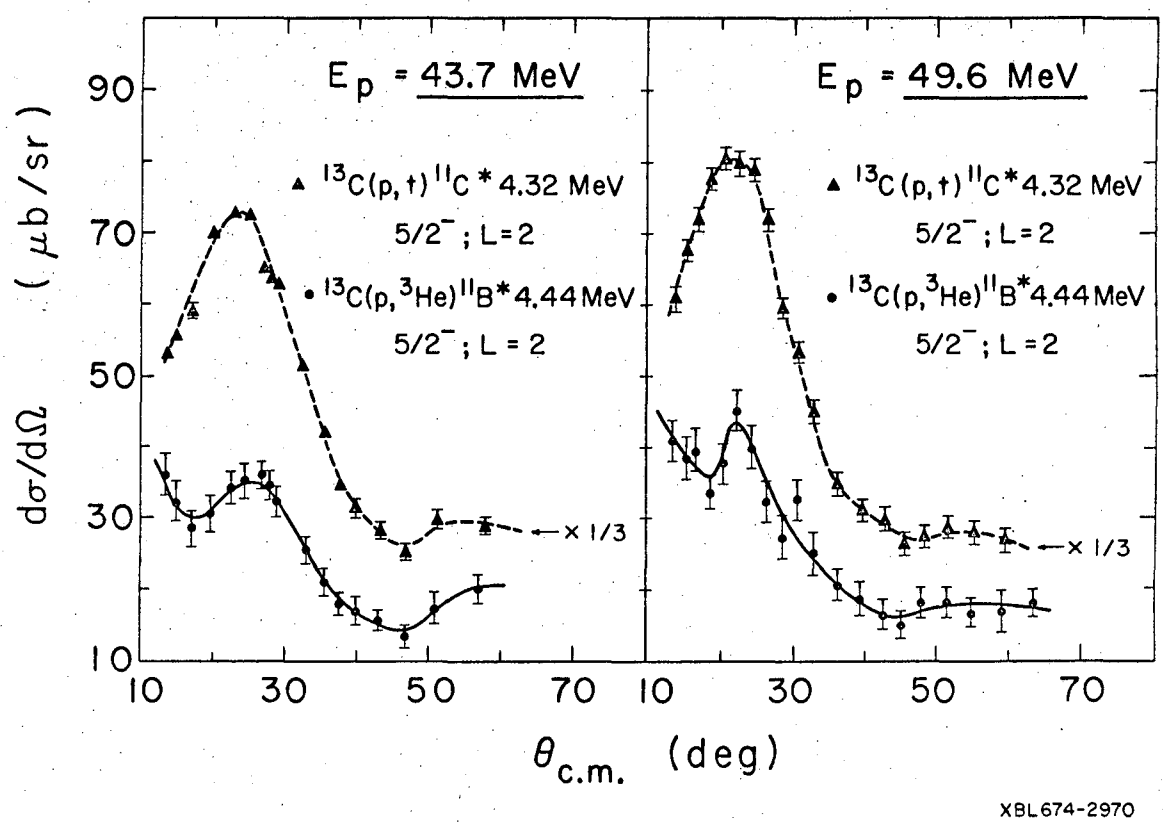


Fig. 38. Angular distributions of the $^{13}C(p,t)^{11}C^*$ 4.32 MeV and $^{13}C(p,^3He)^{11}B^*$ 4.44 MeV transitions at 43.7 and 49.6 MeV incident proton energies. The (p,t) cross sections have been multiplied by 1/3. The curves have no theoretical significance.

the angular distributions of these two transitions on a linear scale for the two beam energies. On this scale, the difference at forward angles between the (p,t) and (p,$^3$He) transitions is quite striking and is reproduced, well outside of statistical errors, at both energies. The fact that this behavior shows up in the (p,$^3$He) angular distribution, and not in the (p,t) has interesting implications for the reaction mechanism and this will be considered in a later discussion.

d. 4.80 MeV [$^{11}$C] and 5.02 MeV [$^{11}$B], $3/2^-$. Angular momentum selection rules for these transitions are the same as for the ground state transition; L=2 for the (p,t) and L=0,2 for the (p,$^3$He). This is the third L=2 transition observed in $^{11}$C and these three are shown together in Fig. 39. They are very similar in shape and in addition are remarkably similar to other L=2 (p,t) angular distributions on light nuclei (Figs. 9 and 15). For comparison the (p,$^3$He) angular distributions for the ground state, 2.12 MeV and the 5.02 MeV transition (all L=0,2 mixtures) are presented in Fig. 40. They show little reproduceable overall structure but in most cases do have the characteristic of rising at forward angles, where the (p,t) transitions are falling. This appears to be a general characteristic of most $1/2^-$ to $3/2^-$ or $1/2^-$ to $1/2^-$ (p,$^3$He) angular distributions on light (T=1/2) target nuclei, as can be further seen in Figs. 11 and 12 for other L=0,2 transitions in the $^{15}$N(p,$^3$He)$^{13}$C reaction.

The DWBA fits to the $^{13}$C(p,t)$^{11}$C$^*$ 4.80 MeV and $^{13}$C(p,$^3$He)$^{11}$B$^*$ 5.02 MeV transitions are given in Fig. 41. Again, the (p,t) transition is insensitive to the pure jj wave functions used to describe these states and the corresponding DWBA fit gives a good account of the data; the (p,$^3$He) fit, on the other hand, is very poor and did not significantly improve with any variation in the optical model parameters.

e. 6.49 MeV [$^{11}$C] and 6.72 MeV [$^{11}$B], $7/2^-$. Assuming that $^{13}$C can be well represented by a pure $(1p)^9$ configuration, then transitions from a $1/2^-$ initial state to a $7/2^-$ final state are not allowed in the (p,t) reaction. The exact nature of how these transitions are forbidden can be understood from the nuclear wave functions of the initial and final states. The intermediate coupling wave functions of Boyarkina[8] show that the first $7/2^-$ state in mass 11 is predominantly composed of the configuration $|^{22}F\rangle$ and $|^{22}G\rangle$, while the ground state wave function

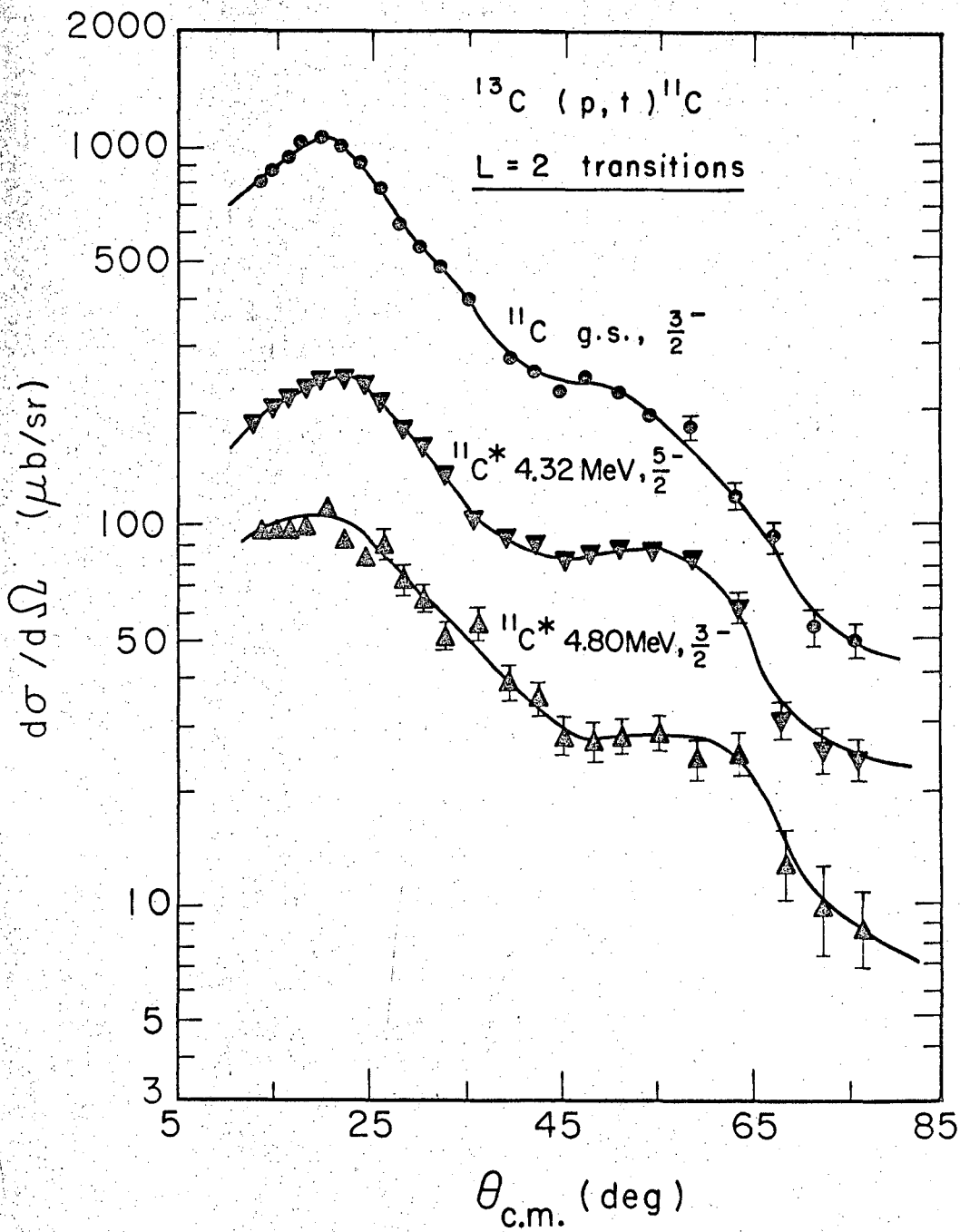


XBL678-3982

Fig. 39. Differential cross sections of the 49.6 MeV (p,t) L=2 transitions on $^{13}C$. The curves have no theoretical significance.

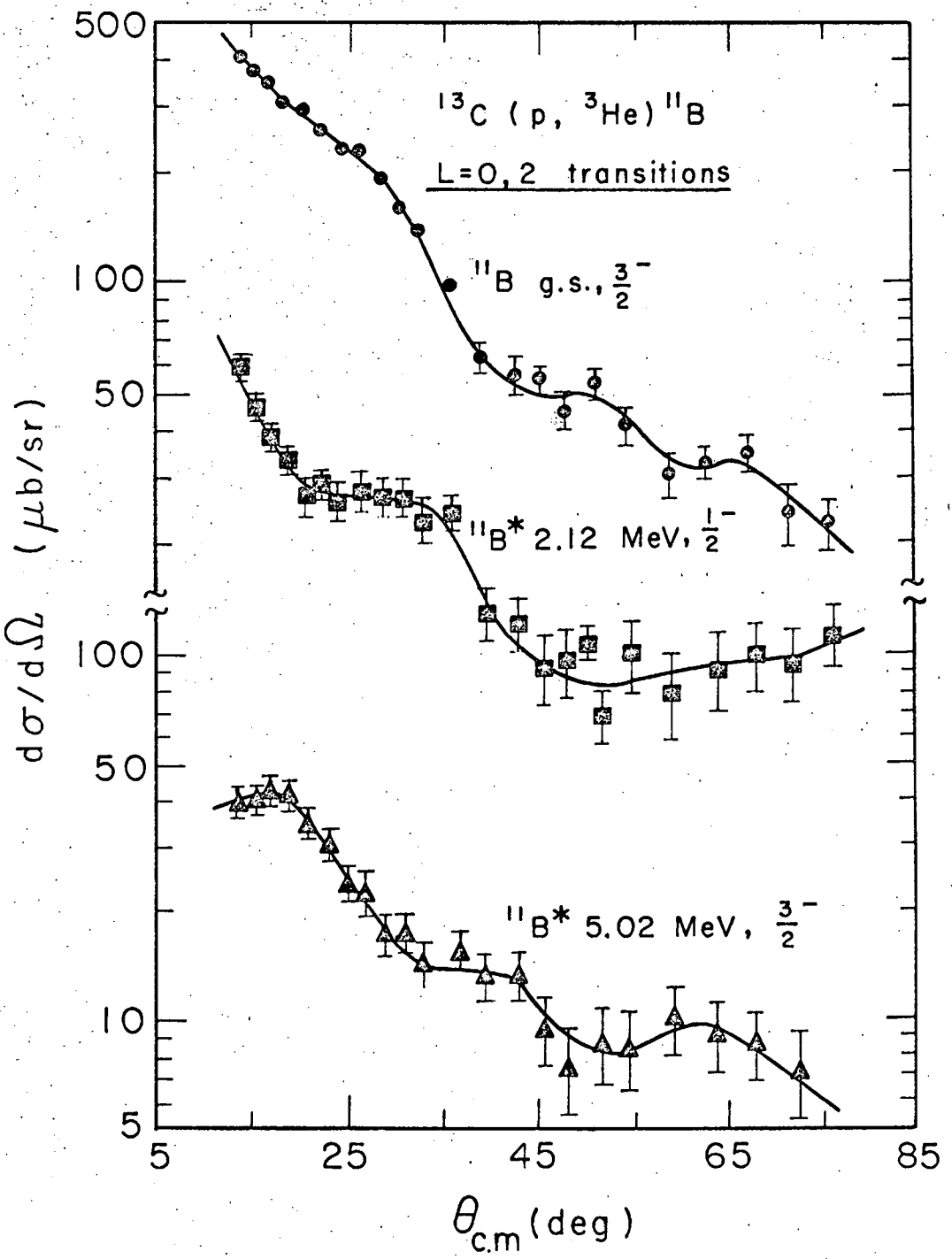


XBL678-3987

Fig. 40. Differntial cross sections of the 49.6 MeV (p,$^{3}$He) L=0,2 transitions on $^{13}$C. The curves have no theoretical significance.

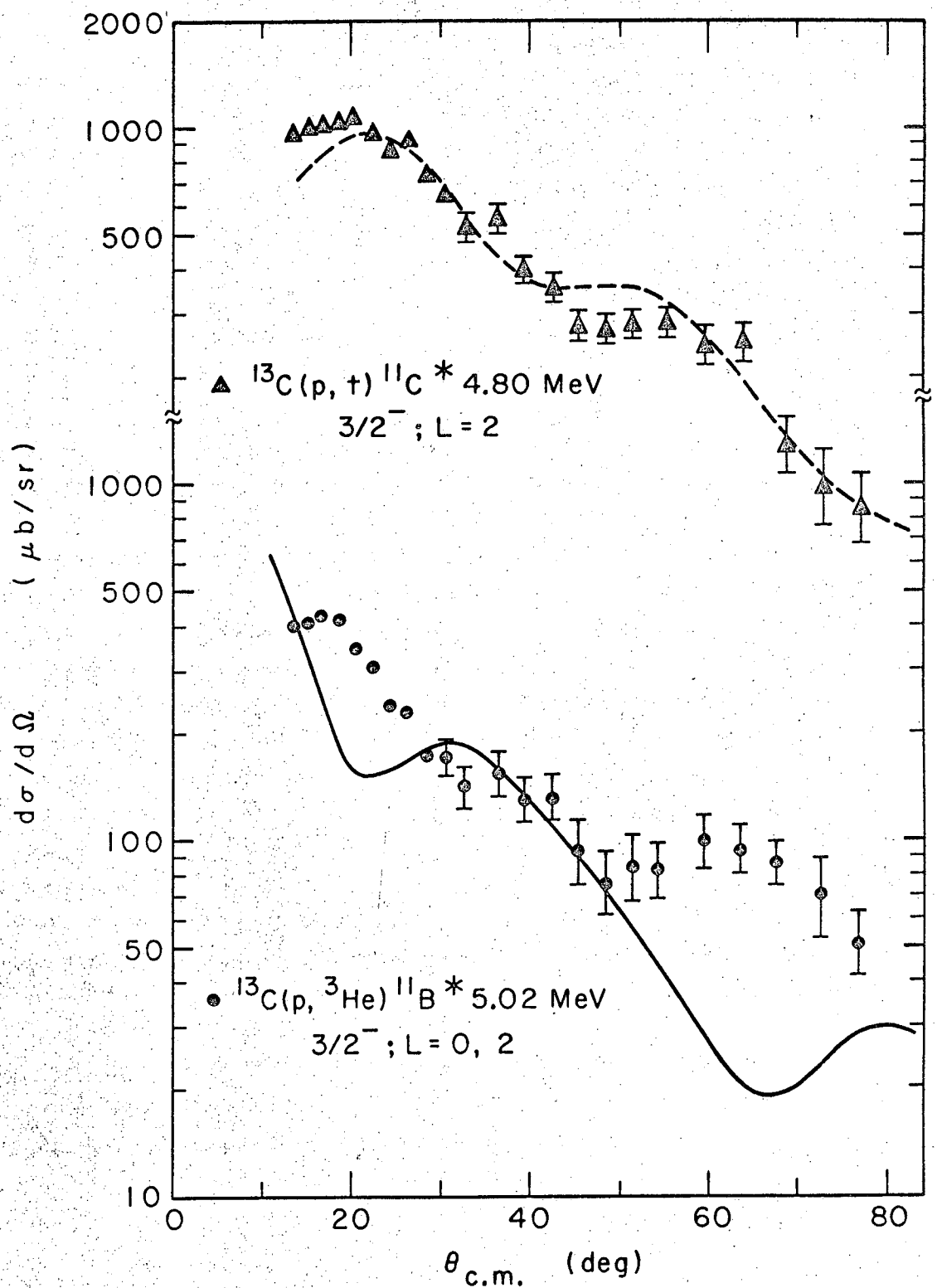


Fig. 41. Normalized DWBA fits to the 49.6 MeV $^{13}C(p,t)^{11}C^*$ 4.80 MeV and $^{13}C(p,{}^3He)^{11}B^*$ 5.02 MeV transitions.

is primarily $|^{22}P\rangle$ and $|^{22}D\rangle$. Thus the transition between initial and final states in the (p,t) reaction (assuming a transfer of two (1p) neutrons) is not "S-forbidden" and is generally not "L-forbidden" (the P→ G transition would not be allowed); it is in fact "J-forbidden", since conservation of angular momentum requires that J = L + S = 3, and this is not allowed in the (p,t) reaction because the spin transfer S is restricted to zero. The (p,$^3$He) transition, on the other hand, is not restricted in this way since S=1 is allowed; therefore, the (p,$^3$He) $1/2^-$ to $7/2^-$ transition proceeds via a pure J = 3, L = 2, S = 1 pickup of a neutron-proton pair.

The angular distributions of these two transitions are presented in Fig. 34 for 43.7 and 49.6 MeV incident protons. The shape of the (p,t) angular distribution is almost isotropic out to 60° and shows nothing of the diffraction structure which has characterized other (p,t) transitions to date. The DWBA fit to the (p,t) transition has been given previously (Fig. 28) and although not shown, it was also possible to get a reasonable fit to the (p,$^3$He) angular distribution.

Since the (p,t) transition is J-forbidden, one would a priori expect a very weak excitation of the $^{11}C^*$ 6.49 MeV ($7/2^-$) level, perhaps proceeding through second order processes such as core excitation or knockout. In fact, this level is relatively strongly excited (Table VII, Fig. 29), with a cross section only slightly smaller than the other $^{11}C$ excited states populated in the $^{13}C(p,t)^{11}C$ reaction. Since compound nuclear contributions can be regarded as insignificant at these high bombarding energies, then other explanations must be sought for the population of this state. Of the two mentioned above, core excitation and knockout, the latter mechanism would seem to be the more unlikely, since, in general, the selective population of final states seen in these reactions could not be understood if knockout were a contributing mechanism (Fig. 29). A core-excitation mechanism, on the other hand, does present a possible explanation for the excitation of this $7/2^-$ level.

Following the treatment outlined earlier (see Theory section), a core-excitation mechanism populating a given final state requires both a strong excitation of some parent state in the target via inelastic

scattering and a favorable overlap of this parent state with the configuration of the final state. Although no proton scattering on $^{13}C$ has been done at higher energies, the $^{13}C(\alpha,\alpha')^{13}C^*$ results of Harvey et al.[100] should give a good indication of which levels in the target nucleus would be strongly excited in the $^{13}C(p,p')^{13}C$ reaction. The data in Ref. 100 show a strong excitation of the $^{13}C^*$ 3.68 MeV $3/2^-$ state and this particular level will be assumed to be the only contributing parent state in the two-step reaction.

The overall matrix element could then be represented schematically as

$$T_2 \propto \langle 7/2^- | {}^1D_2 | 3/2^- \rangle \langle 3/2^- | Y_m^\ell(\hat{r}) | 1/2^- \rangle$$

where $Y_m^\ell(\hat{r})$ characterizes the inelastic scattering step which, in the absence of any "spin-flip", would be a quadrupole excitation. Two nucleon selection rules restrict the pickup of two neutrons in the second step to an L=2 transfer, so that this matrix element is characterized by a ${}^1D_2$ operator. The shape of the overall angular distribution and the strength of the transition will depend on these two amplitudes in such a way that it is probably not too meaningful to talk about a total angular momentum transfer as characterizing the reaction. In particular, if the inelastic excitation shows very little structure as, for example, the $^{12}C(p,p')^{12}C^*$ 4.43 MeV (L=2) transition at 30-50 MeV does,[101,57] then it may be reasonable to expect the kind of shape observed for the angular distribution of the $^{13}C(p,t)^{11}C^*$ $7/2^-$ transition (Fig. 34).

Since there would appear to be a reasonably strong excitation of a parent state (3.68 MeV, $3/2^-$) in the entrance channel, it is of interest to see if the overlap between this state and the $^{11}C^*$ 6.49 MeV ($7/2^-$) level is also favorable. This can be estimated by a nuclear structure calculation using the $^{13}C^*$ 3.68 MeV ($3/2^-$) state as the initial wave function. Using methods described in the Appendix, one finds that the nuclear structure factor for this $3/2^-$ to $7/2^-$ transition ($G_{12021}$) could have a value as large as 0.605, which when compared to those values for the "allowed" transitions in Table X, could be taken as an indication for a very favorable overlap between the $^{13}C^*$ $3/2^-$ and $^{11}C^*$ $7/2^-$ states.

This overlap coupled with a strong excitation of the parent state in the entrance channel could account for the relatively strong population of the 6.49 MeV $7/2^-$ level in the $^{13}C(p,t)^{11}C$ reaction.

It is interesting to note on the basis of the above model for core excitation, that a plausible explanation can also be advanced for the small angle rise observed in the $^{13}C(p,^3He)^{11}B^*$ 4.44 MeV ($5/2^-$) angular distribution. As noted earlier, this transition is restricted to an L=2 transfer and as such should be quite similar to the mirror (p,t) transition. However, as can be seen in Fig. 38, the (p,t) angular distribution does not show the forward angle rise observed in the $(p,^3He)$ angular distribution, the shape of which is reminiscent of an L=0 component in the cross section (compare Figs. 12, 14 and 40). An L=0 contribution to the $(p,^3He)$ cross section of this $5/2^-$ level is strictly forbidden on the basis of a direct pickup, but could be accounted for in a two-step reaction proceeding through the $^{13}C^*$ 3.68 MeV ($3/2^-$) level. Such a $3/2^-$ to $5/2^-$ pickup of a neutron-proton pair could take place by a $^3S_1$ transfer in the $(p,^3He)$ reaction; any such contribution to the mirror (p,t) transition, however, would still be restricted to L=2.

The above discussion, of course, can only be regarded as qualitative, since even if core excitation did play a dominant role in the excitation of the $5/2^-$ and $7/2^-$ levels which were discussed, many more parent states than the $^{13}C^*$ 3.68 MeV ($3/2^-$) level would surely be involved.

On the other hand, the assumption that the $^{13}C$ ground state can be represented by a pure $(1p)^9$ configuration may not be adequate and other admixtures, for example $(1f\ 7/2)^2$, should perhaps be considered. Any $(1f\ 7/2)^2$ mixed into the ground state of $^{13}C$ could account for the $^{13}C(p,t)^{11}C^*$ ($7/2^-$) transition by the <u>direct</u> pickup of a (1p 1f) neutron pair. No explicit calculations exist for the amount of $(1f\ 7/2)^2$ expected in the $^{13}C$ ground state, but other calculations on the amount of this impurity expected in 1p shell nuclei would indicate about 5%.[102] Assuming a 5% admixture of $(1f\ 7/2)^2$, then, the nuclear structure factor $G_{14041}$ for a $(p_{1/2}\ f_{7/2})$ pickup is calculated to be .096. Comparing this value to those of the other $^{11}C$ transitions shown in Table X would seem to imply that the state is too strongly excited to be accounted for by this relatively small structure factor (for example, the $^{11}C^*$ 4.80 MeV

($3/2^-$) transition might be expected to be a factor of 25 times stronger, when in fact the two cross sections are identical). A DWBA calculation, however, predicts a strong cross section for the $7/2^-$ transition. In fact, as is later indicated, its relative cross section, assuming a 5% admixture of $(1f\ 7/2)^2$, is predicted as well as the other negative parity states in the $^{11}C$ spectrum.

Moreover, although the shape of the angular distribution would not be expected to show such a lack of structure for a direct pickup, it is possible to obtain a good fit to the data with a DWBA calculation. Figure 28 presents this fit. As previously described, two curves are shown for this transition, corresponding to different choices of the oscillator parameter for the bound state wave function.

Mitigating against the direct pickup mechanism in the $^{13}C(p,t)^{11}C^*$ ($7/2^-$) transition are (1) uncertainties in the DWBA treatment of such quantities as the form factor for this type of transition, and (2) the absence of relatively strong transitions to positive parity states in $^{11}C$ arising from what would presumably be a greater than 5% admixture of $(2s\ 1d)^2$ in the $^{13}C$ ground state. (The 6.84 MeV ($5/2^+$) level in $^{11}C$ is populated stronges, but with a total cross section of only 33 μb (Table VII))

Of interest in the discussion of the levels to follow, will be Table XI, which presents the dominant configurations of the intermediate coupling wave functions of Boyarkina,[8] for the mass 11 levels in this region of excitation. The angular distributions of the levels to be considered below are presented in Fig. 42.

f. <u>8.10 MeV [$^{11}C$] and 8.52 MeV [$^{11}B$], $\leq 5/2^-$</u>. The 8.10 MeV level in $^{11}C$ was obscured at most angles by the $^{10}C$ ground state arising from the $^{12}C(p,t)^{10}C$ impurity reaction, so that an angular distribution for this level could not be obtained. The analysis of the 8.52 MeV level in $^{11}B$ was similarly obscured by transitions to the $^{10}B^*$ 1.74 and $^{10}B^*$ 2.15 MeV levels, also arising from the $^{12}C$ impurity. Nevertheless, an angular distribution for the $^{13}C(p,{}^3He)^{11}B^*$ 8.52 MeV transition was

Table XI. Dominant LS configurations (in percent) of the mass 11 intermediate coupling wave functions of Boyarkina.[8]

| $J^{\pi}$ | Theoretical Excitation (MeV) | $^2P$ | $^4P$ | $^2D$ | $^4D$ | $^2F$ | $^4F$ | $^2G$ | $^4G$ |
|---|---|---|---|---|---|---|---|---|---|
| $5/2^-$ | 11.1 | | 41 | | 32 | 11 | 10 | | |
| $1/2^-$ | 12.2 | 23 | 9 | | 64 | | | | |
| $3/2^-$ | 12.7 | 27 | 13 | 7 | 30 | | 18 | | |
| $5/2^-$ | 12.7 | | 3 | 4 | 5.0 | 78 | | | |
| $3/2^-$ | 13.7 | 8 | 32 | 19 | | | 36 | | |
| $9/2^-$ | 13.7 | | | | | | 11 | 89 | |
| $7/2^-$ | 15.4 | | | | 6 | 34 | 11 | 55 | |
| $5/2^-$ | 16.4 | | 34 | 22 | 13 | | 25 | | |
| $1/2^-$ | 16.9 | 1 | 78 | | 15 | | | | |
| $7/2^-$ | 17.4 | | | | 48 | | 32 | 16 | |
| $3/2^-$ | 17.9 | 8 | 15 | 7 | 58 | | 10 | | |

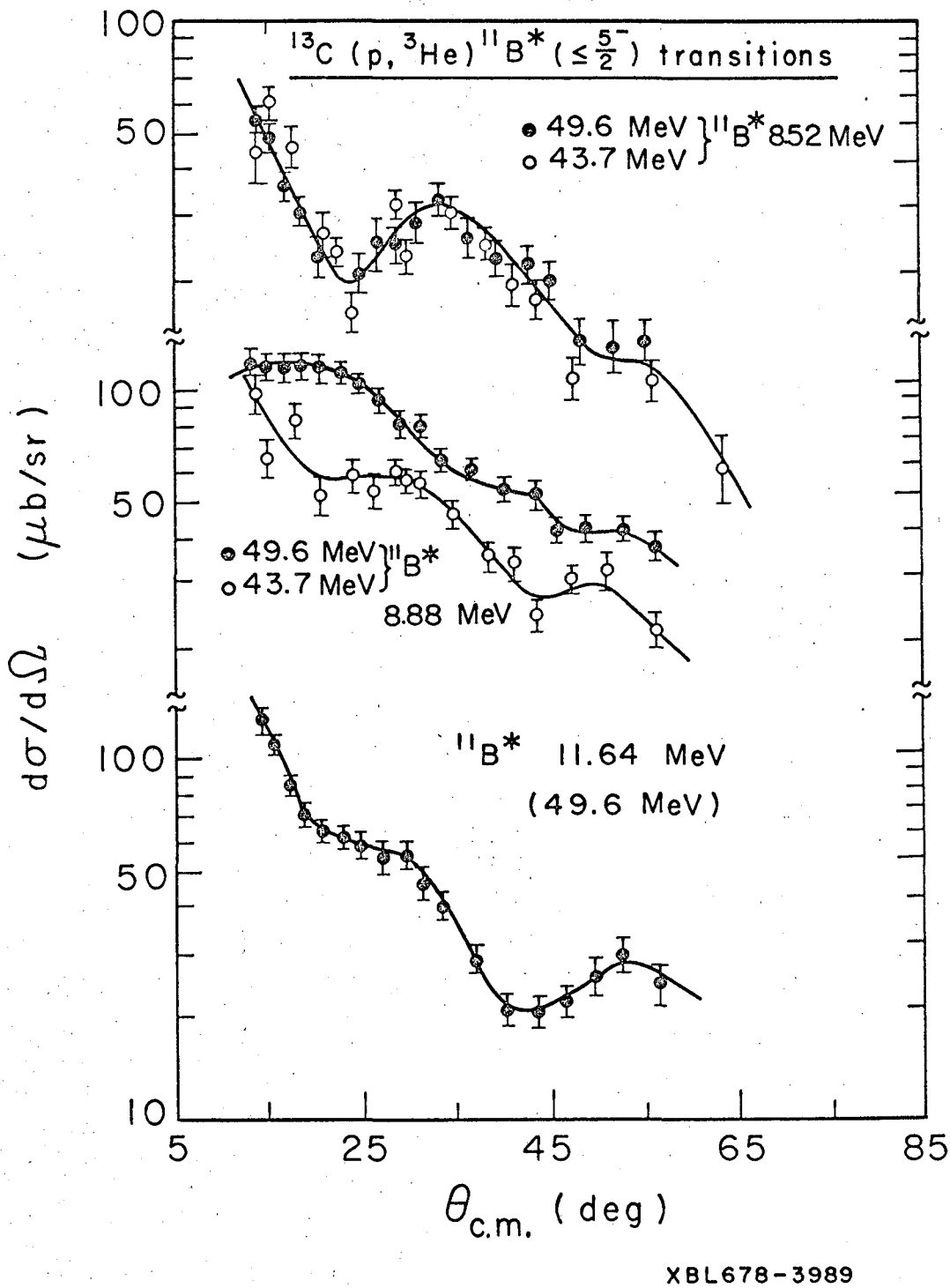


XBL678-3989

Fig. 42. Differential cross sections of some higher excited ($\leq 5/2^-$) transitions in the $^{13}C(p,{}^3He)^{11}B$ reaction at 43.7 and 49.6 incident proton energies. The curves have no theoretical significance.

obtained and is presented in Fig. 42 for the two beam energies considered, 43.7 and 49.6 MeV. The shapes are quite similar at the two energies, both having a sharp rise at forward angles with a structure indicative of a direct L=0, L=2 mixture (compare with Figs. 11, 12 and 40), thus implying a $1/2^-$ or $3/2^-$ spin and parity. These shapes are consistent with the previous assignment of this level as $\leq 5/2^-$. No attempt was made at a DWBA analysis of these data.

g. 8.43 MeV [$^{11}$C] and 8.88 MeV [$^{11}$B], $5/2^-$. The spin and parity of a level at 8.92 MeV in $^{11}$B has been previously determined[52] to be $5/2^-$, and this level likely corresponds to the one observed at 8.88 ± .05 MeV in the $^{13}$C(p,$^3$He)$^{11}$B reaction. The angular distribution is presented in Fig. 42, for 43.7 and 49.6 MeV bombarding energy. At forward angles, the shape of the angular distribution is not reproduceable at both energies and this could be due to unresolved $^{10}$B impurities at the lower energy. The 49.6 MeV data shows a reasonable L=2 shape, although somewhat less structured than those previously observed (compare Figs. 9, 13 and 39)

Although this 8.88 MeV level in $^{11}$B can be clearly seen at most angles, there is little evidence for excitation of the mirror level in $^{11}$C at 8.43 MeV,[52] even at forward angles. This is completely contradictory to almost all of the (p,t) and (p,$^3$He) mirror transitions discussed to date. As previously shown in Tables I, II, VII and VIII, the (p,t) transitions are found to be consistently stronger than their mirror (p,$^3$He) transitions and the implications of this will be considered in some detail later. Unfortunately, lacking proper intermediate coupling wave functions (in jj coupling) to describe the final state, one can only speculate as to the nature of this departure from the now established trend of stronger (p,t) than (p,$^3$He) transitions.

There have been previous examples of severely inhibited (p,t) transitions, notably in the "S-forbidden" transitions discussed in Ref. 10 for the $^7$Li and $^9$Be (p,t) and (p,$^3$He) reactions. On these light nuclei, where LS coupling is likely more appropriate, those final state configurations which are strongly quartet (S=3/2) can not be directly excited in the (p,t) reaction. Although it is less likely that such strongly quartet spin configurations would be present in the final states populated

in the $^{13}C(p,t)^{11}C$ reaction, the intermediate coupling wave functions of Boyarkina (Table XI) do indicate a high percentage of quartet spin states for the mass 11 levels in this region of excitation. On this basis, one would be forced to conclude that the above levels correspond to the calculated level in Table XI at 11.1 MeV, which is the first $5/2^-$ state predicted in this region. (This is actually the second $5/2^-$ state predicted by the intermediate coupling calculations of Ref. 8, the first one lying at 5.2 MeV and thereby corresponding well to the experimental values of 4.32 MeV in $^{11}C$ and 4.44 MeV in $^{11}B$). This particular level is 83% quartet, which would likely enhance the $(p,^3He)$ transition considerably.

If the calculated level at 11.1 MeV does correspond to the 8.43 and 8.88 MeV levels in $^{11}C$ and $^{11}B$, respectively, then this would imply that the levels at 8.10 and 8.52 MeV are either $1/2^-$ or $3/2^-$, since the first $5/2^-$ level would already be assigned. An assignment of either $1/2^-$ or $3/2^-$ to the 8.88 MeV level in $^{11}B$ would be consistent with its angular distribution in the $^{13}C(p,^3He)^{11}B$ reaction (Fig. 42).

h. <u>11.64 MeV [$^{11}B$] ($1/2^-$ or $3/2^-$)</u>. This is a further example of a transition in these mass 11 reactions which is strongly excited in the $(p,^3He)$ reaction but is virtually absent in the (p,t) spectrum. At some angles, there was an indication of a peak in the $^{11}C$ spectrum at about 11.3 MeV of excitation, but it was not possible to obtain an angular distribution. (There is a known[52] broad level at 11.45 MeV). The angular distribution (49.6 MeV data only) for the $(p,^3He)$ transition is presented in Fig. 42 and shows a structure strongly suggestive of a mixture of direct L=0 and L=2 transfers (compare with Figs. 11, 12 and 40), thus implying a spin and parity assignment of $1/2^-$ or $3/2^-$.

There are several known[52] $^{11}B$ levels in this region, most of which have been tentatively assigned as positive parity and as such could not correspond to the 11.64 MeV state by virtue of the strength with which it is excited. The width of this level (FWHM) was found to be 300 ± 70 keV. There is a broad level reported in Ref. 52 at 11.0 MeV, which is tentatively assigned as $5/2^-$, but it seems unlikely that this and the 11.64 MeV level discussed above could be the same state. No attempt was made at a DWBA analysis of this transition. Further spectroscopic comment can not be made without detailed intermediate coupling wave functions.

i. 12.48 MeV [$^{11}$C], 12.84 MeV [$^{11}$B], $1/2^-$, T=3/2. These levels correspond to the lowest 1p shell T=3/2 levels in the mass 11 nuclei. As such, they form the middle members of a quartet composed of $^{11}$Be($T_z$ = +3/2), $^{11}$B($T_z$ = +1/2), $^{11}$C($T_z$ = -1/2) and $^{11}$N($T_z$ = -3/2). Since $^{11}$Be is a shell model anomaly[103]--the 2s 1/2 level appears lower than the 1p 1/2 level-- then the lowest T=3/2 level in $^{11}$B and $^{11}$C could not be directly excited in these $^{13}$C(p,t)$^{11}$C and $^{13}$C(p,$^3$He)$^{11}$B reactions. No evidence has been seen in the previous discussion to indicate any significant admixture of $(2s\ 1d)^2$ in the $^{13}$C ground state; consequently a positive parity state could not be directly excited and the levels above thought to be T=3/2 states must correspond to an excited (negative parity) state of the $^{11}$Be nucleus.

The lowest negative parity T=3/2 states in $^{11}$B and $^{11}$C are expected to lie near 12.8 MeV of excitation, as calculated from the $^{11}$Be mass after correction for Coulomb energy and neutron-hydrogen atom mass differences. This value is in good agreement with the observed excitation of 12.48 MeV in $^{11}$C and 12.84 MeV in $^{11}$B. The first negative parity state in $^{11}$Be is known[52] to have a possible spin and parity of $1/2^-$, $5/2^-$ or $7/2^-$. If the levels described above are indeed the lowest negative parity T=3/2 states, then both the (p,t) and (p,$^3$He) reactions populating them are transitions from the same initial to identical final states and as such both proceed via an S=0, T=1 transfer of the nucleon pair. Two nucleon transfer selection rules then restrict these transitions to L=0, L=2 or L=4 transfers populating $1/2^-$, $5/2^-$ and $7/2^-$ final states, respectively. The angular distributions for these (p,t) and (p,$^3$He) transitions, at both 43.7 and 49.6 MeV, are shown in Fig. 43 (the (p,$^3$He) has been multiplied by the phase space factor, $k_t/k_{^3He}$, of 0.932 and 0.963, respectively); they are virtually identical, as expected for transitions populating T=3/2 final states within the framework of charge independence of nuclear forces. The (p,t) transition is shown again in Fig. 44, along with the $^{13}$C(p,t)$^{11}$C transitions (at 49.6 MeV) populating the $^{11}$C ground state ($3/2^-$, L=2) and first excited states ($1/2^-$, L=0). The T=3/2 transition is quite similar to the $^{11}$C$^*$ 2.00 MeV ($1/2^-$) L=0 angular distribution (the first maximum is shifted slightly inward, which is consistent with

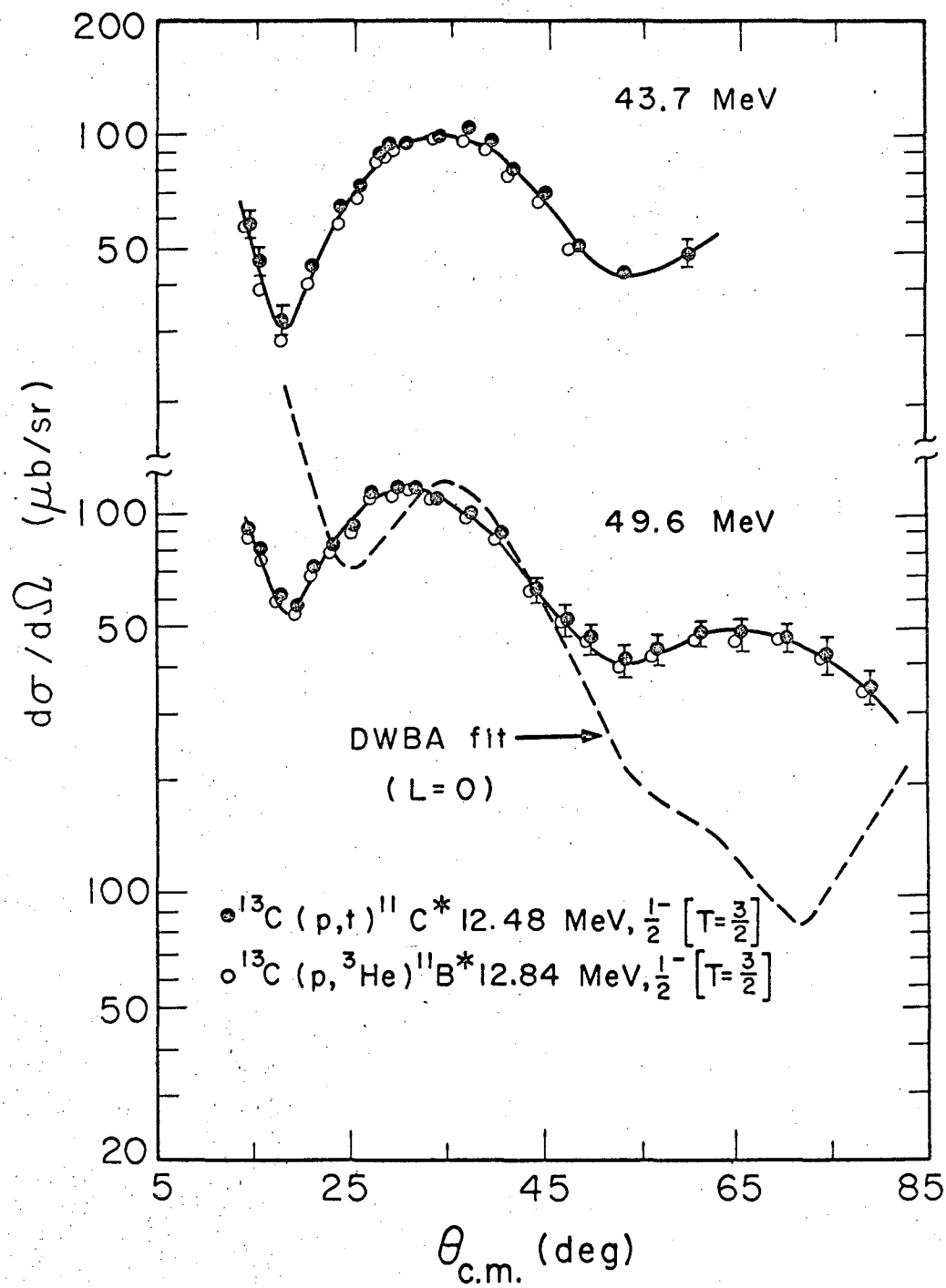


XBL678-3976

Fig. 43. Differential cross sections of the $^{13}C(p,t)^{11}C^*$ 12.48 MeV and $^{13}C(p,^3He)^{11}B^*$ 12.84 MeV ($1/2^-$, T=3/2) transitions at Ep = 43.7 and 49.6 MeV. The (p,$^3$He) cross sections have been multipled by the phase space factors 0.932 and 0.963, respectively. A DWBA fit (L=0) is shown for the 49.6 MeV data.

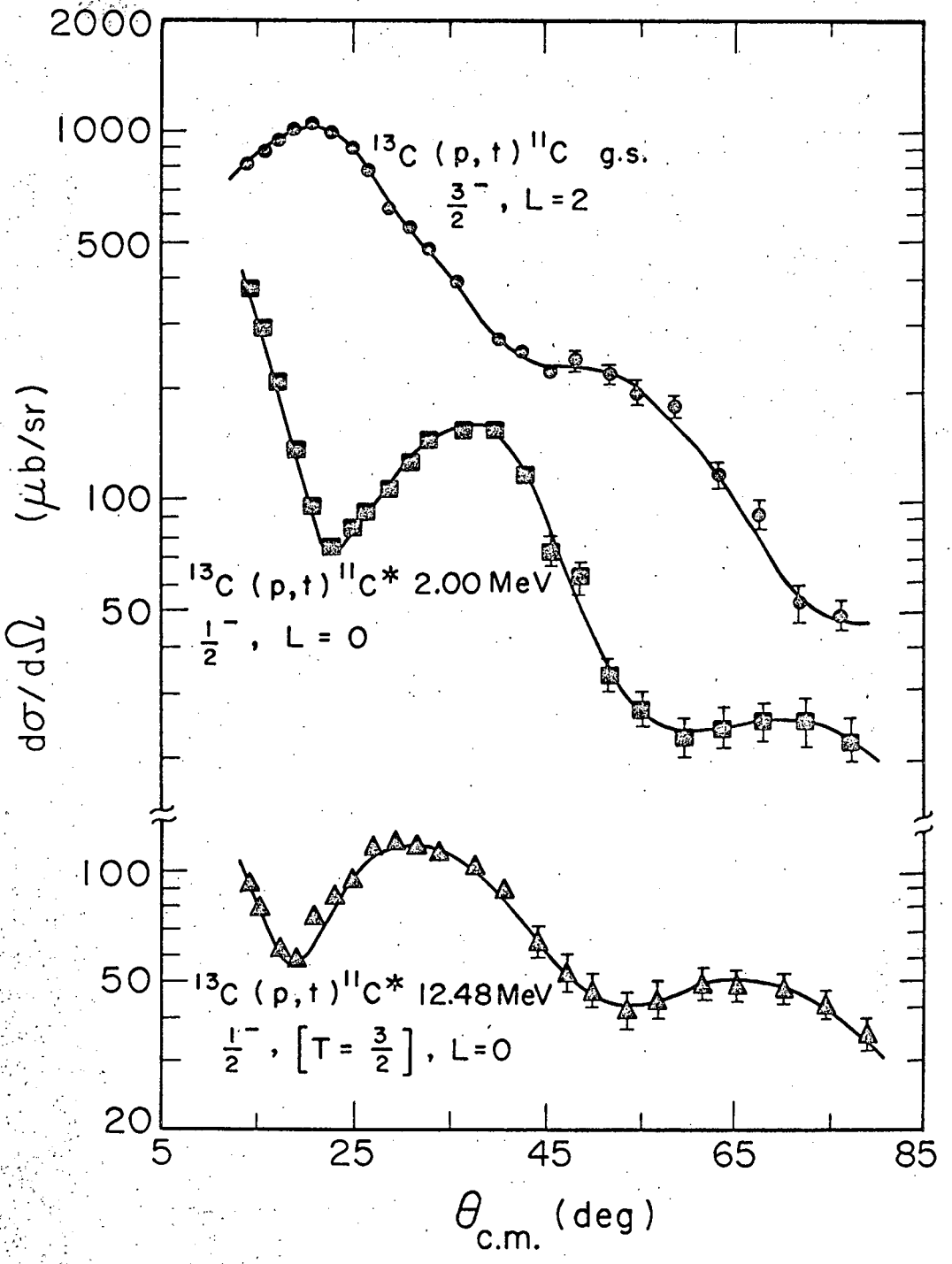


XBL678-3977

Fig. 44. Angular distributions of the 49.6 MeV $^{13}C(p,t)^{11}C$ transitions populating the ground ($3/2^-$), 2.00 MeV ($1/2^-$) and 12.48 MeV ($1/2^-$, T=3/2) states. The curves have no theoretical significance.

other (p,t) L=0 angular distributions to excited states, as can be seen in Fig. 14); it shows nothing of the structure of the $^{11}C$ ground state ($3/2^-$ L=2) angular distribution. This comparison is then a very good indication that these lowest negative parity states are $1/2^-$, and not $5/2^-$ or $7/2^-$. It is very unlikely that a $7/2^-$ state at this excitation would be so strongly excited, even though the $^{13}C(p,t)^{11}C^*$ 6.49 MeV ($7/2^-$) transition (see previous discussion) is surprisingly strong (Table VII); moreover, the angular distribution of this latter transition (Fig. 34) shows nothing of the structure observed in the above T=3/2 angular distributions.

Intermediate coupling calculations[7,8,70] (in the 1p shell alone) predict that the lowest negative parity T=3/2 state in $^{11}C(^{11}B)$ should be of $1/2^-$ spin and parity and should lie at about 13.5 MeV of excitation. In fact, the calculations of Ref. 8 show that a $5/2^-$ and a $7/2^-$ T=3/2 level should be 4 MeV and 12 MeV, respectively, further removed from the first $1/2^-$ T=3/2 level. These calculations and the evidence presented above seem to overwhelmingly indicate that the levels observed at 12.48 MeV in $^{11}C$ and 12.84 MeV in $^{11}B$ in the $^{13}C(p,t)$ and $(p,^3He)$ reactions, respectively, are indeed $1/2^-$ T=3/2 states.

The width (FWHM) of these $1/2^-$ T=3/2 levels are large, being 350 ± 40 keV for the $^{11}B$ state and 550 ± 50 keV for the $^{11}C$ state. However, these T=3/2 levels are expected to be wide since they both have T=3/2 channels energetically allowed for decay; the $^{11}C^*$ 12.48 MeV level can decay to the $^{10}B^*$ (1.74 MeV, T=1) level plus a proton and the $^{11}B^*$ 12.84 MeV level can decay to the $^{10}Be$ ground state ($T_z = +1$) plus a proton. The energies available for these modes of decay are 2.05 MeV and 1.61 MeV, respectively, which is consistent with the larger width observed for the $^{11}C$ state.

The DWBA fit to the 49.6 MeV (p,t) transition (the $(p,^3He)$ fit is the same) is shown in Fig. 43, and compared to the quality of fit previously discussed for the (p,t) reaction (which has always been restricted to a single L value), it is quite poor. The calculated angular distribution does not account for the position of the first minimum and moreover, predicts a minimum at 70° where the experimental data show little structure. However, this was also the case in the DWBA fit to the $^{11}C^*$ 2.00 MeV ($1/2^-$ L=0) transition (Fig. 36) and may reflect a basic inaccuracy in the optical model wave functions.

j. 6.84 MeV [$^{11}$C], $5/2^+$. As noted earlier, positive parity states cannot be directly excited in either the (p,t) or (p,$^3$He) reactions on a $^{13}$C($1/2^-$) target, assuming a pure $(1p)^9$ configuration for the $^{13}$C ground state. A weak level was observed at 6.84 MeV in $^{11}$C, which probably corresponds to the known[52] 6.90 MeV ($5/2^+$) level. (The mirror level at 7.30 MeV in $^{11}$B could not be seen due to contaminant peaks). The angular distribution to this 6.84 MeV ($5/2^+$) level was very similar to those observed in other "forbidden" transitions (Fig. 10) and is not shown. It was, however, relatively very weakly excited, with a total cross section of only 33 μb (Table VII), which may give evidence that the amount of $(d_{5/2})^2$ admixed into the $^{13}$C ground state is very small.

## V. THEORETICAL CROSS SECTIONS

In the prediction of absolute cross sections, single-nucleon transfer reactions have yielded impressive results. In such calculations, one is able to treat the motion of a single nucleon bound in a well quite accurately. Recent $(d,^3He)$,[64] $(d,p)$[58] and $(^3He,d)$[104] calculations have shown that absolute cross sections predicted by theory are in very good agreement with experiment, often to within 20 or 30%. In two-nucleon transfer reactions, however, the motion of the pair is obviously more complicated and the approximations inherent in the theory are correspondingly more suspect. For example, the zero range approximation[105] is probably much more inadequate in two-nucleon[106] than in one-nucleon transfer.[107] Broglia and Riedel,[6] using the theory under discussion, report on calculations of absolute cross sections for the $^{206}Pb(t,p)^{208}Pb$ reaction which are an order of magnitude too low, a difference they attribute as mainly due to the assumed simple (gaussian) structure of the triton wave function. The DWBA code used herein, consequently, is not programmed to calculate absolute cross sections and only <u>relative</u> cross sections will be compared in the discussion to follow.

The two-nucleon transfer theory under discussion has been successfully tested on targets of widely varying mass. Mangelson et al. have obtained good fits to the angular distributions found in the $^{12}C(^3He,p)^{14}N$ reaction[32] and Glendenning[33] has had equally good results in fitting the $^{208}Pb(p,t)^{206}Pb$ reaction. Since the shapes of the (p,t) angular distributions previously discussed (the $(p,^3He)$ being sensitive to the final state configurations) are also well predicted, it can be assumed that the present theory properly takes into account the dynamics of the two-nucleon transfer reaction.

## A. Mirror State Cross Section Ratios

Of interest is the ability of the theory to predict the magnitudes of the (p,$^3$He) transitions relative to the (p,t) transitions. A study of mirror transitions permits such comparisons with minimal uncertainty in the final state wave functions. Although such a study will depend somewhat on the choice of acceptable optical model parameters, the theoretical ratios of (p,t) to (p,$^3$He) cross sections should be relatively insensitive to this choice.

This investigation of mirror state transitions was carried out on the target nuclei $^{15}$N, $^{13}$C, and $^{31}$P. An explanation for the ratios of experimental cross sections from these targets is sought in terms of the theory based on a spin-independent nucleon-nucleon interaction ($A^S = A^T$) as well as the case of a strongly spin-dependent interaction ($A^S = 0.3A^T$). The introduction of this strongly spin-dependent force will alter the relative (p,t) and (p,$^3$He) cross sections and hence alter the ratios to be compared; in addition, it may also change the shapes of those (p,$^3$He) angular distributions in which multiple L values are allowed.

Of particular concern is an understanding of the general implications of the few observed experimental transitions in which the ratio of these cross sections is above the limit of 4/1 predicted by the theory. Two possible explanations, both of which introduce interference terms, are considered: either (1) a coherent sum on the (LS) angular momentum quantum numbers of the transferred pair must be taken into account, or (2) a core-excitation mechanism plays a role in the overall cross section, which is then coherent with the direct reaction path.

### 1. Discussion of Results

a. $^{15}$N(p,t)$^{13}$N and $^{15}$N(p,$^3$He)$^{13}$C transitions. Only the first three "strong" states of those previously discussed will be considered here. As noted earlier, the shapes of these (p,t) angular distributions (Figs. 20 thru 22) are well predicted. In addition, although not quite as well predicted, the (p,$^3$He) angular distributions shown in Figs. 20 thru 22 are also fairly well fit. All these previous (p,$^3$He) fits are for a spin-independent nucleon-nucleon interaction. The effect of

introducing a spin-dependent interaction is to alter the relative amounts of L=0 and L=2 in these (p,$^3$He) transitions, since the factor $C_{ST}^2$ in the differential cross section of Eq. (1) will be altered. The particular choice that has been made ($A^S = 0.3\ A^T$) strongly enhances the S=0 transfer, resulting in a considerable increase of the L=0 component in the ground state transition but causing little difference in the 3.68 MeV transition. The effect of this is shown in Fig. 45 which presents normalized (p,$^3$He) fits to the ground state ($1/2^-$) and 3.68 MeV ($3/2^-$) transitions, utilizing the spin-dependent interaction. The ground state transition is now better fit by the theory, while the $3/2^-$ transition shows no significant change. Although the (AX) optical model parameters used in this study were obtained by interpolation from parameters given in the literature for neighboring nuclei, and as such are certainly subject to inaccuracies, this effect of improving the ground state (p,$^3$He) fit by introducing the spin-dependent force does reproduce for other choices of the helium-3 potential. The fit to the 7.55 MeV ($5/2^-$) angular distribution shown in Fig. 22 is unaffected by a spin-dependent nucleon-nucleon interaction, since two-nucleon selection rules restrict this transition to a pure L=2 transfer. Before comparing (p,t) and (p,$^3$He) cross section ratios, it is of interest to ascertain whether Coulomb and kinematic effects on the relative cross sections are important. With identical structure factors, the DWBA integrated cross sections for (p,t) and (p,$^3$He) transitions to any given mirror pair were virtually identical,[108] so that theory and experiment can be directly compared for each such pair.

Figure 46 presents a comparison of theoretical cross sections with experiment for the (p,t) and (p,$^3$He) ground state transitions--the data are shown in μb/sr and the theory is given in arbitrary units with no relative normalization. Two theoretical comparisons of these transitions are shown--one for a spin-independent interaction and the other for the chosen spin-dependent interaction. Agreement between theory and experiment for the relative magnitudes of these transitions is certainly better in the case of the spin-dependent interaction. Similar comparisons have been made for the other levels and the ratios

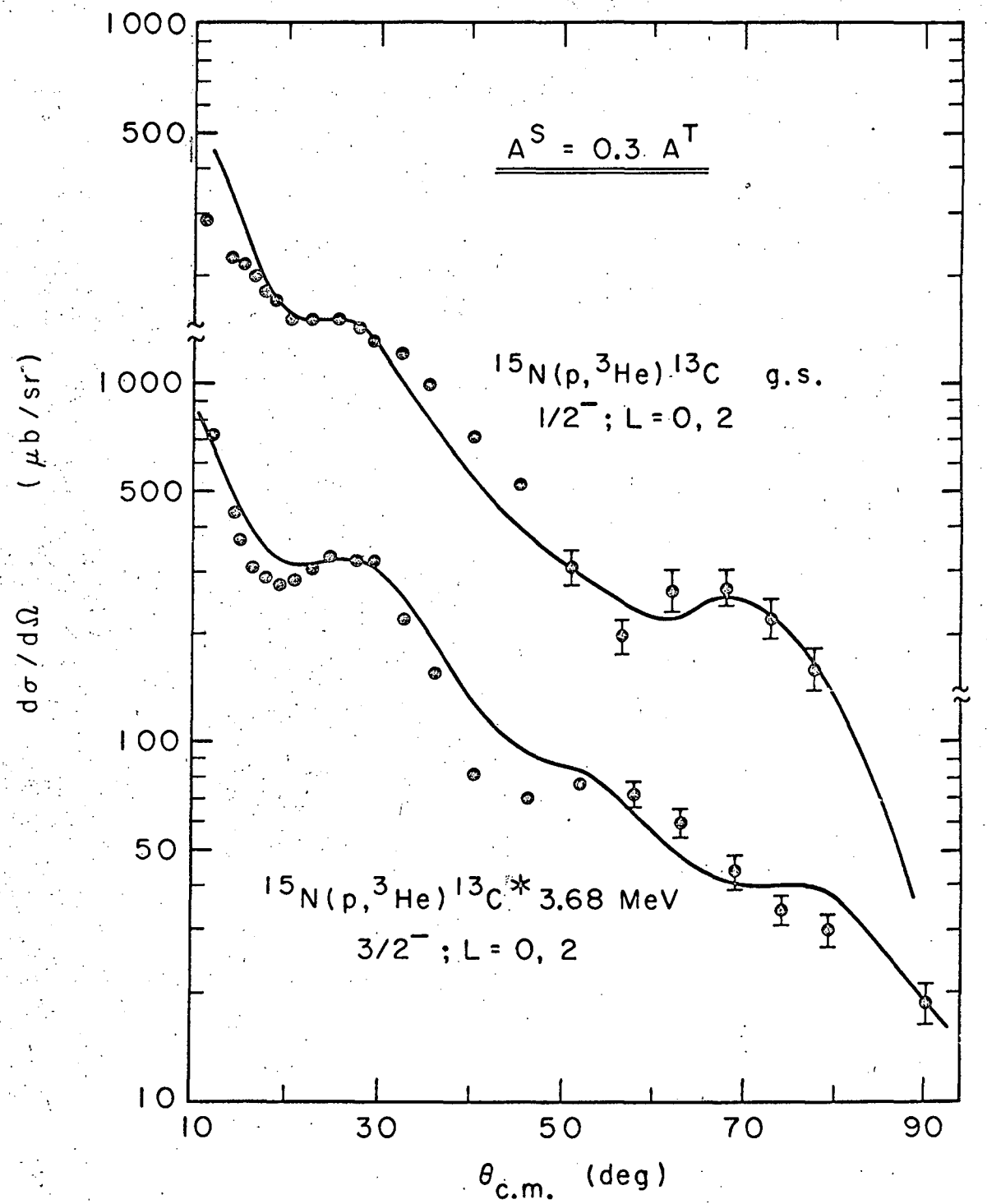


XBL674-2959-A

Fig. 45. The normalized DWBA fits to the $^{15}N(p,{}^3He)^{13}C$ ground and 3.68 MeV transitions utilizing the spin-dependent nucleon-nucleon interaction, $A^S = 0.3\ A^T$.

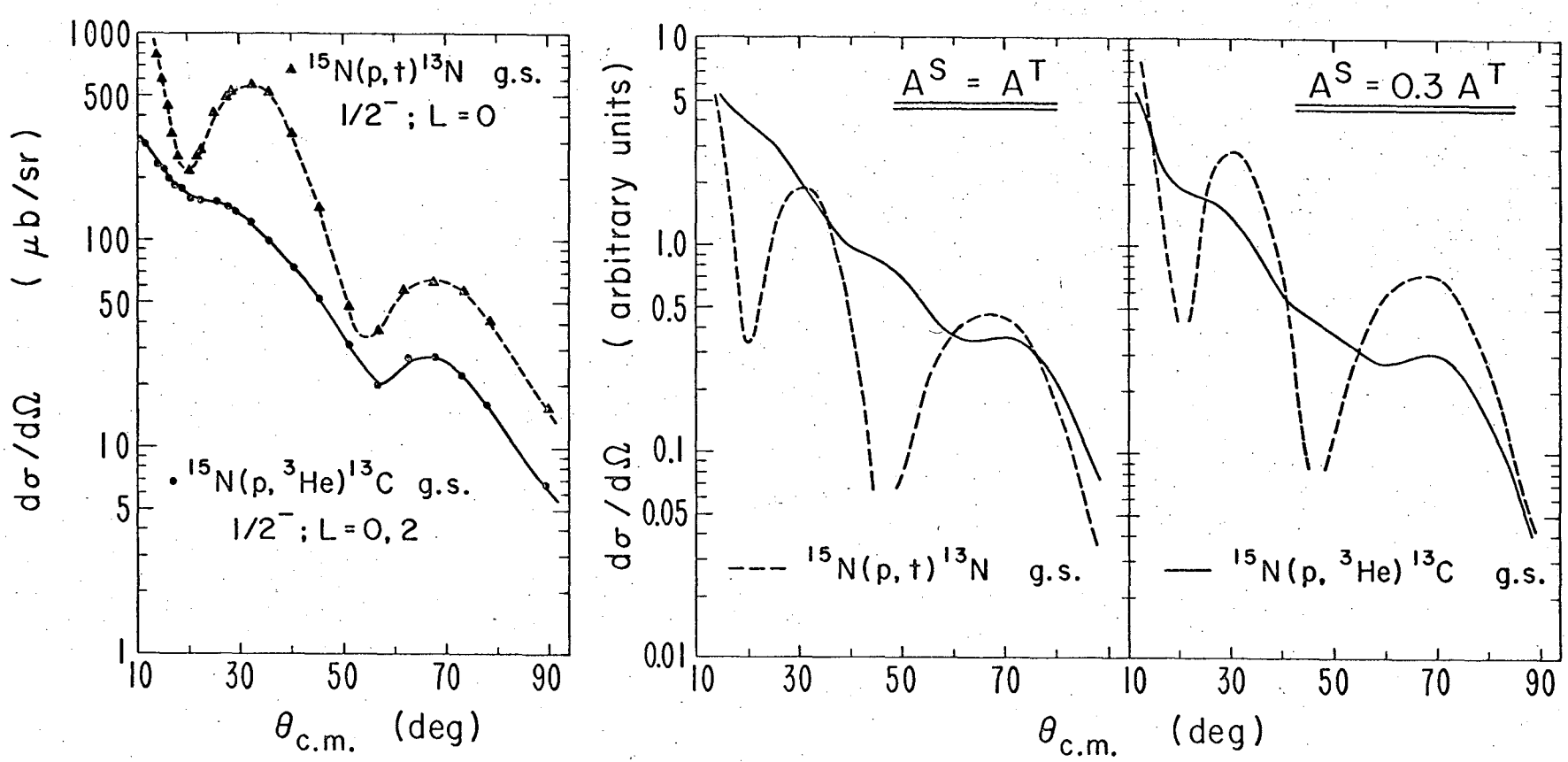


Fig. 46. (a) The $^{15}N(p,t)^{13}N$ and $^{15}N(p,^{3}He)^{13}C$ ground state differential cross sections. The curves have no theoretical significance. (b) Theoretical curves for these transitions utilizing a spin-independent nucleon-nucleon interaction. The dashed line represents the (p,t) cross section and the solid line the (p,3He) cross section. The theoretical cross sections are given in the same units and have not been normalized to each other. (c) as in (b), but with the spin-dependent ($A^S = 0.3\ A^T$) — nucleon-nucleon interaction.

(R) of (p,t) to (p,$^3$He) integrated cross sections (the theory being integrated over the same range as the experiment) are shown in Table XII, along with those for the $^{13}$C discussion which follows. The over-all result is that one has to invoke a strongly spin-dependent force in order to approach reasonable agreement between these theoretical ratios and experiment. Noting the table, it can be seen that the mass 13 $3/2^-$ level is quite well predicted by the choice of a spin dependence while the ground state ($1/2^-$) transition is not. Nevertheless, the average agreement with experiment for these two levels is considerably improved. Of particular interest is the experimental ratio for the $5/2^-$ transition, which is greater than the limit of 4/1. Accordingly, the theoretical ratio for this transition remains in poor agreement with the data, regardless of the value used for the spin-dependent nucleon interaction.

b. <u>$^{13}$C(p,t)$^{11}$C and $^{13}$C(p,$^3$He)$^{11}$B transitions</u>. Only the first four levels of those previously discussed will be considered here. DWBA fits for the (p,$^3$He) transitions have not been calculated for the spin-dependent interaction, as they were for the mass 13 final states, because the jj wave functions used to described these mass 11 final states are too uncertain. The previously discussed DWBA fits (Figs. 35 thru 37 and Fig. 41) are reasonable and should permit a comparison of (p,t) and (p,$^3$He) cross sections.

As observed earlier for transitions to mass 13 final states, the DWBA calculation of the (p,t) and (p,$^3$He) integrated cross sections to the several mass 11 mirror pairs, utilizing (p,t) nuclear structure factors for both, were essentially equal, so that theory and experiment can again be directly compared for each mirror pair. Figure 47 presents such a comparison for the ground state transitions, where the cross sections in μb/sr are compared with theoretical predictions for the case of a spin-independent and the spin-dependent interaction. The theoretical curves are plotted in arbitrary units without relative normalization. As such, they represent how well the theory accounts for the relative magnitudes of these (p,t) and (p,$^3$He) transitions. Note that the agreement is much better with the inclusion of the strongly spin-dependent interaction. Similar comparisons have been made for the other strong states excited in these reactions and the ratios (R) of (p,t) to (p,$^3$He) integrated cross

Table XII. Mass 13 and mass 11 experimental and theoretical integrated cross sections.

| $J^{\pi}$ | $^{15}N(p,t)^{13}N$ $\sigma_T(\mu b)$ (10-90°,c.m.) | $^{15}N(p,^3He)^{13}C$ $\sigma_T(\mu b)$ (10-90°,c.m.) | $R_{exp} = \frac{\sigma_T(p,t)}{\sigma_T(p,^3He)}$ | $R_{theory}$ $A^S = A^T$ | $R_{theory}$ $A^S = 0.3\ A^T$ |
|---|---|---|---|---|---|
| $1/2^-$ | 941 | 308 | 3.16 | .635 | 1.46 |
| $3/2^-$ | 652 | 573 | 1.14 | .686 | 1.50 |
| $5/2^-$ | 1271 | 270 | 4.72 | 1.71 | 2.72 |

| $J^{\pi}$ | $^{13}C(p,t)^{11}C$ $\sigma_T(\mu b)$ (10-80°,c.m.) | $^{13}C(p,^3He)^{11}B$ $\sigma_T(\mu b)$ (10-80°,c.m.) | $R_{exp} = \frac{\sigma_T(p,t)}{\sigma_T(p,^3He)}$ | $R_{theory}$ $A^S = A^T$ | $R_{theory}$ $A^S = 0.3\ A^T$ |
|---|---|---|---|---|---|
| $3/2^-$ | 1320 | 359 | 3.68 | 1.34 | 2.44 |
| $1/2^-$ | 310 | 63 | 4.92 | 1.51 | 2.74 |
| $5/2^-$ | 425 | 90 | 4.72 | .402 | 1.01 |
| $3/2^-$ | 167 | 58 | 2.88 | .875 | 1.84 |

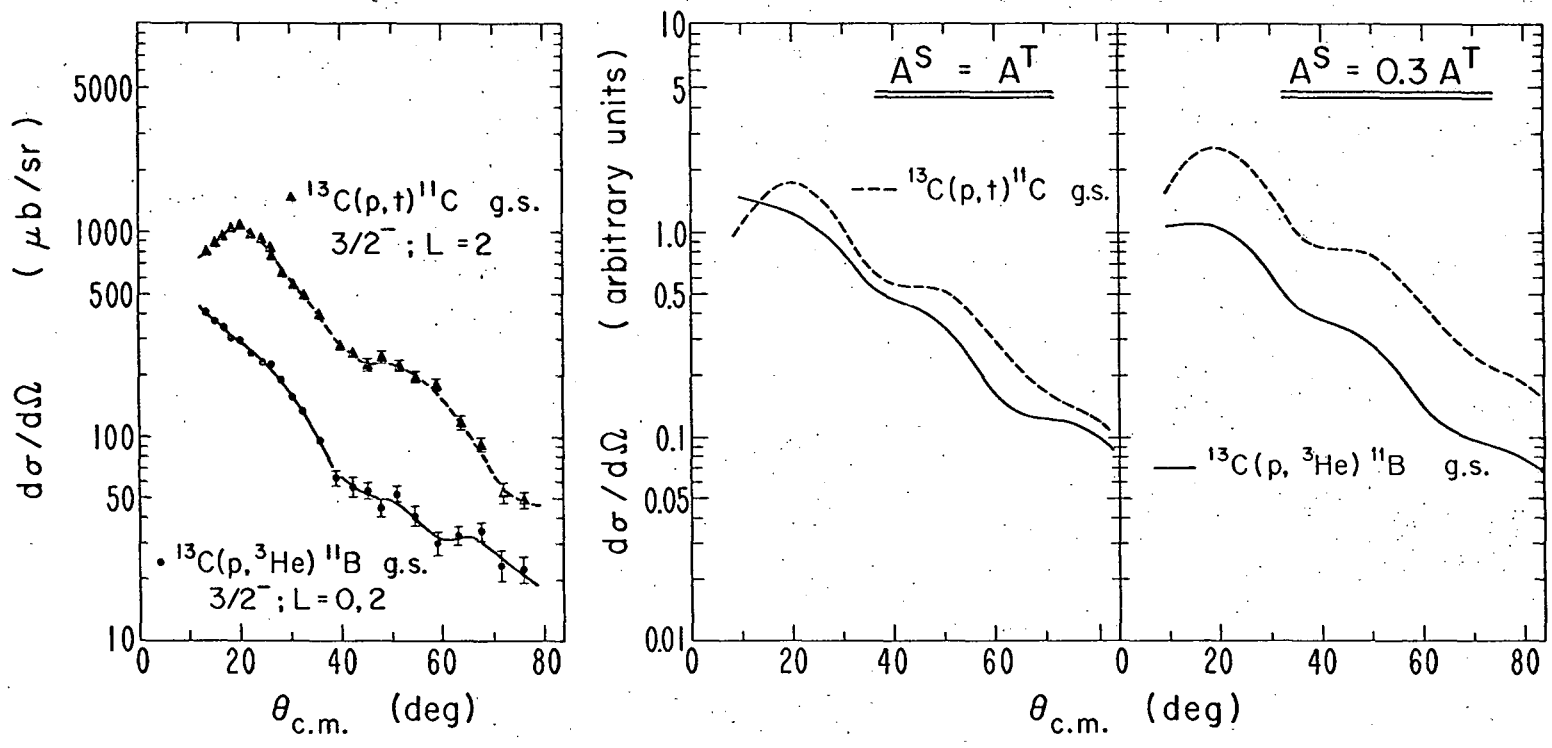


XBL674-2973-A

Fig. 47. (a) The 49.6 MeV $^{13}C(p,t)^{11}C$ and $^{13}C(p,^{3}He)^{11}B$ ground state differential cross sections. The curves have no theoretical significance. (b) Theoretical curves for these transitions utilizing a spin-independent nucleon-nucleon interaction. The dashed line represents the (p,t) cross section and the solid line the (p,$^{3}$He) cross section. The theoretical cross sections are given in the same units and have not been normalized to each other. (c) as in (b) but with the spin-dependent ($A^S = 0.3\ A^T$) nucleon-nucleon interaction.

sections (the theory being integrated over the same range as the experiment) are shown in Table XII. However, and unlike the $^{15}N$ reactions, relatively poor agreement is obtained for each level, even in the limit of a strong spin dependence. Nevertheless, the results for these mass 11 final states are still consistent with what was found for the mass 13 final nuclei--that agreement between theory and experiment improves as one goes to a strongly spin-dependent interaction.

The most important feature of the $^{13}C$ data shown in Table XII is the experimental ratio for the $1/2^-$ and $5/2^-$ integrated cross sections, both of which are well outside the 4/1 limit expected for a pure S=0 transfer of the neutron-proton pair. The theoretical ratios for these transitions, even in the case of strong spin dependence, are in very poor agreement with experiment. In order to emphasize this, the differential cross sections for these $1/2^-$ and $5/2^-$ (p,t) and (p,$^3$He) transitions are shown again in Fig. 48. At forward angles, where direct reaction contributions to the cross section are expected to be at a maximum, the (p,t) transition is favored over the (p,$^3$He) by factors as large as six or seven.

There are now three examples where the ratios of (p,t) to (p,$^3$He) cross sections are beyond the limit predicted by theory. Table XIII presents the total cross section of these cases integrated just over the forward angles of the data and compares the results with those obtained over the total angular range considered earlier. Also shown are the theoretical predictions for the spin-independent interaction, integrated over the same angular range. For the mass 11 levels, the disagreement between theory and experiment is much more striking when considered over this limited range of angles.

c. <u>$^{31}P(p,t)^{29}P$ and $^{31}P(p,^3He)^{29}Si$ g.s. transition</u>. All the other available data on T=1/2 targets [those of $^7Li$, $^9Be$ (Ref. 10) $^{27}Al$ (Ref. 44), $^{31}P$ (Ref. 44) and $^{39}K$ (Refs. 45, 109)] are consistent with the previously mentioned general trend, that unless inhibited by nuclear structure considerations, the (p,t) transition is stronger than the corresponding mirror (p,$^3$He) transition. This is shown in Table XIV where the experimental results for the cross section ratios of (p,t) to (p,$^3$He) reactions on these targets are given. Two values are shown:

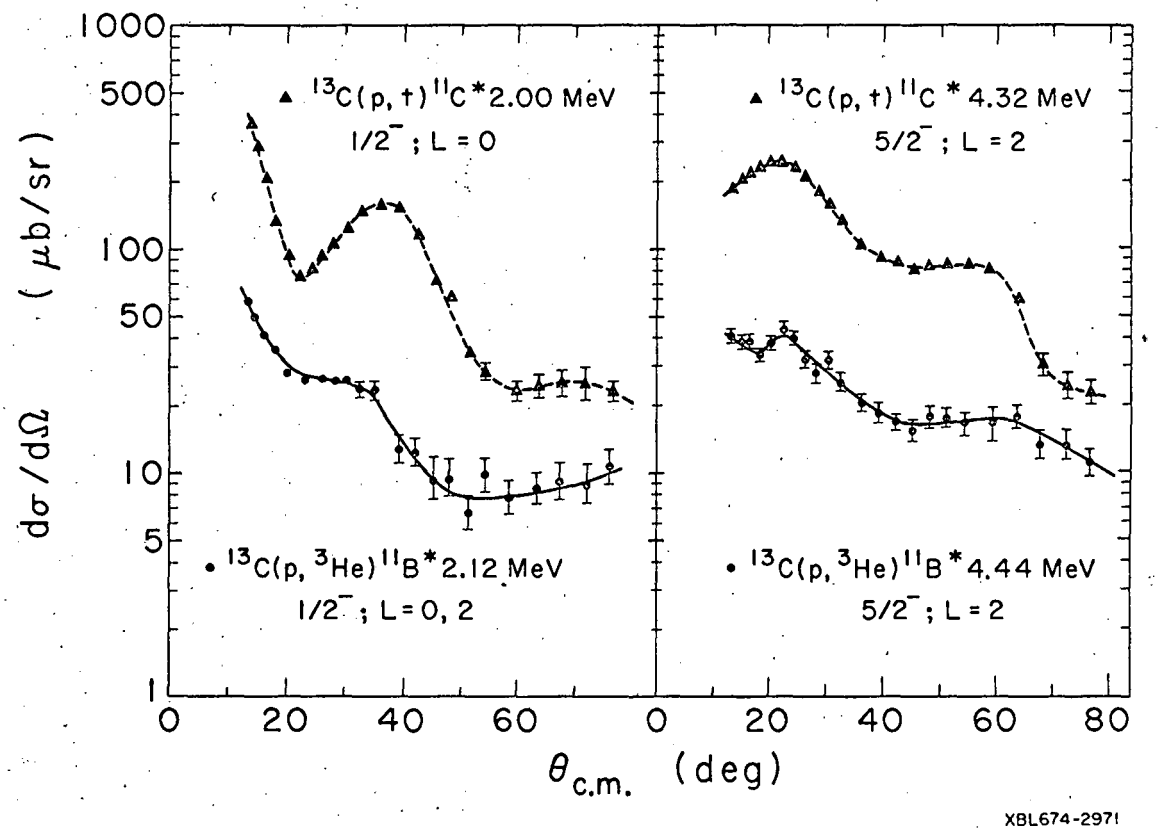


Fig. 48. Differential cross sections at 49.6 MeV for the (a) $^{13}C(p,t)^{11}C^*$ 2.00 MeV and $^{13}C(p,^3He)^{11}B^*$ 2.12 MeV transitions and (b) $^{13}C(p,t)^{11}C^*$ 4.32 MeV and $^{13}C(p,^3He)^{11}B^*$ 4.44 MeV transitions. The curves have no theoretical significance.

Table XIII. Integrated (p,t) and (p,$^3$He) cross section ratios for those levels exceeding the pure $^{13}$S transfer limit of the theory.

| | $J^\pi$ | Excitation (MeV) | R(10-80°) experiment | R(10-45°) experiment | $R_{theory}$ (10-45°) $A^S = A^T$ |
|---|---|---|---|---|---|
| $^{13}$N, $^{13}$C | 5/2$^-$ | 7.38 | 4.72[a] | 4.44 | 1.66 |
| $^{11}$C, $^{11}$B | 1/2$^-$ | 2.00, 2.12 | 4.92 | 5.88 | 1.55 |
| $^{11}$C, $^{11}$B | 5/2$^-$ | 4.32, 4.44 | 4.72 | 5.64 | 0.380 |

[a]Cross sections integrated to 90°.

Table XIV. (p,t)/(p,$^3$He) cross section ratios for other data available on T=1/2 targets.

| Reaction | $J^\pi$ | Excitation (MeV) | Peak Angle Ratio | Integrated ($\sigma_T$) Ratio | Reference |
|---|---|---|---|---|---|
| $^7Li \rightarrow {}^5He, {}^5Li$ | $3/2^-$ | g.s. | 3.0 | 2.3 | 10 |
| $^9Be \rightarrow {}^7Be, {}^7Li$ | $3/2^-$ | g.s. | 3.3 | 2.5 | 10 |
| $\rightarrow {}^7Be^*, {}^7Li^*$ | $1/2^-$ | 0.478 | 2.9 | 1.5 | 10 |
| $\rightarrow {}^7Be^*, {}^7Li^*$ | $7/2^-$ | 4.63 | 1.8 | 1.3 | 10 |
| $^{27}Al \rightarrow {}^{25}Al, {}^{25}Mg$ | $5/2^+$ | g.s. | 3.7 | 3.3 | 44 |
| $\rightarrow {}^{25}Al^*, {}^{25}Mg^*$ | $7/2^+$ | 1.61 | 2.0 | 1.9 | 44 |
| $^{31}P \rightarrow {}^{29}P, {}^{29}Si$ | $1/2^+$ | g.s. | 4.1 | 3.0 | 44 |
| $\rightarrow {}^{29}P^*, {}^{29}Si^*$ | $5/2^+$ | 2.04 | 1.0 | 0.80 | 44 |
| $^{39}K \rightarrow {}^{37}K, {}^{37}A$ | $3/2^+$ | g.s. | 4.5 | 3.8 | 45,109 |

1) the differential cross section ratio arising from the peak angle in the (p,t) reaction and the corresponding angle in the (p,$^3$He) reaction, and 2) the ratio of integrated cross sections over the angular range observed. Not shown are data concerning the "S-forbidden" transitions in the $^9$Be(p,t)$^7$Be and $^7$Li(p,t)$^5$Li reactions,[10] which are virtually absent in those spectra. Those ratios which are close to unity in Table XIV can presumably be understood on the basis of nuclear structure effects inhibiting the (p,t) transition. Other than the striking cases of this inhibition discussed in Ref. 10, further examples were previously pointed out in the $^{13}$C(p,t)$^{11}$C and $^{13}$C(p,$^3$He)$^{11}$B discussion.

Of the above data, the $^{31}$P(p,t)$^{29}$P and $^{31}$P(p,$^3$He)$^{29}$Si reactions appeared the most tractable for detailed consideration, since nuclear wave functions were available and two-nucleon spectroscopic factors were readily calculable. This experiment was done by Hardy and Skyrme,[44] using the 40 MeV proton beam from the Rutherford Linac. The ground state angular distributions and DWBA fits are shown in Fig. 49. Although only a small angular range is covered by these data, it is still worthwhile to present the DWBA fits in order to show that the theory is properly accounting for the experimental angular distributions. The calculated curves are arbitrarily normalized to the data and the optical model parameters used are given in Table III. Note that the (p,t) transition is again much stronger than the mirror (p,$^3$He) transition, with their cross sections at the peak angle differing by about a factor of four. Nuclear structure factors have been calculated from wave functions[110] based on a model of three nucleons outside a $^{28}$Si core. As observed previously, the theoretical cross sections for mirror state transitions utilizing (p,t) nuclear structure factors for both were essentially the same and one can again directly compare theory and experiment. Figure 50 shows the ground state cross section compared with the theory for the spin-independent and spin-dependent nucleon-nucleon interaction discussed earlier. The theoretical curves represent the relative magnitude of these (p,t) and (p,$^3$He) transitions and, as observed earlier, agreement with experiment is much improved for the case of a strongly spin-dependent nucleon-nucleon interaction.

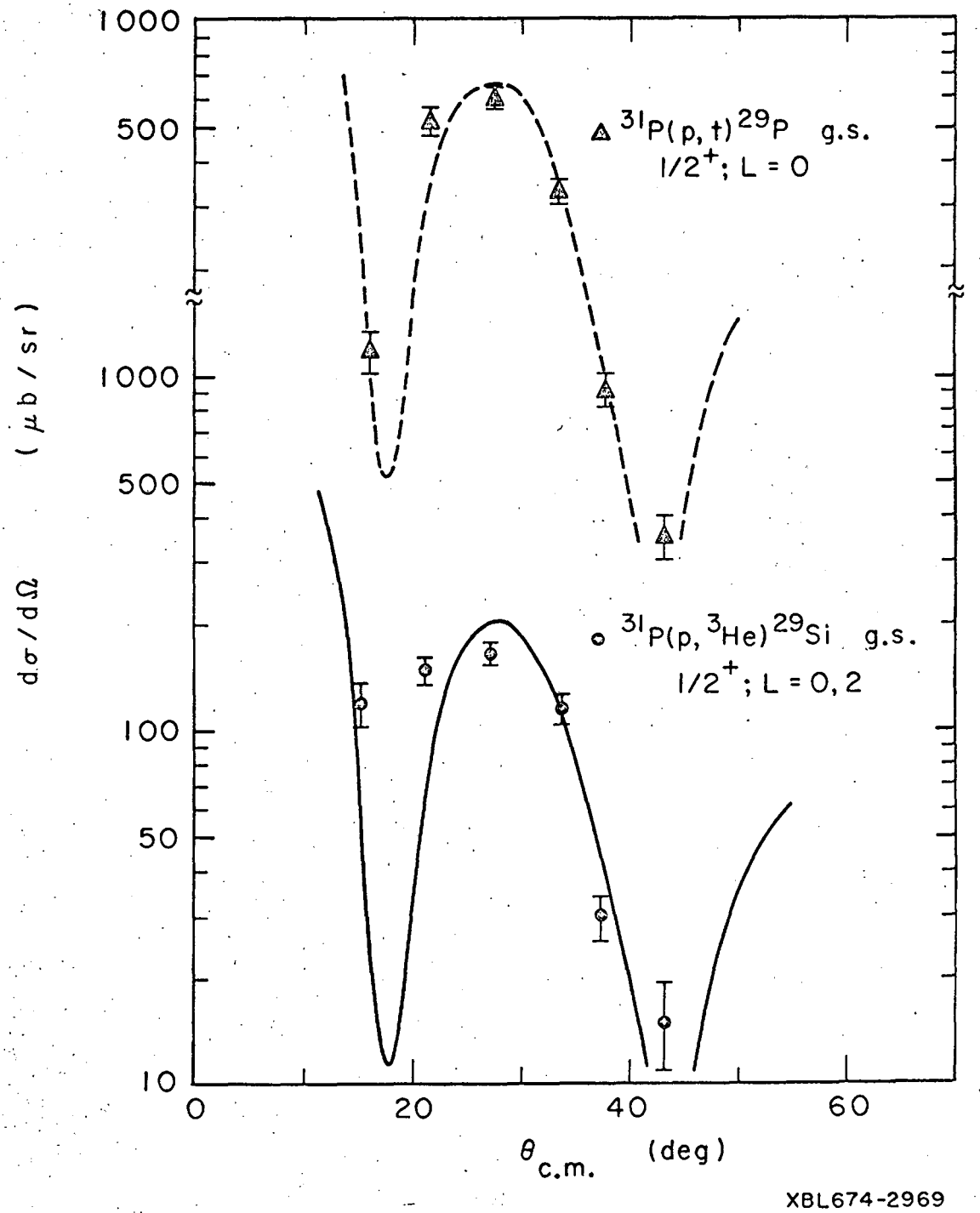


Fig. 49. Ground state differential cross sections and DWBA fits to the $^{31}P(p,t)^{29}P$ and $^{31}P(p,^{3}He)^{29}Si$ transitions.[44]

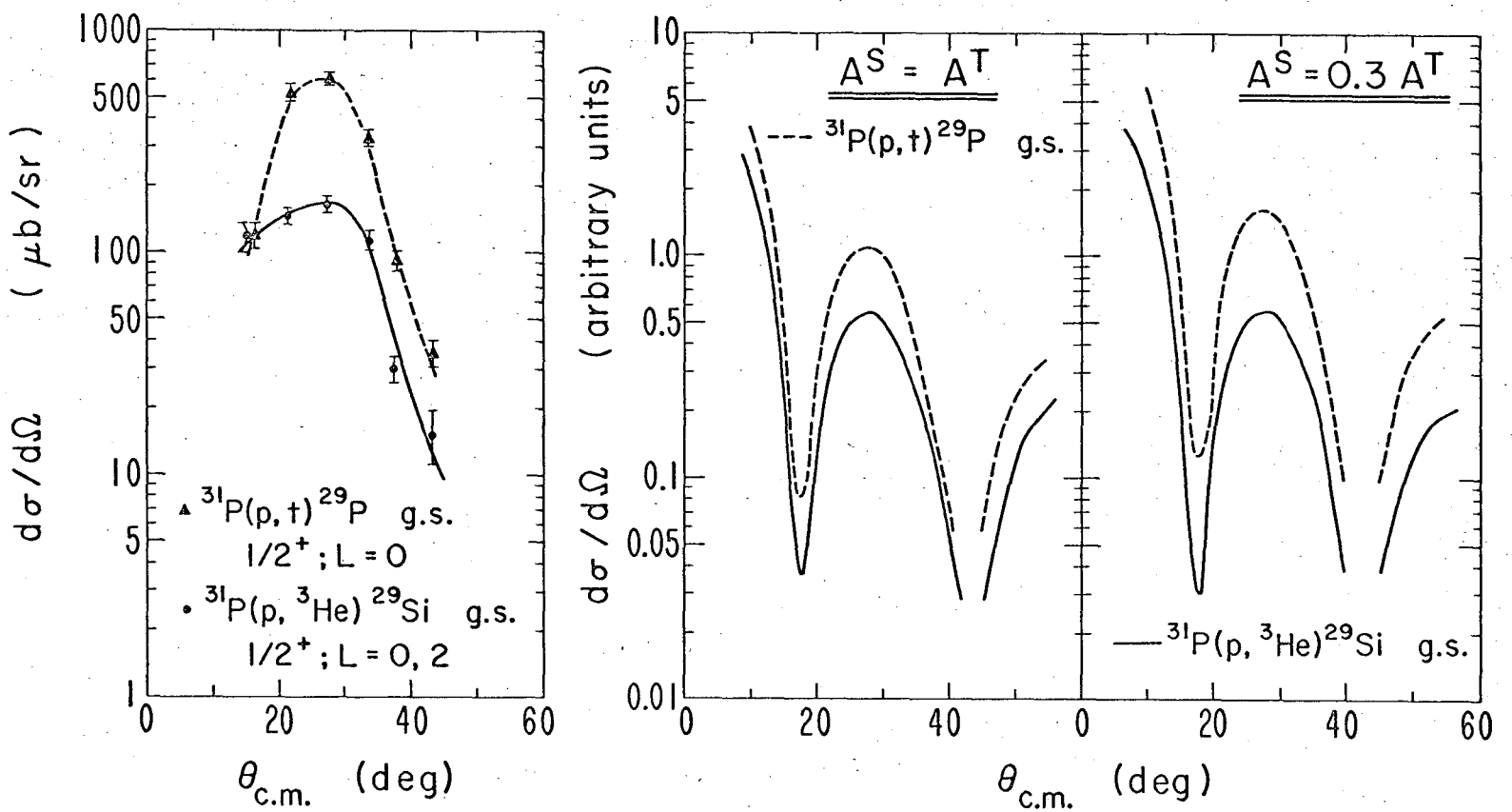


XBL674-2974-A

Fig. 50. (a) The $^{31}P(p,t)^{29}P$ and $^{31}P(p,^{3}He)^{29}Si$ ground state differential cross sections. The curves have no theoretical significance. (b) Theoretical curves for these transitions utilizing a spin-independent nucleon-nucleon interaction. The dashed line represents the (p,t) cross section and the solid line the $(p,^{3}He)$ cross section. The theoretical cross sections are given in the same units and have not been normalized to each other. (c) as in (b) but with the spin-dependent ($A^{S} = 0.3\ A^{T}$) nucleon-nucleon interaction.

2. Possible Explanations

Although the theory generally gives a good account of the shapes of the (p,t) angular distributions, it is unable, in almost every case, to account for the ratios of cross sections observed for (p,t) and (p,$^3$He) transitions to T=1/2 mirror states. It is found that the introduction of a strongly spin dependent term ($A^S = 0.3A^T$) in the nucleon-nucleon interaction considerably improves the agreement between theory and experiment for these ratios, but even so, it was not possible to fit the overall average behavior of the data. Moreover, three examples now discussed lie outside the pure S=0 limit of the present theory. An explanation for these results is sought in either one, or both, of the following: 1) that the neglect of spin-dependent interactions in the optical potential is not justified, so that the angular momentum quantum numbers of the transferred pair would interfere, or 2) that a two-step reaction mechanism may be competitive with the direct reaction mode.

a. Coherence arising from the spin-orbit interaction. The present theory assumes that the incident particle interacts only with the two nucleons to be transferred and has no other interactions except its interaction with the nucleus through the optical potential; the further assumption of the absence of a spin-orbit force leads to an incoherent sum on all the angular momentum quantum numbers of the transferred pair. However, when a spin-orbit force is included in the optical potential, the orbital angular momentum (L) and the spin angular momentum (S) transferred in the reaction are no longer incoherent (although the sum on the total angular momentum (J) remains incoherent) and one must consider a coherent sum on these quantum numbers.[36]

The coherence introduced through the spin-orbit interaction will not affect the (p,t) reaction, since the spin transfer is zero.[111] The (p,$^3$He) reaction, on the other hand, might be expected to undergo a considerable change since now a separation between the L and S transferred in the reaction cannot be achieved. In this case, representing the entrance and exit channel spins by $S_a$ and $S_b$ respectively, the differential cross section can be written as

$$\frac{d\sigma}{d\Omega}(p,{}^3He) \propto \sum_{\substack{JM \\ m_a m_b}} \left| \sum_{M' m_a' m_b'} \sum_{LS} C_{ST} \left( \sum_N G_{NLSJT} \, B_{NLSJ}^{M,M',m_a,m_a',m_b,m_b'} \right) \right|^2 \qquad (19)$$

where the distorted wave amplitude now contains discrete sums over the channel spin projections $(M',m_a',m_b')$. (See Ref. 2 or Ref. 36 for a more complete discussion).

The strong influence of the S=1 transfer in the $(p,{}^3He)$ reaction can be seen in those transitions where multiple L values are allowed. For most of these cases the $(p,{}^3He)$ angular distribution is quite unlike the corresponding (p,t) transition where only a single L value is allowed. The coherence introduced with the S=1 transfer could have a marked effect on the $(p,{}^3He)$ cross section, possibly reducing it with respect to the mirror (p,t) transition, so that agreement between theory and experiment could be considerably improved over what has been heretofore presented based on an incoherent sum. Such interference effects might also alter the shapes of the $(p,{}^3He)$ angular distributions, possibly in such a way as to improve the overall agreement between theory and experiment. However, the theoretical shapes that have been obtained for the ${}^{15}N(p,{}^3He){}^{13}C$ transitions (neglecting the reactions on ${}^{13}C$ since the final wave functions are too uncertain), assuming an incoherent sum on the angular momentum quantum numbers, are already in reasonable agreement with experiment.

As previously discussed, the DWBA code being used cannot calculate the influence of such interference terms on the cross section, since it contains no spin-orbit potential. To get an indication of whether interference terms could explain the results, a very preliminary analysis with the Oak Ridge code JULIE was conducted on the ${}^{15}N(p,t)$ and $(p,{}^3He)$ transitions populating the $5/2^-$ levels at 7.38 MeV in ${}^{13}N$ and 7.55 MeV in ${}^{13}C$. The results are only tentative, but using the AX optical potential given in Table III, a considerable improvement was found in the ratios of (p,t) to $(p,{}^3He)$ cross sections as compared to the previously discussed (incoherent sum) calculations, although a spin dependence was still required. Clearly, much more extensive and detailed theoretical analysis is necessary to establish any quantitative results on the significance of spin-orbit interference terms in two-nucleon transfer reactions.

b. Coherence arising from core excitation. In addition to spin-orbit interference terms, other coherent effects, such as those arising through core excitation, could also possibly account for the observed ratios of mirror (p,t) and (p,$^3$He) transitions. Following the treatment presented earlier (see Theory), the overall cross section for a given reaction, with the inclusion of a core-excitation step, can be written[51] as

$$\sigma \propto |T_1 + T_2|^2 = |T_1|^2 + |T_2|^2 + 2\mathrm{Re}(T_1 \cdot T_2^*) \qquad (20)$$

where $T_1$ and $T_2$ are again the transition amplitudes for the direct step and the core-excitation step (which consists of terms like the one shown in Eq. (18)), respectively. The last term in the above equation is an interference term between the direct transition and the core-excitation transition. It has been noted previously that the $^{11}C^*$ $7/2^-$ state is excited with an appreciable cross section in the $^{13}C(p,t)^{11}C$ reaction and insofar as this can be taken as evidence for a core-excitation pickup reaction, then interference effects could presumably be quite large. For a two-nucleon transfer reaction in the absence of spin-orbit coupling, the orbital angular momentum (L) and total angular momentum (J) transferred in each reaction path will be coherent. Although this coherence could account for the observed ratios of (p,t) and (p,$^3$He) mirror state transitions, its effect is by no means clear, since, due to the S=1 spin transfer, many more interference terms would be present in the (p,$^3$He) reaction than in the corresponding mirror state (p,t) transition.

## B. Comparison of Relative Cross Sections

### 1. $^{15}N(p,t)^{13}N$ and $^{15}N(p,^3He)^{13}C$ transitions

Before discussing the DWBA predictions for these transitions it is well to review how the form factor is treated in the calculation. Since the bound state wave function is represented by a harmonic oscillator, it is matched at the nuclear surface to a Hankel function tail. For a pickup reaction, the increasing separation energy of the pair with excitation has a damping effect on the magnitude of the Hankel function and this results in an increase in the matching radius with increasing excitation. For a

given L transfer, this tends to cause an increase in the predicted two-nucleon cross section with excitation, although the magnitude of this increase can be quite sensitive to the chosen optical model potential, as will be indicated later. A more reasonable method might be to match the Hankel function tail at the same radius for all excited states, which necessitates a slight increase in the oscillator parameter $\nu$ with excitation. Both approaches have been tried and noticeably better results are obtained with the latter.

Relative cross sections for these two calculations are compared with experiment in Table XV for two choices of the optical-model potential, AX and AZ (Table III), and using the nuclear structure factors calculated from the Cohen and Kurath (CK) wave functions (Table VI). Both calculations have been arbitrarily adjusted to give the best agreement with experiment. The calculation in which the oscillator parameter is fixed at $\nu$=0.32 and the matching radius is correspondingly increased gives noticeably poorer results for relative cross sections than the procedure adopted whereby the matching radius is fixed (at the ground state value of 3.60f) and the oscillator parameter adjusted. The variation in agreement of the experimental and theoretical relative cross sections is indicated by the quantity B, which is defined as the average value minus one of the larger ratio of experimental and theoretical relative cross sections for all the indicated levels (B=0 for perfect agreement). In Table XV, B varies from a value of 1.51 (AX potential with constant $\nu$) to a value of 0.31 (AZ potential with a constant R=3.60f and a 17 percent variation in $\nu$). Since the method of requiring the Hankel function tail to match the oscillator at the same radius for all the excited states gives a significant improvement in this agreement, its use is adopted hereafter. For both calculations, the theoretical results using optical potential AZ are in much better agreement with experiment than those using potential AX. Other choices were tried (including those of Table III) and in no case was there a significantly greater difference than between AX and AZ. It is disappointing that potential AX shows the worst agreement in reproducing the relative cross sections, since it gives better overall fits to the data and is the potential used in the previous discussion. However, potential AZ shows the best fit to the ground state transition (Fig. 16) and also gives a reasonable fit to all the excited states (an example is shown in Fig. 17).

Table XV. $^{15}N(p,t)^{13}N$ relative cross sections for different form factors and optical model potentials.

| $J^{\pi}$ | Excitation (MeV) | $\sigma_T$(μb) exp. (10-90, c.m.) | Relative $\sigma_T$ (exp.) | $\nu$ = 0.32 Matching R(f) | AX $\sigma_T$ (Rel.) | AZ $\sigma_T$ (Rel.) | $R_{match}$ = 3.60f $\nu$ | AX $\sigma_T$ (Rel.) | AZ $\sigma_T$ (Rel.) |
|---|---|---|---|---|---|---|---|---|---|
| $1/2^-$ | 0.0 | 941 | 1.00 | 3.58 | .174[a] | .445 | .318 | .408[a] | .822 |
| $3/2^-$ | 3.51 | 652 | .693 | 3.70 | .386 | .457 | .334 | .690 | .641 |
| $5/2^-$ | 7.38 | 1271 | 1.35 | 3.82 | 1.79 | 1.71 | .348 | 2.26 | 1.80 |
| $1/2^-$ | 10.78 | 17.6 | .0187 | 3.89 | .0239 | .0217 | .357 | .0187 | .0196 |
| $3/2^-$ | 11.88 | 93 | .0988 | 3.94 | .104 | .0800 | .362 | .0872 | .0600 |
| $3/2^-$ | 15.07 | 115 | .122 | 4.03 | .473 | .320 | .372 | .268 | .188 |
| [T=3/2] | | | | B = | 1.51 | 0.674 | | .578 | .312 |

[a]The ground state is expected to show poor agreement for the AX potential since this potential produced a relatively poor fit to the data (Fig. 14).

In Table XVI the relative integrated cross sections of all the (p,t) transitions are compared using nuclear structure factors (Table VI) calculated from both pure jj and intermediate coupling (CK) configurations, for the optical model potentials AX and AZ discussed above. Both calculations have been arbitrarily adjusted to give the best agreement with experiment. The average relative cross sections for these two potentials, utilizing the CK structure factors, agree with experiment to within an average B value of 0.45. This is the first time that such comparisons have been extended to cover such a wide range of excitation and the agreement must be considered as very good. Insofar as the theory is to be regarded as a test of the nuclear wave functions being used, then the intermediate coupling calculations of Cohen and Kurath[70] give good results for the $^{15}N(p,t)^{13}N$ reaction; moreover, insofar as these wave functions have been previously tested (Ref. 70), the two-nucleon transfer theory[3] under discussion is found to perform very well. The relative cross sections predicted in Table XVI using pure jj configurations to describe the final state are, on the other hand, in relatively poor agreement with experiment.

Two further points of interest appear in Table XVI. First, it is important to note that the cross section to the very weakly excited 10.78 MeV level in $^{13}N$, which was earlier assigned as $1/2^-$, is in good agreement with calculation. In fact, assuming this level to be the next $3/2^-$ state, gives a theoretical value for the cross section (shown in brackets in the table) which, on the average, is about a factor of five too large. Second, of equal interest is the transition to the 8.93 MeV ($1/2^-$) state, for which the relative cross section is predicted to be a factor of <u>six hundred</u> too low. It is unlikely that this gross discrepancy between theory and experiment is due to the nuclear wave functions because of the good agreement obtained in $^{14}N(p,d)^{13}N$ [54] and $^{14}N(^3He,\alpha)^{13}N$ [53] calculations for this level. This large discrepancy is not understood; it can perhaps be explained through coherent admixtures of other configurations or by a very complex reaction mechanism.

Table XVI. $^{15}N(p,t)^{13}N$ relative cross sections for constant form factor calculated from jj and intermediate coupling wave functions.[70]

| $J^{\pi}$ | Excitation (MeV) | $\sigma_T(\mu b)$ exp (10-90°,c.m.) | Relative $\sigma_T$ (exp.) | $\nu$ | jj AX $\sigma_T$ (Rel.) | jj AZ $\sigma_T$ (Rel.) | CK AX $\sigma_T$ (Rel.) | CK AZ $\sigma_T$ (Rel.) |
|---|---|---|---|---|---|---|---|---|
| $1/2^-$ | 0.0 | 941 | 1.00 | .318 | .212[a] | .416 | .408[a] | .822 |
| $3/2^-$ | 3.51 | 652 | .693 | .334 | .313 | .281 | .690 | .641 |
| $5/2^-$ | 7.38 | 1271 | 1.35 | .348 | 1.96 | 1.51 | 2.26 | 1.80 |
| $1/2^-$ | 8.93 | 130 | .138 | .351 | - | - | [.00021 | .00022][b] |
| $1/2^-$ | 10.78 | 17.6 | .0187 | .357 | - | - | .0187 | .0196 |
| | | | | | | | [.0975 | .0702 ][b] |
| $3/2^-$ | 11.88 | 93 | .0988 | .362 | .338 | .234 | .0872 | .0600 |
| $3/2^-$ [T=3/2] | 15.07 | 115 | .122 | .372 | .249 | .171 | .268 | .188 |
| | | | | B = | 1.77 | .952 | .578 | .312 |

[a] The ground state is expected to show poor agreement for the AX potential since this potential produced a relatively poor fit to the data (Fig. 14).

[b] Not included in the calculation of B.

Table XVII presents the relative integrated cross sections for the $^{15}N(p,^{3}He)^{13}C$ reaction and DWBA comparisons similar to those of Table XVI. Calculations for the intermediate coupling (CK) configurations only are shown. The matching radius for the 3.68 MeV $(3/2^{-})$ transition was held constant and the theoretical cross sections are again arbitrarily adjusted to give the best agreement with experiment. Two values of B are shown in the table, $B_1$ and $B_2$. The $B_1$ value arises from all the levels shown in Table XVII while $B_2$ is calculated only for the mirror transitions corresponding to those in Table XVI.

The earlier discussion has shown that the ratios of (p,t) to $(p,^{3}He)$ cross sections for mirror transitions were significantly improved with the introduction of a strong spin dependence in the nucleon-nucleon interaction. Since this can only affect the $(p,^{3}He)$ relative cross sections, calculations for both a spin-independent ($A^S = A^T$) and the strongly spin-dependent interaction ($A^S = 0.3\ A^T$) are presented in Table XVII. There appears to be little difference between the spin independent and the spin dependent results for the $B_1$ calculation but the $B_2$ calculation shows a definite preference for the spin-independent interaction for such <u>relative</u> cross section comparisons. However, the previous discussion of cross section ratios has shown that a spin dependence is to be preferred, although it could not account for all of the data. One of the further suggestions made was that a coherent sum on the (LS) quantum numbers of the transferred pair in the $(p,^{3}He)$ reaction should be taken into account. Since the $(p,^{3}He)$ calculations described above have not included this coherence, one would expect that the agreement in relative cross sections for these transitions should be significantly worse than for the mirror (p,t) transitions discussed earlier (Table XVI). Comparing the two over the same range of excitation and for the same optical potential, however, the (p,t) cross sections are found to be only in somewhat better agreement with experiment. In fact, the agreement in these $(p,^{3}He)$ cross sections is certainly acceptable -- the present theory predicting fairly well those states which are strongly or weakly excited.

It would appear from the above results on the $^{15}N(p,^{3}He)^{13}C$ reaction that a comparison of experimental <u>relative</u> cross sections with theory (in a $(p,^{3}He)$ reaction on a T=1/2 target) does not clarify the discussion presented earlier, which indicated 1) a necessity for some

Table XVII. $^{15}N(p,{}^{3}He)^{13}C$ relative cross sections for different spin-dependent interactions and optical potentials.

| $J^{\pi}$ | Exc. (MeV) | $\sigma_T(\mu b)$ exp. (10-90°,c.m.) | Relative $\sigma_T$ (exp.) | $A^S = A^T$ AX $\sigma_T$ (Rel.) | $A^S = A^T$ AZ $\sigma_T$ (Rel.) | $A^S = 0.3\ A^T$ AX $\sigma_T$ (Rel.) | $A^S = 0.3\ A^T$ AZ $\sigma_T$ (Rel.) | $\nu$ |
|---|---|---|---|---|---|---|---|---|
| $1/2^-$ | 0.0 | 308 | 1.00 | .650 | 1.00 | .612 | .997 | .308 |
| $3/2^-$ | 3.68 | 573 | 1.86 | 1.04 | 1.44 | 1.04 | 1.28 | .323 |
| $5/2^-$ | 7.55 | 270 | .878 | 1.41 | 1.26 | 2.00 | 1.66 | .337 |
| $1/2^-$ | 8.86 | 61 | .198 | .271 | .329 | .198 | .226 | .342 |
| $(1/2^-)$ | 11.09 | 52 | .169 | .0690 | .0588 | .0571 | .0479 | .350 |
| $(3/2^-)$ | 11.80 | 137 | .445 | .444 | .364 | .361 | .276 | .352 |
| $7/2^-$ | 12.40 | 100 | .325 | 1.31 | 1.02 | .954 | .693 | .354 |
| $3/2^-$ [T=3/2] | 15.11 | 115[a] | .358 | .319 | .246 | .699 | .395 | .363 |
| | | | $B_1$ = | 0.863 | 0.760 | 0.972 | 0.733 | |
| | | | $B_2$[b] = | 0.498 | 0.426 | 0.899 | 0.710 | |

[a] This cross section assumed identical to the (p,t) [T=3/2] cross section due to the lack of large angle data.

[b] This calculation does not include the 8.86 MeV ($1/2^-$) and 12.40 MeV ($7/2^-$) levels.

spin-dependent nucleon-nucleon interaction in the two-nucleon transfer theory and 2) the probable necessity for including spin-orbit coupling in the optical potential. DWBA calculations that reliably predicted absolute cross sections for these two-nucleon transfer reactions and could incorporate these effects would certainly resolve the problem. Insofar as the first effect is considered, a comparison of experimental and theoretical relative cross sections for $(p,{}^3He)$, [or $({}^3He,p)$] transitions on T=0 targets would be expected to be much more sensitive to the presence of a spin-dependent nucleon-nucleon force, since here the neutron-proton pair is transferred in unique ${}^3S$, T=0 or ${}^1S$, T=1 states.

2. $^{13}C(p,t)^{11}C$ Transitions

Table XVIII presents the relative integrated cross sections for all of the $^{13}C(p,t)^{11}C$ transitions previously discussed. The optical potentials used in the DWBA calculation were again AX($R_w$ = 1.45) and AZ of Table III, and the matching radius of the ground state transition (3.63f) was held constant (although here this procedure did not appear to be necessary to obtain good agreement with experiment). Calculations of relative cross sections have not been carried out for the $^{13}C(p,{}^3He)^{11}B$ transitions because of the ambiguities inherent in such comparisons on a T=1/2 target, as previously pointed out in the discussion of the $^{15}N(p,{}^3He)^{13}C$ reaction, and also because of the assumed simple jj configurations of these mass 11 final states -- such calculations could hardly yield meaningful results.

For the (p,t) transitions, it is surprising that the agreement (again denoted by B -- the larger ratio of experiment and theory minus one) between experiment and theory indicated in Table XVIII is so good. In fact, over 12.5 MeV of excitation (excluding the 6.49 MeV $(7/2^-)$ transition), the average value of B for the optical potentials shown is 0.52. When this is compared to the value of 1.4 obtained earlier in a similar calculation using jj configurations for the $^{15}N(p,t)^{13}N$ reaction, then the agreement for these mass 11 transitions appears to be quite striking. That the pure jj configurations assumed for these states are indeed a poor representation of their structure can be seen by projecting out the appropriate intensities from the complete (intermediate coupling)

Table XVIII. $^{13}C(p,t)^{11}C$ relative cross sections for contant form factor and different optical model potentials.

| $J^{\pi}$ | Excitation (MeV) | $\sigma_T(\mu b)$ exp. (13-77°,c.m.) | Relative $\sigma_T$ (exp.) | $\nu$ | AX $\sigma_T$ (Rel.) | AZ $\sigma_T$ (Rel.) |
|---|---|---|---|---|---|---|
| $3/2^-$ | 0.0 | 1324 | 1.00 | .323 | .920 | 1.00 |
| $1/2^-$ | 2.00 | 310 | .234 | .327 | .236 | .226 |
| $5/2^-$ | 4.32 | 425 | .321 | .337 | .366 | .336 |
| $3/2^-$ | 4.80 | 167 | .126 | .339 | .247 | .221 |
| $7/2^-$ | 6.49 | 167 | .126 | .456 | [.120 | .0812][a] |
| $1/2^-$ | 12.84 | 294 | .222 | .362 | .0862 | .0856 |
| [T=3/2] | | | | B = | 0.556 | 0.486 |

[a]Assuming a 5% $(f7/2)^2$ admixture in the $^{13}C$ ground state and a $(p_{1/2}\ f_{7/2})$ pickup. Not included in the calculation of B.

wave functions. Calculations of this by Kurath[70] show the following: the ground $(3/2^-)$ state, 2.00 MeV $(1/2^-)$ state and the 4.32 MeV $(5/2^-)$ state are only 46%, 55% and 53% pure jj, respectively. It is somewhat dissapointing, then, that the calculated cross sections agree as well as they do.

## VI. CONCLUSIONS

The comparative measurement of (p,t) and (p,$^3$He) reactions populating mirror final states has proven to be a useful spectroscopic tool. In particular, these reactions were found to be ideal probes of the nuclear configurations which characterize highly excited analogue final states. Two-nucleon structure factors for mirror (p,t) and (p,$^3$He) reactions were calculated from assumed nuclear configurations and then tested for consistency with experiment, utilizing the DWBA theory of Glendenning.[3] In general, good results were obtained for the angular distributions and the theoretical comparison of relative cross sections populated in the $^{15}$N(p,t)$^{13}$N reaction has indicated that the (p,t) reaction may, in general, be a good test of the wave functions used to describe the initial and final nuclear states.

The theoretical comparison of cross section ratios of mirror (p,t) and (p,$^3$He) transitions led to the incorporation of a strong spin dependence in the nucleon-nucleon interaction, in an attempt to account for the generally much stronger (p,t) transitions. This led to a modification of the computed ratio in the correct direction, but did not in itself provide a satisfactory account of the data. Several transitions were observed in which this ratio was greater than the 4/1 limit expected for pure S=0 transfer of the nucleon pairs and interference terms arising either through spin-orbit coupling in the optical potential or through core excitation were suggested as accounting for this result. The former explanation is somewhat preferred, since the examples which are outside this limit generally arise from the most highly populated final states. In fact, until the exact nature of this interference effect is understood, the spectroscopic utility of (p,$^3$He) or ($^3$He,p) reactions on T≠0 targets is greatly hindered.

## ACKNOWLEDGEMENTS

I take particular pleasure in thanking:

My research director, Professor Joseph Cerny, for suggesting these experiments, for his continued guidance and encouragement throughout the course of this work and for his careful reading of the manuscript.

Dr. Norman K. Glendenning and Dr. Martin G. Redlich for their many helpful discussions concerning the theoretical interpretation of the experimental results and especially to Dr. Norman K. Glendenning for the use of his two-nucleon transfer DWBA program.

Mr. Robert Lothrop and his staff for providing me with several excellent semiconductor detectors.

Mr. Creve C. Maples for the use of several of his computer programs and for his help in setting up the experimental apparatus.

Dr. Sam W. Cosper for his assistance in setting up the experimental apparatus and for several valuable discussions.

Dr. Claude Detraz, Dr. Robert L. McGrath, Mr. Nolan F. Mangleson, Mr. Gordon C. Ball and many other colleagues for several relevant and helpful discussions.

Mr. John Meneghetti, Mr. Wayne Oltoff, Mr. Don Stiver, Mr. Don Fong, Mr. Frank Hart and the other members of the machine shop for their help in setting up the supporting equipment used in these experiments.

My wife for putting up with me during the course of this work and especially during the last month of it.

This work was performed under the auspices of the U.S. Atomic Energy Commission.

# APPENDIX

## TWO-NUCLEON STRUCTURE FACTORS ($G_{NLSJT}$)

### A. Derivation of Two-Nucleon Parentage Factors

#### 1. Even-Even Nuclei

The target wave function has zero spin and can be written in the form

$$|\psi_T\rangle = |(j_a)_0^{n_a} (j_b)_0^{n_b};\ 0\rangle$$

where $n_a$ and $n_b$ are even.

(a) For a pair of like nucleons added or taken out of a given shell, say $j_b$, then the final state wave function has the form

$$|\psi_F\rangle = |(j_a)_0^{n_a} (j_b)_J^{n_b-2};\ J_f = J\rangle$$

and the parentage factor relating this configuration to that of the initial state is just simply the two-nucleon coefficient of fractional parentage. Thus

$$\beta^{\gamma}(j_b)_J^2 = \left(\frac{n_b(n_b-1)}{2}\right)^{1/2} ((j_b)_{vJ}^{n_b-2}\ (j_b)_J^2;\ 0|\}(j_b)_0^{n_b})$$

For states of minimum seniority (maximum T), this coefficient is discussed by Schwartz and de-Shalit.[112] One finds that

$$((j_b)_{vJ}^{n_b-2}\ (j_b)_J^2;\ 0|\}(j_b)_0^{n_b}) = \left(\frac{2(n_b-2)(2J+1)}{(n_b-1)(2j_b-1)(2j_b+1)}\right)^{1/2}_{v=2,J\neq 0}$$

$$= \left(\frac{2j_b+3-n_b}{(n_b-1)(2j_b+1)}\right)^{1/2}_{v=0,J=0}$$

Other cases are discussed in Ref. 3 or Ref. 112.

(b) For any pair of nucleons transferred across shells or a pair of unlike nucleons transferred within the same shell (neutron-proton pair), the final state wave function has the form

$$|\psi_F\rangle = |[(j_a)^{n_a-1}_{j_a} (j_b)^{n_b-1}_{j_b}]_J;\ J_f = J\rangle$$

and the parentage factor relating this configuration to that of the initial state is derived as follows: (this type of calculation is treated in more detail below). The target state wave function is expanded in the form

$$|\psi_T\rangle = |[(j_a)^{n_a-1}_{j_a},\ j_a][(j_b)^{n_b-1}_{j_b},\ j_b]_0;\ 0\rangle$$

$$= \sum_J \begin{bmatrix} j_a & j_a & 0 \\ j_b & j_b & 0 \\ J & J & 0 \end{bmatrix} |(j_a j_b)_J,\ [(j_a)^{n_a-1}_{j_a} (j_b)^{n_b-1}_{j_b}]_J;\ 0\rangle$$

so that the pair is immediately separated from the core. Thus the parentage factor has the form

$$\beta^{\gamma}(j_a j_b)_J = (n_a n_b)^{1/2} \begin{bmatrix} j_a & j_a & 0 \\ j_b & j_b & 0 \\ J & J & 0 \end{bmatrix} = (n_a n_b)^{1/2} \left(\frac{2J+1}{(2j_a+1)(2j_b+1)}\right)^{1/2}$$

2. <u>Odd-A Nuclei</u>

The target wave function has spin $j$ and is written in the form

$$|\psi_T\rangle = |(j_a)^{n_a}_0 (j_b)^{n_b}_0,\ j;\ j\rangle$$

where $n_a$ and $n_b$ are even and $j$ is the spin of the odd nucleon.

(a) For a pair of like nucleons added or taken out of a given shell, say $j_b$, then the final state wave function has the form

$$|\psi_F\rangle = |(j_a)^{n_a}_0 (j_b)^{n_b-2}_J,\ j;\ J_f\rangle$$

and the parentage factor relating this configuration to that of the initial state is derived as follows:

The target wave function is first expressed in terms of the transferred pair and the core. Thus

$$|\psi_T\rangle = ((j_b)^{n_b-2}_{vJ}\ (j_b)^2_J;\ 0|\}(j_b)^{n_b}_0)$$
$$\times\ |[(j_b)^2_J\ (j_b)^{n_b-2}_J]_0\ (j_a)^{n_a}_0,\ j;\ j\rangle$$

where the square bracket denotes vector coupling. The transferred pair must now be separated from the final state and this is achieved by a recoupling coefficient,[49]

$$|\psi_T\rangle = ((j_b)^{n_b-2}_{vJ}\ (j_b)^2_J;\ 0|\}(j_b)^{n_b}_0)$$
$$\times \sum_{J_f} \sqrt{2J_f+1}\ \ W(JJjj;\ 0\ J_f)$$
$$\times\ |(j_b)^2_J,\ [(j_b)^{n_b-2}_J,\ (j_a)^{n_a}_0,\ j]_{J_f};\ j\rangle$$

The angular momentum of the transferred pair is $J$, $J_f$ is the spin of the final state and the vector - coupled expression in the brackets is just the configuration of the final state. For a particular $J_f$,

$$\sqrt{2J_f+1}\ \ W(JJjj;\ 0\ J_f) = (-)^{J_f-J-j}\left(\frac{2J_f+1}{(2J+1)(2j+1)}\right)^{1/2}$$

and

$$|\psi_T\rangle = ((j_b)^{n_b-2}_{vJ}\ (j_b)^2_J;\ 0|\}(j_b)^{n_b}_0)\times(-)^{J_f-J-j}$$
$$\times\left(\frac{2J_f+1}{(2J+1)(2j+1)}\right)^{1/2}\times|(j_b)^2_J,[(j_b)^{n_b-2}_J\ (j_a)^{n_a}_0,\ j]_{J_f};\ j\rangle$$

and the parentage factor (defined with respect to core × particles) relating this configuration to that of the final state is given by,

$$\beta^{\gamma}(j_b)^2_J = \left(\frac{n_b(n_b-2)}{2}\right)^{1/2}((j_b)^{n_b-2}_{vJ}\ (j_b)^2_J;\ 0|\}(j_b)^{n_b}_0)\left(\frac{2J_f+1}{(2J+1)(2j+1)}\right)^{1/2}$$

where the expression $(|\})$ is a two-nucleon coefficient of fractional parentage, as defined previously.

(b) For a pair of nucleons transferred across shells or a pair of unlike nucleons (neutron-proton pair) transferred within the same shell, the final state wave function has the form

$$|\psi_F\rangle = |[(j_a)^{n_a-1}_{j_a}(j_b)^{n_b-1}_{j_b}]_J, j;\ J_f\rangle$$

where the square bracket again denotes vector coupling. Following the procedure outline above, then

$$|\psi_T\rangle = ((j_a)^{n_a-1}_{j_a},\ j_a;\ 0|\}(j_a)^{n_a}_0)((j_b)^{n_b-1}_{j_b},\ j_b;\ 0|\}(j_b)^{n_b}_0)$$

$$\times\ |[(j_a)^{n_a-1}_{j_a},\ j_a]_0\ [(j_b)^{n_b-1}_{j_b},\ j_b]_0,\ j;\ j\rangle$$

For $n_a$ and $n_b$ even, the single nucleon coefficients of fractional parentage are just unity,[2] and can thus be dropped from the above expression. Hence

$$|\psi_T\rangle = |[(j_a)^{n_a-1}_{j_a},\ j_a]_0\ [(j_b)^{n_b-1}_{j_b},\ j_b]_0,\ j;\ j\rangle$$

$$= \sum_J \begin{bmatrix} j_a & j_a & 0 \\ j_b & j_b & 0 \\ J & J & 0 \end{bmatrix} |\{(j_a j_b)_J, [(j_a)^{n_a-1}_{j_a}(j_b)^{n_b-1}_{j_b}]_J\}_0,\ j;\ j\rangle$$

Now recoupling of the angular momentum yields

$$|\psi_T\rangle = \sum_{J_f,J} \begin{bmatrix} j_a & j_a & 0 \\ j_b & j_b & 0 \\ J & J & 0 \end{bmatrix} \sqrt{2J_f+1}\ \ W(JJjj;\ 0\ J_f)$$

$$\times\ |(j_a j_b)_J,\ \{[(j_a)^{n_a-1}_{j_a}(j_b)^{n_b-1}_{j_b}]_J,\ j\}_{J_f};\ j\rangle$$

where $J$ is the angular momentum transferred in the reaction and the expression in curly brackets is just the configuration of the final state. For the total angular momentum transfer $J$, then

$$\begin{bmatrix} j_a & j_a & 0 \\ j_b & j_b & 0 \\ J & J & 0 \end{bmatrix} = (2J+1) \begin{Bmatrix} j_a & j_a & 0 \\ j_b & j_b & 0 \\ J & J & 0 \end{Bmatrix} = (-)^{J-j_a-j_b}\ \sqrt{2J+1}$$

$$\times\ W(j_a j_a j_b j_b;\ 0\ J)$$

Thus $$|\psi_T\rangle = \sum_{J_f,J} (-)^{J-j_a-j_b} \sqrt{(2J+1)2J_f+1}\; W(JJjj;\, 0\, J_f)$$

$$\times\, W(j_a j_a j_b j_b;\, 0\, J)\,|(j_a j_b)_J,\, \{[(j_a)^{n_a-1}_{j_a}\,(j_b)^{n_b-1}_{j_b}]_J,\, j\}_{J_f};\, j\rangle$$

where

$$W(j_a j_a j_b j_b;\, 0\, J)\; W(JJjj;\, 0\, J_f) = \frac{(-)^{J_f-j-j_a-j_b}}{((2J+1)(2j+1)(2j_a+1)(2j_b+1))^{1/2}}$$

therefore

$$|\psi_T\rangle = \sum_{J_f,J} (-)^{J_f+J-j} \times \left(\frac{2J_f+1}{(2j_a+1)(2j_b+1)(2j+1)}\right)^{1/2}$$

$$\times\, |(j_a j_b)_J,\, \{[(j_a)^{n_a-1}_{j_a}\,(j_b)^{n_b-1}_{j_b}]_J,\, j\}_{J_f};\, j\rangle$$

Note that on odd-A nuclei, for an across shell transfer the total angular momentum transfer $J$ enters only in the phase of the above equation, unlike the similiar case discussed earlier for even-even nuclei. The parentage factor relating this configuration to that of the final state is defined with respect to core $\times$ particles and has the form

$$\beta^{\gamma}(j_a j_b)_J = (n_a n_b)^{1/2} \left(\frac{2J_f+1}{(2j_a+1)(2j_b+1)(2j+1)}\right)^{1/2}$$

## B. Numerical Examples of Nuclear Structure Calculations

In the following discussion, several nuclear structure factors are computed on the basis of assumed pure $jj$ wave functions to describe the final state. In many of the DWBA calculations previously presented, these factors were in fact constructed from a complete intermediate coupling wave function,[70] which introduces a coherent sum over the various configurations. Each separate shell-model configuration, however, is calculated as shown below. Only the (p,t) transitions are considered; the extension to the S=1 transfer for the (p,$^3$He) reaction is straightforward. The configurations of initial and final states are written in terms of neutrons and protons, where $\nu$ refers to neutron and $\pi$ to proton.

1. $^{15}N(p,t)^{13}N$ Transitions

The $^{15}N$ ground state wave function is written in the form

$$|^{15}N\rangle = |(p_{3/2}{}^{\nu})^4_0(p_{3/2}{}^{\pi})^4_0(p_{1/2}{}^{\nu})^2_0\, p_{1/2}{}^{\pi};\ 1/2^-\rangle$$

(a) For the ground state transition, the final state wave function has the form

$$|^{13}N\ g.s.\rangle = |(p_{3/2}{}^{\nu})^4_0(p_{3/2}{}^{\pi})^4_0\, p_{1/2}{}^{\pi};\ 1/2^-\rangle$$

This is actually an especially simple case since the pair of neutrons to be transferred is already separated from the final state. Thus, using the notation developed above

$$\beta(1/2\ 1/2)_0 = 1.0 \times 1.0 = 1.0$$

and in LS coupling,

$$\beta_{LSJ} = \beta_{000} = \begin{bmatrix} 1 & 1/2 & 1/2 \\ 1 & 1/2 & 1/2 \\ 0 & 0 & 0 \end{bmatrix} = +0.577$$

Since this (p,t) reaction is a $1/2^-$ to $1/2^-$ transition, it is restricted by angular momentum selection rules to an L=J=S= 0 and T=1 transfer. The two-nucleon structure factor is defined as

$$G_{NLSJT} = \sum_{\gamma} g^{\gamma}\beta^{\gamma}_{LSJT}\, \Omega_n\, \langle n0,\ NL;\ L|n_1\ell_1,\ n_2\ell_2;\ L\rangle$$

The selection rule for transforming to relative and center-of-mass coordinates is given by

$$2(n_1 + n_2) + \ell_1 + \ell_2 = 2(n + N) + \lambda + \Lambda$$

which for $\lambda = 0$ becomes

$$2(n_1 + n_2) + \ell_1 + \ell_2 = 2(n + N) + L$$

Now, for an L=0 transition in the 1p shell, both n=1, N=2 and n=2, N=1 are allowed values of the relative, center-of-mass principal quantum numbers. Assuming a Gaussian wave function for the triton, the overlap integral between the transferred pair and this wave function has the form[3]

$$\Omega_n = \frac{(2n-1)^{1/2}}{2^{n-1}(n-1)!} (xy)^{3/2} (1-x)^{n-1}; \; n=1,2,\ldots.$$

Thus

$$\Omega_1 = (xy)^{3/2} \quad \text{and} \quad \Omega_2 = \frac{\sqrt{6}}{2} (xy)^{3/2} (1-x)$$

The parameters x and y are defined as

$$x = \frac{2\nu}{(2a\eta^2+\nu)} \quad \text{and} \quad y = \eta\left(\frac{2a}{\nu}\right)^{1/2}$$

where $\nu$ refers to the oscillator parameter of the single particle (harmonic oscillator) wave functions being used to describe the transferred pair. The value of $\nu$ used is 0.32, which is the same value employed by True.[72] The parameter a is 3 for $^3$H ($^3$He) and the size parameter $\eta$ of the light particle is related to its mean square radius by

$$\eta^2 = \frac{1}{6\langle r^2\rangle} \quad \text{for } ^3\text{H and } ^3\text{He}.$$

For the triton, $\eta = 0.242$ (0.206 for $^3$He) which in conjunction with the value of $\nu$, yields for the triton

$$\Omega_1 = 1.00 \quad \text{and} \quad \Omega_2 = +\ .0575$$

The Moshinsky bracket -$\langle n0,\ NL;\ ^1L|n_1\ell_1, n_2\ell_2;\ L\rangle$- has the values

$$\langle 10,20;\ 0|11,11;\ 0\rangle = +\ 0.707$$

$$\langle 20,10;\ 0|11,11;\ 0\rangle = -\ 0.707$$

thus the product,

$$\Omega_1\ \langle 10,20;\ 0|11,11;\ 0\rangle = +\ 0.707$$

$$\text{and}\ \ \Omega_2\ \langle 20,10;\ 0|11,11;\ 0\rangle = -\ 0.0407$$

and these numbers, along with the evaluation of the parentage factor, $\beta^{\gamma}_{LSJT}$, yield for the nuclear structure factor, $G_{NLSJT}$, the values

$$G_{10001} = 0.577 \times -.0407 = -0.023$$

$$G_{20001} = 0.577 \times 0.707 = +0.408$$

Thus, although two values of N are allowed, the transition is dominated by the N=2 term. This is a general result for two-nucleon transfer <u>within the same shell</u>; namely, the largest value of the principal quantum number N always dominates the cross section. However, these structure factors enter coherently into the cross section (Eq. (1)) through a sum on N and for cross shell transitions, such a coherence can be quite important.

(b) For the 7.38 MeV $5/2^-$ transition, the final state wave function has the form

$$|^{13}N^* \ 7.38 \text{ MeV}\rangle = |(p_{3/2}{}^{\pi})^4_0[(p_{3/2}{}^{\nu})^3_{3/2}\, p_{1/2}{}^{\nu}]_2, p_{1/2}{}^{\pi}; 5/2\rangle$$

In order to excite this configuration in the $^{15}N(p,t)^{13}N$ reaction, a pair of neutrons must be transferred across the $p_{1/2}p_{3/2}$ shells. The parentage factor for this transfer is given by

$$\beta^{\gamma}(j_a j_b)_J = (n_a n_b)^{1/2} \left( \frac{2J_f+1}{(2j_a+1)(2j_b+1)(2j+1)} \right)^{1/2}$$

Thus, for a $5/2^-$ final state

$$\beta(1/2\ 3/2)_2 = (2\cdot 4)^{1/2} \left(\frac{6}{2\cdot 4\cdot 2}\right)^{1/2} = \sqrt{3}$$

For a $1/2^-$ to $5/2^-$ transition the (p,t) reaction is restricted to a pure L=J=2, S=0 transfer, so that in LS coupling,

$$\beta_{LSJ} = \beta_{202} = \sqrt{3} \times \begin{bmatrix} 1 & 1/2 & 1/2 \\ 1 & 1/2 & 3/2 \\ 2 & 0 & 2 \end{bmatrix} = 1.00$$

The two-nucleon structure factor has the form

$$G_{NLSJT} = \sum_{\gamma} g^{\gamma}\beta^{\gamma}_{LSJT}\ \Omega_n \langle n0,\ NL;\ L|n_1\ell_1, n_2\ell_2;\ L\rangle$$

and for this L=2 transfer, $g^{\gamma} = \sqrt{2}$ and n=N=1 are the only principal quantum numbers allowed by selection rules. Thus the product

$$\Omega_1\ \langle 10,12;2|11,11;2\rangle = +0.707$$

and

$$G_{12021} = \sqrt{2} \times 1.00 \times .707 = 1.00$$

2. <u>$^{13}C(p,t)^{11}C$ Transitions</u>

Most of the transitions in this reaction involve picking two neutrons out of the $p_{3/2}$ shell. The $^{13}C$ ground state wave function has the form

$$|^{13}C\ g.s.\rangle = |(p_{3/2}{}^{\nu})^4_0(p_{3/2}{}^{\pi})^4_0\ p_{1/2}{}^{\nu};\ 1/2\rangle$$

Then for a pair of like nucleons removed from the same shell, the final state wave function, for the $^{11}C^*$ 2.00 MeV $1/2^-$ level, for example, has the form

$$|^{11}C^*\ 2.00\ MeV\rangle = |(p_{3/2}{}^{\pi})^4_0(p_{3/2}{}^{\nu})^2_0\ p_{1/2}{}^{\nu};\ 1/2\rangle$$

and the parentage factor is given by

$$\beta^{\gamma}(j_b)^2_J = \left(\frac{n_b(n_b-)}{2}\right)^{1/2} ((j_b)^{n_b-2}_{vJ}\ (j_b)^2_J;\ 0|\}(j_b)^{n_b}_0)\ \left(\frac{2J_f+1}{(2J+1)(2j+1)}\right)^{1/2}$$

which in the case of $j_b$=3/2, $J_f$=1/2, J=0 and j=1/2, has the value

$$\beta(3/2)^2_0 = \sqrt{6} \times ((3/2)^2_0(3/2)^2_0;0|\}(3/2)^4_0) \times \left(\frac{2}{1.2}\right)^{1/2}$$

$$= \sqrt{6} \times \frac{1}{\sqrt{6}} \times 1.0 = 1.0$$

However, in this case such is not the final result, because removing two neutrons from the $p_{3/2}$ shell leaves an intermediate state of T=1 which can then couple with the odd nucleon (j=1/2, t=1/2) to give an isobaric

spin of T=3/2 or T=1/2 for the final state. Thus the parentage factor must include the appropriate Clebsch-Gordon coefficient, which is $\sqrt{2/3}$ for T=1/2 final states, and the value of $\beta$ is then given by

$$\beta(3/2)^2_0 = 1.0 \times \sqrt{2/3} = \sqrt{2/3}$$

and in LS coupling (L=J=S=0),

$$\beta_{LSJ} = \beta_{000} = \sqrt{2/3} \times \begin{bmatrix} 1 & 1/2 & 3/2 \\ 1 & 1/2 & 3/2 \\ 2 & 0 & 2 \end{bmatrix} = 2/3$$

which leads to the $G_{NLSJT}$ values of

$$G_{10001} = 2/3 \times -.0407 = -.0271$$

$$G_{20001} = 2/3 \times .707 = +.472$$

## REFERENCES


1. M. H. MacFarlane and J. B. French, Rev. Mod. Phys. 32, 567 (1960).
2. N. K. Glendenning, Ann. Rev. Nucl. Sci. 13, 191 (1963).
3. N. K. Glendenning, Phys. Rev. 137B, 102 (1965).
4. C. L. Lin and S. Yoshida, Prog. Theo. Phys. (Tokyo) 32, 885 (1964); E. M. Henley and D. V. L. Yu, Phys. Rev. 133B, 1445 (1964); B. Bayman, Argonne National Laboratory Report, ANL-6878, 1964 (unpublished) p. 335; A. Y. Abul-Magd and M. El Nadi, Nucl. Phys. 77, 182 (1966); C. L. Lin, Prog. Theo. Phys. (Tokyo) 36, 251 (1966).
5. J. R. Rook and D. Mitra, Nucl. Phys. 51, 96 (1964); J. R. Rook and V. S. Mathur, Nucl. Phys. A91, 305 (1967).
6. R. A. Broglia and C. Riedel, Nucl. Phys. A92, 145 (1967); A93, 241 (1967).
7. D. Kurath, Phys. Rev. 101, 216 (1956).
8. A. N. Boyarkina, Adademia Nauk, SSSR (English trans.) Physical Series, 28, 255 (1964).
9. F. C. Barker, Nucl. Phys. 45, 467 (1963).
10. J. Cerny, C. Detraz and R. H. Pehl, Phys. Rev. 152, 950 (1966).
11. J. B. Ball and C. D. Goodman, Phys. Rev. 120, 488 (1960); J. B. Ball, C. B. Fulmer and C. D. Goodman, Phys. Rev. 130, 2342 (1963); C. G. Hoot, M. Kondo and M. E. Rickey, Nucl. Phys. 71, 449 (1965); L. C. McIntyre, Phys. Rev. 152, 1013 (1966).
12. G. Bassani, N. M. Hintz, C. D. Kavaloski, Phys. Rev. 136B, 1006 (1964); G. Bassani, N. M. Hintz, C. D. Kavaloski, J. R. Maxwell and G. M. Reynolds, Phys. Rev. 139B, 830 (1965); J. R. Maxwell, G. M. Reynolds and N. M. Hintz, Phys. Rev. 151, 1000 (1966); J. R. Maxwell, G. M. Reynolds and N. M. Hintz, Phys. Letts. 22, 454 (1966); G. M. Reynolds, J. R. Maxwell and N. M. Hintz, Phys. Rev. 153, 1283 (1967).
13. J. R. Maxwell, G. M. Reynolds and N. M. Hintz, University of Minnesota Annual Progress Report, 1965 (unpublished), p. 98.
14. J. C. Legg, Phys. Rev. 129, 272 (1963); H. D. Holmgren and C. B. Fulmer, Phys. Rev. 132, 2644 (1963); D. Bachelier, M. Bernas, I. Brissaud, P. Radvanyi and M. Roy, Phys. Letters 16, 304 (1965); J. C. Hardy, D. J. Skyrme and I. S. Towner, Phys. Letters 23, 487 (1966); J. W. Verba, H. Willmes, R. F. Carlson, I. Slaus, J. R. Richardson and E. L. Peterson,

Phys. Rev. 153, 1127 (1967); W. Benenson, G. M. Crawley, J. D. Dreisbach and W. P. Johnson, Nucl. Phys. A97, 510 (1967).

15. J. G. Jenkin, L. G. Earwaker and E. W. Tittertas, Phys. Letters 4, 142 (1963); R. E. Brown, N. M. Hintz, C. G. Hoot, J. R. Maxwell and A. Scott, University of Minnesota Annual Progress Report, 1966 (unpublished) p. 70; J. C. Hardy and D. J. Skyrme, University of Oxford Report No. 189, Nuclear Physics Laboratory, 1967 (unpublished).
16. R. K. Cole, R. Dittman, H. S. Sandhu and C. N. Waddell, Nucl. Phys. A91, 665 (1967).
17. J. Cerny, R. H. Pehl and G. T. Garvey, Phys. Letters 12, 234 (1964); see also the discussion by B. Bayman, Isobaric Spin and Nuclear Physics, J. Fox and O. Robson, eds., Academic Press, 1966, p. 503.
18. C. Detraz, J. Cerny and R. H. Pehl, Phys. Rev. Letters 14, 708 (1965).
19. H. E. Conzett and B. G. Harvey, Nucleonics 24, 48 (1966).
20. C. Williamson and J. P. Boujot, Center for Nuclear Study, Saclay, France, 1962.
21. G. Dearnley and D. G. Northrup, Semiconductor Counters for Nuclear Radiations, John Wiley and Sons, Inc., N. Y., 1963; F. S. Goulding, Lawrence Radiation Laboratory Report, UCRL-16231; J. M. Hollander, Nucl. Inst. and Methods 43, 65 (1966).
22. F. S. Goulding, D. A. Landis, J. Cerny and R. H. Pehl, Nucl. Inst. and Methods 31, 1 (1964).
23. Hamilton Watch Co., Lancaster, Pa.
24. M. El Nadi, Proc. Phys. Soc. (London) A70 62 (1957); M. El Nadi, Phys. Rev. 119, 242 (1960); H. C. Newns, Proc. Phys. Soc. (London) A76 (1960) 489; M. El Nadi and H. Sherif, Proc. Phys. Soc. A80, 1041 (1962); N. K. Glendenning, Nucl. Phys. 29, 109 (1962); I. Manning and A. H. Aitken, Nucl. Phys. 32, 524 (1962); S. Yoshida, Nucl. Phys. 33, 685 (1962).
25. G. E. Fischer and V. K. Fischer, Phys. Rev. 114, 533 (1959); J. Cerny, B. G. Harvey and R. H. Pehl; Nucl. Phys. 29, 120 (1962); S. W. Cosper, B. T. Lucas and O. E. Johnson, Phys. Rev. 139B, 763 (1965); J. L. Wiza, and R. M. Middleton, Phys. Rev. 143, 676 (1966); R. Jahr, K. Kayser, A. Koska and J. P. Wurm, Nucl. Phys. 76, 79 (1966); M. Krick and G. J. F. Legge, Nucl. Phys. 89, 63 (1966); W. R. McMurray,

P. VanderMerwe and J. VanHeerden, Nucl. Phys. A92, 401 (1967); S. Hinds, H. Marchant and R. Middleton, Phys. Letters 24B, 34 (1967).

26. H. D. Holmgren and C. B. Fulmer, Phys. Rev. 132, 2644 (1963); R. H. Pehl, J. Cerny, E. Rivet and B. G. Harvey, Phys. Rev. 140B, 605 (1965); J. H. Towle and B. E. F. Macefield, Nucl. Phys. 66, 65 (1965); R. W. Zurmuhle, C. M. Fou and L. W. Swenson, Nucl. Phys. 80, 259 (1966).

27. B. Buck, R. N. Maddison and P. E. Hodgson, Phil. Mag. 5, 1181 (1960); R. H. Bassel, R. M. Drisko and G. R. Satchler, Oak Ridge National Laboratory Report, ORNL-3240, 1962 (unpublished); P. E. Hodgson, The Optical Model of Elastic Scattering , Oxford University Press, 1963.

28. R. M. Drisko and F. Rybicki, Phys. Rev. Letters 16, 275 (1966).

29. T. A. Brody and M. Moshinsky, Tables of Transformation Brackets (monografias del Insituto de Fisica, Mexico), 1960.

30. J. M. Blatt, G. H. Derrick and J. N. Lyness, Phys. Rev. Letters 8, 323 (1962); R. Pascual, Phys. Letters 19, 221 (1965); B. F. Gibson, Phys. Rev. 139B, 1153 (1965).

31. J. J. Wesolowski, L. F. Hansen, J. G. Vidal and M. L. Stelts, Phys. Rev. 148, 1063 (1966); J. Vervier, Phys. Letters 22, 82 (1966); 24B, 603 (1967).

32. N. F. Mangelson and B. G. Harvey, Lawrence Radiation Laboratory Annual Report, UCRL-17299, 1966 (unpublished) p. 97, and N. F. Mangelson, private communication.

33. N. K. Glendenning, Phys. Rev. 156, 1344 (1967).

34. N. M. Hintz, Argonne National Laboratory Report, ANL-6878, 1966 (unpublished)., p. 425.

35. This is only strictly true in the zero-range approximation or when neglecting $\lambda \neq 0$ amplitudes in the wave function of the light particle (see Ref. 36).

36. G. R. Satchler, Nucl. Phys. 55, 1 (1964).

37. J. C. Hardy and I. S. Towner, University of Oxford, Nuclear Physics Laboratory Report No. 25, 1967.

38. J. L. Gammel and R. M. Thaler, Phys. Rev. 107, 291, 1337 (1957); P. S. Signel and R. E. Marshak, Phys. Rev. 109, 1229 (1958); K. E. Lassila, M. J. Hull, H. M. Ruppel, F. A. McDonald and G. Breit, Phys. Rev. 126, 881 (1962).

39. T. Hamada and I. D. Johnston, Nucl. Phys. 34, 383 (1962).

40. C. L. Storrs and D. H. Frisch, Phys. Rev. 95, 1252 (1954); L. Hulthen and M. Sugawara, Encyc. of Physics (Handbuch der Physik) 39, 1 (1957); M. A. Preston, Physics of the Nucleus, Addison-Wesley Publishing Co. (1962) p. 25.

41. W. J. S. Y. Young, Nucl. Phys. 55, 84 (1964).

42. T. T. S. Kuo and G. E. Brown, Nucl. Phys. 85, 40 (1966); N. Freed and P. Goldhammer, Phys. Letters 23, 564 (1966); G. E. Brown and T. T. S. Kuo, Nucl. Phys. A92, 481 (1967).

43. S. G. Nillson, J. Sawicki and N. K. Glendenning, Nucl. Phys. 33, 239 (1962); A. Kallio and K. Koltveit, Nucl. Phys. 53, 87 (1964).

44. J. C. Hardy and D. J. Skyrme, University of Oxford, Nuclear Physics Laboratory Report No. 189, 1966.

45. G. Butler, J. Cerny, S. W. Cosper and R. L. McGrath, submitted to the Physical Review.

46. M. Chabre, D. L. Hendrie, H. G. Pugh and C. Detraz, Lawrence Radiation Laboratory Annual Report, UCRL-16580, 1965 (unpublished), p. 68.

47. Actually this ratio (ignoring the slight kinematic and Coulomb effects) would be slightly greater (about 4.1/1) since the spatial overlap between the A=3 ground state and the transferred pair is slightly greater for tritons than for $^3$He.

48. Parentage factors for even-even nuclei have also been given by Glendenning (Ref. 3), and are included here for completeness.

49. A. R. Edmonds, Angular Momentum in Quantum Mechanics, Princeton University Press, 1957; A. de-Shalit and I. Talmi, Nuclear Shell Theory, Academic Press, N. Y., 1963.

50. R. Bock H. H. Duhum, R. Rudel and R. Stock, Phys. Letters 13, 151 (1964); T. A. Belote, W. E. Dorenbusch, O. Hansen and J. Rapaport, Nucl. Phys. 73, 321 (1965); B. Kozlowsky and A. de-Shalit, Nucl. Phys. 77, 215 (1966); F. S. Levin, Phys. Rev. 147, 715 (1966).

51. S. K. Penny, Ph.D. Thesis, University of Tennessee, 1966 (unpublished); S. K. Penny and G. R. Satchler, Nucl. Phys. 53, 145 (1964).

52. F. A. Selove, private communication, and to be published; T. Lauritsen and F. Ajenberg-Selove, Energy Levels of Light Nuclei, May, 1962.

53. G. Ball and J. Cerny, to be published, and G. Ball, private communication.

54. D. Bachelier, M. Bernas, I. Brissaud, P. Radvanyi and M. Roy, Nucl. Phys. 88, 307 (1966); R. L. Kozub, L. A. Kull and E. Kashy, Nucl. Phys. A99, 540 (1967).

55. M. P. Fricke and G. R. Satchler, Phys. Rev. 139B, 567 (1965); E. T. Boschitz, M. Chabre, H. E. Conzett and R. J. Slobodrian, Lawrence Radiation Laboratory Annual Report, UCRL-16580, 1965 (unpublished), p. 118.

56. A. E. Glassgold and P. J. Kellog, Phys. Rev. 109, 1291 (1958).

57. J. A. Fannan, E. J. Burge, D. A. Smith and N. K. Ganguly, Nucl. Phys. A97, 263 (1967).

58. L. L. Lee, Jr., J. P. Schiffer, B. Zeidman, G. R. Satchler, R. M. Drisko and R. H. Bassel, Phys. Rev. 136B, 971 (1964).

59. C. Glashausser and M. E. Rickey, Phys. Rev. 154, 1033 (1967); E. F. Gibson, B. W. Ridley, J. J. Kraushaar and M. E. Rickey, Phys. Rev. 155, 1194 (1967).

60. F. Bjorklund, Tallahassee Conference on the Nuclear Optical Model, Florida State University, Tallahassee, Florida, 1959.

61. R. N. Glover and A. D. W. Jones, Phys. Letters 16, 69 (1965); J. R. Rook, Nucl. Phys. 61, 219 (1965); K. R. Greider and W. R. Dodd, Phys. Rev. 146, 671 (1966); W. R. Dodd and K. R. Greider, Phys. Rev. 146, 675 (1966).

62. R. N. Glover and A. D. W. Jones, Nucl. Phys. 81, 277 (1966).

63. W. W. Daehnick, Phys. Rev. 135B, 1168 (1964); B. Johansson, Nucl. Phys. 67, 289 (1965); J. Stevens, H. F. Lutz and S. F. Eccles, Nucl. Phys. 76, 129 (1966); A. J. Frasca, R. W. Finlay, R. O. Koshel and R. L. Cassola, Phys. Rev. 144, 854 (1966).

64. J. C. Hiebert, E. Newman and R. H. Bassel, Phys. Rev. 154, 898 (1967).

65. P. E. Hodgson, Proceedings of the Rutherford Jubilee International Conference, J. B. Birks, Ed., 1961, p. 407; H. M. Sen Gupta, J. Rotblatt, P. E. Hodgson and J. B. A. England, Nucl. Phys. 38, 361 (1962).

66. F. G. Perey, Phys. Rev. 131, 745 (1963); P. C. Sood, Nucl. Phys. 84, 106 (1966).

67. D. R. Inglis, Rev. Mod. Phys. 25, 390 (1953).

68. A. M. Lane, Proc. Phys. Soc. (London) A66, 977 (1953), A68, 197 (1954).

69. E. C. Halbert, Y. E. Kim and T. T. S. Kuo, Phys. Letters 20, 657 (1966).

70. S. Cohen and D. Kurath, Nucl. Phys. 73, 1 (1963); D. Kurath, private communication.

71. F. C. Barker, Nucl. Phys. 83, 418 (1966).

72. W. M. True, Phys. Rev. 130, 1530 (1963).

73. The interpretation of relative cross sections for the (p,$^3$He) reaction is not straightforward, as is later discussed.

74. Both of these levels could not be resolved from neighboring $5/2^+$ states at 3.56 MeV in $^{13}$N and 3.85 MeV in $^{13}$C. However, as is later discussed, any contribution of these levels to the cross sections of the $3/2^-$ states is thought to be small.

75. G. G. Shute, D. Robson, V. R. McKenna and A. T. Bertiss, Nucl. Phys. 37, 535 (1962).

76. H. S. Adams, J. D. Fox, N. P. Heydenburg and G. M. Temmer, Phys. Rev. 124, 1899 (1961); M. Nomoto, Nucl. Phys. 30, 513 (1962).

77. F. C. Barker, Nucl. Phys. 45, 449 (1963).

78. A. Gallman, D. E. Alburger, D. H. Wilkinson and F. Hibou, Phys. Rev. 129, 1765 (1963).

79. G. G. Shute and A. M. Baxter, Nucl. Phys. 83, 460 (1966).

80. D. Lister and A. Sayres, Phys. Rev. 143, 745 (1966).

81. R. McPherson, R. A. Esterlund, A. M. Poskanzer, and P. L. Reeder, Phys. Rev. 140B, 1513 (1965).

82. A. Marques, A. J. P. L. Policarpo and W. R. Phillips, Nucl. Phys. 36, 45 (1962).

83. D. E. Grace and B. D. Sowerby, Nature 206, 494 (1965).

84. T. W. Bonner, A. A. Kraus, Jr., J. B. Marion and J. P. Schiffer, Phys. Rev. 102, 1348 (1956); J. H. Gibbons and R. H. Macklin, Phys. Rev. 137B, 1508 (1965).

85. There is a known (Ref. 52, 75) $7/2^-$ state at lower excitation--10.36 MeV in $^{13}N$--which is excited by an f wave resonance in $^{12}C + p$ scattering. As such, it does not appear in an intermediate coupling calculation restricted to the 1p shell. This 10.36 MeV ($7/2^-$) level is very weakly excited in the $^{15}N(p,t)^{13}N$ reaction and there is no evidence for a level at this excitation in the $(p,^3He)$ spectrum.

86. G. A. Jones, Ph.D. Thesis, University of Cambridge, 1953.

87. D. C. Hensley and C. A. Barnes, Bull. Am. Phys. Soc. 10, 1194 (1963).

88. E. Adelberger and C. A. Barnes, Bull. Am. Phys. Soc. 10, 1195 (1965).

89. D. J. Bredin, O. Hansen, G. M. Temmer and R. Van der Bree, Isobaric Spin in Nuclear Physics, J. Fox and D. Robson, Eds. Academic Press, N. Y., 1966, p. 472; H. M. Kuan and S. S. Hanna, Phys. Letters 24B, 566 (1967).

90. W. M. MacDonald, Nuclear Spectroscopy, Part B, F. Ajenberg-Selove, Ed., Academic Press, N. Y., 1960, p. 932; W. M. MacDonald, Phys. Rev. 100, 51 (1955); Phys. Rev. 101, 271 (1956).

91. G. Strobel, Phys. Rev. 154, 941 (1967).

92. Only the (p,t) transitions will be considered in detail because, as is later discussed, interference effects in the $(p,^3He)$ reaction render its interpretation ambiguous.

93. D. G. Fleming, C. C. Maples and J. Cerny, unpublished data.

94. N. Austern, Phys. Rev. 136B, 1743 (1964); R. Sherr, B. F. Bayman, E. Rost, M. E. Rickey and C. G. Hoot, Phys. Rev. 139B, 1272 (1965); C. Glashausser, M. Kondo, M. E. Rickey and E. Rost, Phys. Letters 14, 113 (1965).

95. F. C. Barker, Nucl. Phys. 28, 96 (1961 ); T. Sebe, Prog. of Theor. Physics (Tokyo) 30, 290 (1963).

96. B. G. Harvey, E. J-M. Rivet, A. Springer, J. R. Meriwether, W. B. Jones, J. H. Elliott and P. Darriulat, Nucl. Phys. 52, 465 (1964); J. Kokame, K. Fukunaga, N. Inoue and H. Nakamura, Phys. Letters 8, 342 (1964); D. Dehnhard and J. L. Yntema, Phys. Rev. 155, 1261 (1967).

97. A. Bussiere, N. K. Glendenning, B. G. Harvey, J. Mahoney and J. R. Meriwether, Phys. Letters 16, 296 (1965).

98. C. P. Browne and F. H. O'Donnell, Phys. Rev. 149, 767 (1966).

99. S. W. Cosper, H. Brunnader, J. Cerny and R. L. McGrath, Phys. Letters, in press.

100. B. G. Harvey, J. Meriwether, J. Mahoney, A. Bussiere de Nercy and D. J. Horen, Phys. Rev. 146, 712 (1966).

101. J. K. Dickens, D. A. Haner and C. N. Waddell, Phys. Rev. 129, 743 (1963); T. Stovall and N. M. Hintz, Phys. Rev. 135, 330 (1964).

102. D. Kurath, Phys. Rev. 140, 1190 (1965); D. H. Wilkinson, J. T. Sample and D. E. Alburger, Phys. Rev. 146, 662 (1966).

103. D. J. Pullen, A. E. Litherland, S. Hinds and R. Middleton, Nucl. Phys. 36, 1 (1962); I. Talmi, Rev. of Mod. Phys. 34, 704 (1962); I. Talmi and I. Unna, Phys. Rev. Letters 4, 469 (1960); D. E. Alburger, C. Chasman, K. W. Jones, J. W. Olness and R. A. Ristinen, Phys. Rev. 136B, 916 (1964).

104. R. H. Bassel, Phys. Rev. 149, 791 (1966).

105. N. Austern, Selected Topics in Nuclear Theory, F. Janouch, Ed. (I.A.E.A., Vienna), 1963, p. 17.

106. Gy. Bencze and J. Zimanyi, Nucl. Phys. 81, 76 (1966).

107. N. Austern, R. M. Drisko, E. C. Halbert and G. R. Satchler, Phys. Rev. 133B, 3 (1964); R. M. Drisko and G. R. Satchler, Phys. Letters 9, 342 (1964).

108. In the majority of cases, the (p,$^3$He) transitions were 5 to 10% larger than the corresponding mirror (p,t) transitions. In no case was the (p,t) transition more than 5% greater than the mirror (p,$^3$He) transition.

109. G. Butler and J. Cerny, unpublished data.

110. P. W. M. Glaudemans, G. Wichers and P. J. Brussard, Nucl. Phys. 56, 548 (1964).

111. The spin-orbit coupling will modify the elastic scattering states in the (p,t) reaction and the effect of this might appear in the shape of the angular distribution. However, this effect is expected to be small.[58,59]

112. C. Swhartz and A. de-Shalit, Phys. Rev. 94, 1257 (1954).

This report was prepared as an account of Government sponsored work. Neither the United States, nor the Commission, nor any person acting on behalf of the Commission:

A. Makes any warranty or representation, expressed or implied, with respect to the accuracy, completeness, or usefulness of the information contained in this report, or that the use of any information, apparatus, method, or process disclosed in this report may not infringe privately owned rights; or

B. Assumes any liabilities with respect to the use of, or for damages resulting from the use of any information, apparatus, method, or process disclosed in this report.

As used in the above, "person acting on behalf of the Commission" includes any employee or contractor of the Commission, or employee of such contractor, to the extent that such employee or contractor of the Commission, or employee of such contractor prepares, disseminates, or provides access to, any information pursuant to his employment or contract with the Commission, or his employment with such contractor.